
Universidad de Valladolid

Departamento de Bioquímica y Biología Molecular y Fisiología e

Instituto de Biología y Genética Molecular (UVa-CSIC)

TESIS DOCTORAL:

# THE ROLE OF Kv1.3 CHANNELS IN CELL PROLIFERATION: MECHANISMS AND MOLECULAR DETERMINANTS

Presentada por LAURA JIMÉNEZ PÉREZ para optar al grado de doctor por la Universidad de Valladolid

Dirigida por:

Dra. Mª Teresa Pérez García

Dr. José Ramón López López

# FINANCIACIÓN

Este trabajo de investigación ha sido posible gracias a la financiación concedida en convocatorias públicas competitivas de los siguientes proyectos de investigación:

- **Determinantes genéticos y ambientales de la disfunción vascular en la hipertensión y en la cardiopatía isquémica (Red HERACLES, RD06/009/0013).**

  Entidad financiadora: Ministerio de Sanidad y Consumo, Instituto de Salud Carlos III

  Duración: desde: 2007 hasta: 2013

  Investigador Responsable: José Ramón López López

- **Papel de los canales iónicos del músculo liso en el remodelado vascular (BFU2010-15898).**

  Entidad financiadora: Ministerio de Ciencia e Innovación (Plan Nacional I+D+i)

  Duración: desde: 2011 hasta: 2013

  Investigador Responsable: Mª Teresa Pérez García

- **Estudio de los mecanismos que asocian la expresión del canal Kv1.3 con la proliferación en tejidos arteriales humanos (VA094A11-2).**

  Entidad financiadora: JCYL Consejería de Educación

  Duración: desde: 2011 hasta: 2013

  Investigador Responsable: José Ramón López López

- **Los canales iónicos del músculo liso como dianas terapéuticas en el remodelado vascular (BFU 2013-45867).**

  Entidad financiadora: Ministerio de Economía y Competitividad (Programa Estatal I+D+i)

  Duración: desde: 2013 hasta: 2016

  Investigador Responsable: José Ramón López López

# DIVULGACIÓN CIENTÍFICA

Parte de los resultados de esta Tesis Doctoral han dado lugar a comunicaciones en Congresos (publicadas como Abstracts) y a publicaciones como artículos en revistas internacionales.

## Artículos en Revistas:

Pilar Cidad[1], **Laura Jiménez-Pérez[1]**, Daniel García-Arribas, Eduardo Miguel-Velado, Sendoa Tajada, Christian Ruiz-McDavitt, José R. López-López, M. Teresa Pérez-García ([1]co-authors). "*Kv1.3 channels can modulate cell proliferation during phenotypic switch by an ion-flux independent mechanism*". Arterioscler Thromb Vasc Biol. 2012; 32: 1299-1307.

Pilar Cidad[1], Eduardo Miguel-Velado[1], Christian Ruiz-McDavitt, Esperanza Alonso, **Laura Jiménez-Pérez**, Agustín Asuaje, Yamila Carmona, Daniel García-Arribas, Javier López, Yngrid Marroquín, Mireia Fernández, Mercè Roqué, M. Teresa Pérez-García and José Ramón López-López. "*Kv1.3 channels modulate human vascular smooth muscle cells proliferation independently of mTOR signaling pathway*". Pflugers Arch. Epub ahead of print.

**Laura Jiménez-Pérez**, Pilar Cidad, Inés Álvarez-Miguel, Alba Santos-Hipólito, Esperanza Alonso, Miguel Ángel de la Fuente, José Ramón López-López, M. Teresa Pérez-García. "*Molecular Determinants of Kv1.3-induced proliferation".* To be submitted.

## Comunicaciones a Congresos:

J.R. López-López, P. Cidad**, L. Jiménez-Pérez**, E. Alonso, E. Miguel-Velado and M.T. Pérez-García. *"Contribution of Kv1.3 channels expression to the proliferative response of Vascular Smooth Muscle Cells: Molecular determinants"*. Red Española de Investigación Cardiovascular (HERACLES). Granada (España) 2010. Comunicación oral.

J.R. López-López, P. Cidad, **L. Jiménez-Pérez**, E. Alonso, E. Miguel-Velado and M.T. Pérez-García. "Role of Kv1.3 in vascular smooth muscle proliferation". 3ª Reunión Española de Canales Iónicos (RECI III). Tenerife (España) 2011. Comunicación oral.

**Laura Jiménez-Pérez**, Daniel García-Arribas, Eduardo Miguel-Velado, Esperanza Alonso, José R López-López, M. Teresa Pérez-García and Pilar Cidad. *"Modulation of HEK293 proliferation by Kv1.3 channels expression"*. The Physiological Society, Oxford (Reino Unido) 2011. Comunicación en póster.

Cidad P., Novensa L., **Jiménez-Pérez L**, Alonso E., Roqué M., Heras M., López-López JR and Pérez-García MT. *"Role of Kv1.3 channel in vascular smooth muscle cells proliferation in a porcine model of coronary restenosis"*. The Physiological Society, Oxford (Reino Unido) 2011. Comunicación en póster.

Cidad P, Miguel-Velado E, Novensa L, **Jiménez-Pérez L**, Ruiz-McDavitt C, Alonso E, Roqué M, Heras M, Pérez-García MT and López-López JR. *"Role of Kv1.3 channels in Vascular Smooth Muscle Remodeling"*. NYAS, Barcelona (España) 2011. Comunicación en póster.

**Laura Jiménez-Pérez**, Pilar Cidad, Inés Álvarez-Miguel, Rebeca Torres-Merino, Esperanza Alonso, Miguel A. de la Fuente, José R. López-López and M. Teresa Pérez-García. "*Molecular Mechanisms involved in the effects of Kv1.3 and Kv1.5 channels on cell proliferation"*. The Physiological Society, Oxford (Reino Unido) 2014. Comunicación en póster.

Mercè Roqué, Manel Garabito, Solanes Nuria, Montserrat Rigol, Pilar Cidad, M Teresa Pérez-García, Víctor Ramos, José Ramón López-López, Salvador Borros, Esperanza Alonso, **Laura Jiménez-Pérez**. *"Role of Kv1.3 Channel in Vascular Smooth Muscle Cells Proliferation in a Porcine Model of Restenosis"*. American College of Cardiology (ACC), San Diego, CA (EEUU) 2015. Comunicación en póster.

Ruby A. Fernandez, **Laura Jiménez-Pérez**, Shanshan Song, Haiyang Tang, and Jason X.-J. Yuan. *"The Functional Coupling of CaSR and TRPC6 Contributes to Enhanced Proliferation in Pulmonary Arterial Smooth Muscle Cells"*. Experimental Biology, Boston, MA (EEUU) 2015. Comunicación en poster.

# ABBREVIATIONS INDEX

| | |
|---|---|
| 6TM1P | Six Transmembrane segments and one Pore-forming region |
| ATP | Adenosine Triphosphate |
| BKCa | Large Conductance Calcium-activated Potassium channel |
| C- | COOH |
| cAMP | cyclic Adenosine Monophosphate |
| cDNA | complementary Deoxyribonucleic Acid |
| cGMP | cyclic Guanosine Monophosphate |
| $C_t$ | Cycle threshold |
| DAG | Diacylglycerol |
| DMEM | Dulbecco's Modified Eagle's Medium |
| DMSO | Dimethyl Sulfoxide |
| dNTP | deoxyribonucleotide / Nucleoside Triphosphate |
| DPO-1 | diphenyl phosphine oxide-1 |
| EAG | ether-à-go-go potassium channel |
| EDTA | Ethylenediaminetetraacetic Acid |
| EdU | 5-ethynyl-2'-deoxyuridine |
| EGFP | Enhanced Green Fluorescent Protein |
| EGFr | Epidermal Growth Factor Receptor |
| EGTA | Ethylene Glycol Tetraacetic Acid |
| Em | Emission |
| ER | Endoplasmic Reticulum |
| ERK1/2 | Extracellular-Regulated Kinase 1/2 |
| ERR | Endoplasmic Reticulum Retention |
| Ex | Excitation |
| FBS | Fetal Bovine Serum |
| GFP | Green Fluorescent Protein |
| hCA | human Coronary Artery |
| HEK | Human Embryonic Kidney |
| HEPES | 4-(2-hydroxyethyl)-1-piperazineethanesulfonic acid |
| hRA | human Renal Artery |
| HRP | Horseradish Peroxidase |

| | |
|---|---|
| hSV | human Saphenous Vein |
| hUA | human Uterine Artery |
| IC50 | Inhibitory Concentration of 50 % |
| $IP_3$ | Inositol Triphosphate |
| $[K^+_e]$ | Extracellular Potassium concentration |
| $K_{Ca}$ | Calcium activated Potassium channel |
| KDa/KD | Kilodaltons |
| $K_{IR}$ | Inward Rectifier Potassium channel |
| Kv | Voltage-gated Potassium channel |
| $R^2$ | R-Squared or Coefficient of Determination |
| LTRs | Long Terminal Repeats |
| MAPK | Mitogen Activated Protein Kinase |
| MEK1/2 | Mitogen-activated protein/extracellular signal-regulated Kinase 1/2 |
| MgTx | Margatoxin |
| MLCK | Myosin Light Chain Kinase |
| MLCP | Myosin Light Chain phosphatase |
| MOI | Multiplicity of Infection |
| MRB | Modified RIPA Buffer |
| mRNA | messenger Ribonucleic Acid |
| N- | NH2 |
| NA | Numerical Aperture |
| NMDG | N-Methyl-D-Glucamine |
| NO | Nitric Oxide |
| PAP-1 | 5-(4-phenoxybutoxy) psoralen |
| PBS | Phosphate Buffered Saline |
| PBST | PBS 0.1 % Tween 20 |
| PCR | Polymerase Chain Reaction |
| PDGF | Platelet Derived Growth Factor |
| PI3K | phosphatidylinositol 3 Kinase |
| PKA | Protein Kinases A |
| PKG | Protein Kinases G |
| PKs | Protein Kinases |
| PLCγ | Phosphor Lipase C gamma |
| PPs | Protein Phosphatases |

| | |
|---|---|
| pTyr | phosphotyrosine |
| PVDF | Polyvinylidene difluoride membrane |
| $Q_{on}/Q_{off}$ | gating charges |
| qPCR | quantitative PCR |
| RFP | Red Fluorescent Protein |
| RIPA | Radio Immunoprecipitation Assay |
| RT-PCR | Reverse Transcriptase PCR |
| SDS-PAGE | Sodium Dodecyl Sulfate PolyAcrylamide Gel Electrophoresis |
| SEM | Standard Error of the Mean |
| Ser/S | Serine |
| SH2 | Src Homology 2 domain |
| SH3 | Src Homology 3 domain |
| siRNA | Small interference Ribonucleic Acid |
| SR | Sarcoplasmic Reticulum |
| TdT | Deoxynucleotidyl Transferase |
| Thr/T | Threonine |
| TRP | Transient Receptor Potential Channel |
| Tyr/Y | Tyrosine |
| $V_{1/2}$ | membrane potential at half activation/inactivation |
| VDCCs | Voltage-Dependent Calcium Channels |
| $V_M$ | Membrane Potential |
| VSM | Vascular Smooth Muscle |
| VSMCs | Vascular Smooth Muscle Cells |
| v-Src | Viral Src |
| WT | Wild Type |

# INDEX

INTRODUCTION ..... 1

1.1. The Cardiovascular System ..... 3

1.1.1. The Vascular Wall ..... 4

1.2. Vascular Smooth Muscle Cells ..... 6

1.2.1. Phenotypic Modulation ..... 9

1.2.2. Ion Channels in VSMCs ..... 12

1.2.3. Ion Channels Involved in the Phenotypic Modulation of VSMCs ..... 14

1.3. Voltage-gated potassium channels ..... 19

1.3.1. Structure of Kv channels ..... 20

1.3.2. Pore and Selectivity Filter of Kv channels ..... 22

1.3.3. Voltage Sensor of Kv channels ..... 24

1.3.4. Inactivation Domains of Kv channels ..... 25

1.3.5. T1 domain of Kv channels ..... 28

1.3.6. Kvβ subunits ..... 31

1.3.7. Post-translational modifications of Kv1 channels ..... 32

1.4. Voltage-Dependent $K^+$ Channels Kv1.3 and Kv1.5 ..... 37

1.5. Mechanisms involved in the pro-proliferative effect of Kv1.3 ..... 39

OBJECTIVES ..... 45

MATERIALS AND METHODS ..... 49

3.1. Plasmid construction ..... 51

3.1.1. Reporter Gene Vectors ..... 53

3.1.2. Bicistronic Vectors ..... 55

3.1.3. Fusion Protein Vectors ..... 56

3.1.4. Mutant Kv1.3 Vectors ..... 58
3.1.5. Chimeric Kv1.3-Kv1.5 Vectors ..... 61
3.1.6. Lentiviral Vectors ..... 68
3.2. Cells and Culture ..... 70
3.3. Drugs ..... 72
3.4. Transfection ..... 73
3.5. Lentivirus Production and Titering ..... 74
3.5.1. Production ..... 74
3.5.2. Titering ..... 75
3.6. Lentiviral Vector Transduction ..... 78
3.7. Coating coverslips with Poly-L-Lysine ..... 79
3.8. Proliferation assays ..... 80
3.9. Apoptosis assays ..... 82
3.10. Immunocytochemistry ..... 82
3.11. Inmunoblot ..... 84
3.12. Immunoprecipitation ..... 85
3.13. Electrophysiological recordings ..... 87
3.14. Statistical Analysis ..... 93
RESULTS ..... 95
Chapter 4.1. Molecular mechanisms involved in Kv1.3-induced proliferation ..... 97
4.1.1. Validation of the heterologous system HEK293 cells to overexpress Kv1.3 and Kv1.5 ..... 98
4.1.2. Kv1.3EGFP fusion proteins as tools to generate Kv1.3 mutant channels ..... 104
4.1.3. Characterization of WT-Kv1.3 channel and Kv1.3-AYA, Kv1.3-W389F, and Kv1.3-WF3x mutant channels ..... 105
4.1.4. Modulation of proliferation by Kv1.3-pore and gating mutant channels ..... 111

4.1.5. Effects of Kv1.3 pore blockers on Kv1.3W389F-induced proliferation ..... 113

Chapter 4.2. Identification of Kv1.3 and Kv1.5 intracellular domains involved in cell proliferation ..... 114

4.2.1. Characterization of K5C3 and K5N3 chimeric constructs ..... 115

4.2.2. Effects of K5C3 and K5N3 on cell proliferation ..... 121

4.2.3. Characterization of Kv1.3 C-terminal point mutants..... 125

4.2.4. Effects of single mutations Kv1.3 C-terminal residues on cell proliferation..... 128

4.2.5. Characterization of K3YS, K5-532YS and K5-613YS chimeric channels..... 129

4.2.6. Role of YS fragment on cell proliferation..... 132

4.2.7. Study of the involvement of Kv1.3 Y447 and S459 residues in the pro-proliferative signaling pathway..... 133

Chapter 4.3. Lentiviral vector transduction as a tool to manipulate Kv1.3 and Kv1.5 expression levels in proliferating VSMCs ..... 138

**DISCUSSION ..... 141**

Chapter 5.1. Kv1.3 channels can modulate proliferation by an ion-flux independent mechanism..... 143

5.1.1. Kv1.3 overexpression increases proliferation in HEK293 cells, whereas Kv1.5 has an opposite effect..... 144

5.1.2. Kv1.3 pore and gating mutants as tools to explore the pro-proliferative mechanisms..... 146

5.1.3. Kv1.3-mediated proliferation requires gating movement but not $K^+$ permeation..... 147

5.1.4. Kv1.3 pore blockers inhibit the effect of Kv1.3W389F on proliferation by affecting gating movement..... 149

Chapter 5.2. Identificacion of the molecular determinants and signalling pathways involved in the pro-proliferative mechanism induced by Kv1.3..... 150

5.2.1. The effects of Kv1.3 and Kv1.5 on HEK cells proliferation seem to be mediated by their cytoplasmic COOH domains ..... 151

5.2.2. Single mutations of the C-terminal tyrosine Y447A or serine S459A abolish the pro-proliferative effect of Kv1.3 ..... 157

5.2.3. YS fragment plays a prominent but not exclusive role in the pro-proliferative effect by means of the interaction with signaling proteins ..... 159

5.2.4. Y447 phosphorylation is essential for Kv1.3-mediated MAPK signaling pathway ..... 161

5.2.5. Kv1.3-mediated signaling is regulated by channel conformation ..... 162

Chapter 5.3. Optimized lentiviral vector transduction to manipulate Kv1.3 and Kv1.5 levels of expression in human VSMCs ..... 165

**CONCLUSIONS ..... 144**

**REFERENCES ..... 175**

**RESUMEN ..... 178**

8.1. Introducción ..... 201

8.2. Objetivos ..... 203

8.3. Materiales y Métodos ..... 203

8.4. Resultados ..... 204

8.5. Discusión y Conclusiones ..... 206

# 1

# INTRODUCTION

## 1.1. The Cardiovascular System

The main function of the cardiovascular system is to maintain the homeostasis and supply every single cell with oxygen and nutrients as well as remove carbon dioxide and metabolic waste products from the tissue. It is also necessary to transport hormones and other substances required for proper organ function, to regulate the body temperature and to maintain an appropriate environment in all the tissue fluids of the body for optimal survival and function of the cells.

The cardiovascular system comprises the heart and the network of blood vessels: arteries, veins, and capillaries that transport blood throughout the body, allowing a rapid exchange of substances between the tissues and the blood (Levy & Pappano, 2007).

The blood vessels in the cardiovascular system can be classified according to their structure into elastic and muscular arteries; and according to their function into resistance, exchange and capacitance vessels (Levick J.R., 2010).

The elastic arteries are the largest arteries, examples include the pulmonary artery, the aorta and their major branches. These vessels are rich in elastic fiber and their main function is to keep a more continuous flow in the arteries by expanding with systole and recoiling during diastole.

Muscular arteries are medium-size arteries, such as coronary arteries, whose main function is to distribute blood to different parts of the body. The tunica media in muscular arteries is thicker than in elastic arteries. These arteries contain more smooth muscle and less elastic tissue than the elastic

arteries. They have a rich sympathetic innervation and can contract or relax. The process of constricting or relaxing the arterial wall is mediated by the vascular smooth muscle and it is called vascular tone modulation. Vascular tone is the tension exerted by the vascular smooth muscle cells (VSMCs) within the media layer and determines the vessel diameter, a major determinant of blood flow.

Terminal arteries and arterioles are resistance vessels due to their narrow lumen and limited number. They regulate blood pressure, which dramatically drops when traversing these vessels, as well as blood flow to the capillaries by adjusting the vessel diameter. Terminal arteries are innervated by sympathetic nerves.

Exchange vessels are the smallest vessels in the cardiovascular system: the capillaries. Their wall is reduced to a single layer of endothelial cells. Through these vessels is achieved the exchange of nutrients and gases between the blood in the capillaries and the surrounding tissue.

The capacitance vessels comprise venules and veins. Venules and veins are different in size and number but all comprise an intima, a thin media of smooth muscle and collagen, and an adventitia. They work as a blood reservoir, controlling the returning of blood to the heart.

### 1.1.1.The Vascular Wall

All vessels, except for the capillaries (exchange vessels), have the same basic structure as illustrated for an elastic artery in figure 1.1. Only the composition of the layers and the fraction of different cells in the layers are

dependent on vessel type. The vessel wall is arranged in three layers; tunica intima, tunica media and tunica adventitia.

**Tunica intima**: it is the innermost layer, which constitutes the main barrier to the escape of plasma. This layer consists of endothelial cells surrounded by a thin layer of connective tissue.

**Tunica media**: it is the middle layer of the vessel wall and the principal determinant of mechanical properties of the arteries. The Tunica media consists of vascular smooth muscle cells that are helically arranged and embedded in a matrix of elastic and collagen fibers. The internal and external elastic laminas connect the tunica media to the intima and adventitia. Thus, endothelial cells from the intima make contact with VSMCs by transmitting signals through the internal elastic lamina.

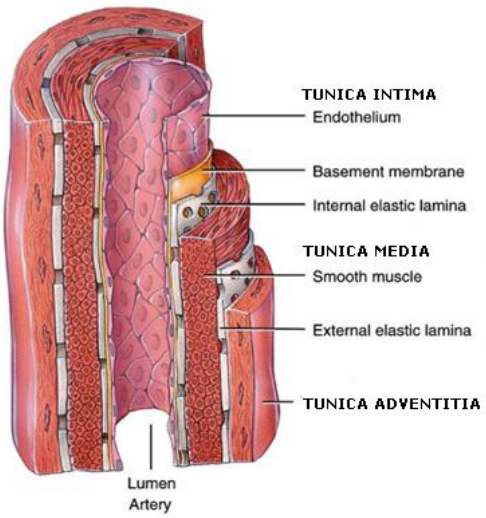


**Figure 1.1. Schematic description of an elastic artery composed of three layers: intima, media and adventitia, with different distributions of endothelial cells and collagen, elastic and smooth muscle fibers. (*Principles of Anatomy and Physiology* by J. Tortora, 2007. John Wiley and Sons, Inc).**

**Tunica adventitia**: it is the outermost layer and is covered by loose connective tissue. The adventitia of most vessels contains sympathetic fiber terminals or autonomic nerves (*nervi vasorum*). Through the varicosities of these terminals, the vasoconstrictor agent noradrenaline is released, regulating bood flow and local resistance. In larger arteries, this layer also contains a network of small blood vessels supplying or nourishing the vessel, the *vasa vasorum* (vessels of vessels) (Levick J.R., 2010).

## 1.2. Vascular Smooth Muscle Cells

The tunica media of blood vessels contains smooth muscle cells (vascular myocytes), which are spindle-shaped cells arranged in a helical pattern and have an extremely low proliferation rate. VSMCs are composed of highly differentiated contractile machinery, calcium stores, cell junctions and caveolae.

The contractile machinery is a sarcomere-like unit composed of thick filaments of myosin surrounded by thin filaments of actin. The actin filaments are attached to cytoplasmic dense bodies and insert into the cell membrane at dense bands.

VSMCs contain poor developed smooth endoplasmic reticulum (ER), which has releasable store of $Ca^{2+}$ ions that are not sufficient to cause contraction. Thus, an influx of extracellular $Ca^{2+}$ is also needed for normal contraction. Cell junctions in VSMCs are formed by the protein connexin and allow ionic currents to flow between cells, transmitting depolarization from cell to cell. Finally, caveolae are tiny invaginations that may be involved in calcium

transport and trafficking of membrane proteins to the cell surface (Levick J.R., 2010).

The physiological state of most arteries is a continuous and partial contraction called basal tone. There exist mechanisms to increase the vascular tone (vasoconstriction) or reduce it (vasodilatation).

Contraction is induced by agonists such as sympathetic nerves releasing noradrenaline (along with some ATP), circulating hormones (adrenaline, noradrenaline), local hormones or cell depolarization. Agonists cause a rise in cytosolic $Ca^{2+}$ concentration by opening voltage-dependent calcium channels (VDCCs) when the cell depolarizes (electromechanical coupling), by opening receptor-operated channels (ROCs) (pharmacomechanical coupling) in the sarcolemma, and by releasing the internal store via a second messenger. $Ca^{2+}$ release from the internal store is triggered by agonists of the G-protein-coupled receptors (GPCR) such as phenylephrine, angiotensin II or endothelin-1. These agonists stimulate phospholipase C (PLC) and generate $IP_3$ and diacylglycerol (DAG). $IP_3$ activates $IP_3$-$Ca^{2+}$ release channels located on the sarcoplasmic reticulum (SR), leading to $Ca^{2+}$ release and a transient increase in $[Ca^{2+}]_i$. This $Ca^{2+}$ increase, as well as DAG, induces depolarization, activating L-type voltage-dependent calcium channels. DAG is also responsible of ROC activation. Therefore, extracellular $Ca^{2+}$ influx through the activated VDCCs, and also through ROCs, raises the cytosolic $Ca^{2+}$ concentration (figure 1.2A).

When $Ca^{2+}$ rises, it forms a complex with calmodulin, which activates the myosin light chain kinase (MLCK). MLCK catalyses phosphorylation of

myosin heads by ATP, causing myosin-actin crossbridge formation and development of tension.

Relaxation consists on reducing the active tension in VSMCs. This is due to a decrease in cytosolic $Ca^{2+}$ concentration and MLCK activity; and an increased activity of the myosin light chain phosphatase (MLCP), which removes the phosphate group of myosin light chain. Thus, the formed crossbridges detach, leading to vasodilatation (Somlyo & Somlyo, 1994). Vasodilatation can be also induced by hyperpolarization, reducing the open probability of VDCCs and therefore, the cytosolic $Ca^{2+}$.

The fall in cytosolic $Ca^{2+}$ concentratrion is brought about by vasodilators, such as β-adrenergic agonists and Nitric oxide (NO), which activate cAMP and cGMP mechanisms, activating protein kinases A (PKA) and G (PKG). These kinases stimulate $Ca^{2+}$ $^{-}$ATPase pumps in the cell membrane and sarcoplasmic reticulum membrane to reduce free cytoplasmic $Ca^{2+}$ concentration (Levick J.R., 2010). PKA and PKG phosphorylate and thereby inhibit MLCK, as well as phosphorylate and activate $K^{+}$ channels, which results in hyperpolarization and the consequent VDCC closure (Cox, 2005) (figure 1.2B). Moreover, the release of $Ca^{2+}$ sparks from the ryanodine receptors (RyRs) in the SR membrane, raises the $Ca^{2+}$ concentration in the subsarcolemmal region, activating $Ca^{2+}$ dependent $K^{+}$ channels and leading to hyperpolarization (Nelson *et al.*, 1995).

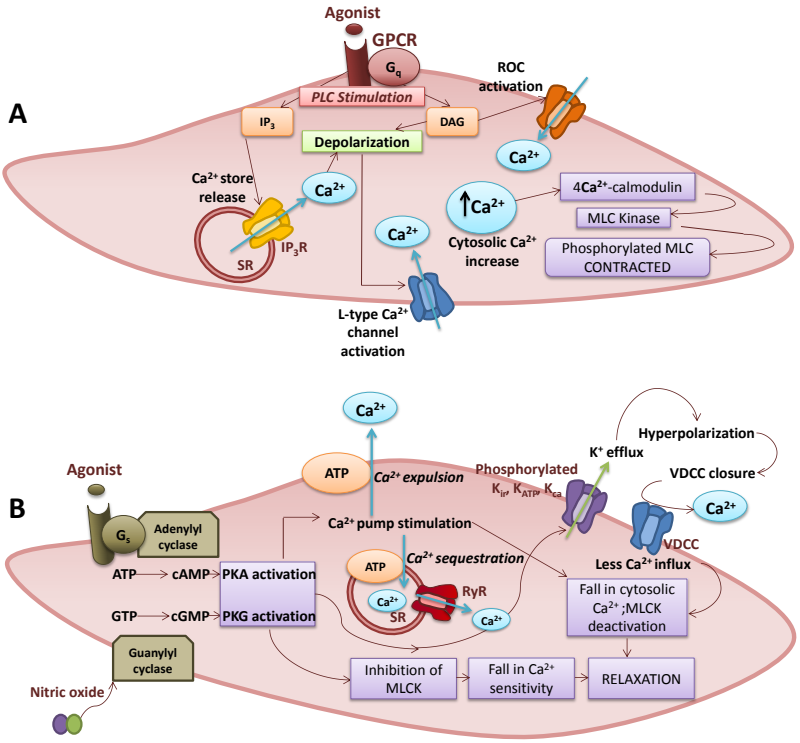


Figure 1.2. Pathways mediating vasoconstriction (A) and vasodilatation (B) in VSMC.

### 1.2.1. Phenotypic Modulation

VSMCs described so far are highly specialized cells whose principal function is contraction; they normally exist in a quiescent state and express proteins that are important for contractility, ion channels, and signaling molecules that allow these cells to regulate systemic blood pressure through the modulation of vascular tone. Unlike the majority of terminal differentiated cells, VSMCs retain remarkable plasticity and can undergo reversible changes in phenotype in response to changes in local environmental cues (Owens, 1998).

VSMCs can switch between a differentiated or contractile state and a dedifferentiated or synthetic phenotype. Differentiated smooth muscle phenotype is characterized by low rates of proliferation, migration, extracellular matrix synthesis and high levels of contractile gene expression that include smooth muscle α-actin (Gabbiani *et al.*, 1981), smooth muscle myosin heavy chain (Nagai *et al.*, 1989), calponin (Gimona *et al.*, 1992), SM-22α (Solway *et al.*, 1995), and h-caldesmon (Frid *et al.*, 1992). In contrast, dedifferentiated VSMCs show low expression of contractile genes and have increased rates of proliferation, migration, and production of extracellular matrix proteins.

VSMC phenotype modulation is critically important for the resolution of vascular injury. In the process of vascular tissue repair after an injury or mechanical stress of arteries, phenotypic switch provides VSMCs with the ability to rapidly fill or replace damage to the vessel. This plasticity is physiologically advantageous and once the injury is resolved, VSMCs return to a nonproliferative, contractile phenotype.

However, plasticity makes VSMCs very susceptible to both physiological and pathophysiological stimuli and can also turn disadvantageous. Deregulation of VSMC phenotype switching contributes to the development and progression of vascular pathologies. This deregulated process plays an important role in the progression of proliferative and obstructive vascular diseases, such as post-angioplasty restenosis or atherosclerosis, inducing VSMC migration from the tunica media to the intima and proliferation, which leads to neointima formation (Owens, 1995;Owens *et al.*, 2004;Thyberg, 1996;Shanahan & Weissberg, 1998).

Phenotypic modulation depends on the integration of several environmental cues and signaling pathways, which define the expression profile of the transcription factors, determining the VSMC phenotype. These signals comprise extracellular matrix interactions, injury, mechanical forces, cell-cell contact, cell adhesions, and various cytokines, such as platelet-derived growth factor (PDGF) (Owens *et al.*, 2004).

In particular, growth factor/cytokine signaling can dramatically affect the differentiation status of VSMCs. The transition from a contractile to a proliferative phenotype also occurs when VSMCs are established in culture in the presence of the mitogen PDGF (Blank & Owens, 1990). The activation of the PDGF receptor leads to the engagement of multiple downstream signaling cascades, activating phosphatidylinositol 3 kinase (PI3K), Ras-MAPK (mitogen activated protein kinase) and phosphor lipase C gamma (PLCγ) signaling pathways, and enhancing transcription of growth related proteins. Besides increasing the rate of proliferation and migration, PDGF reduces expression of contractile genes (Mack, 2011). In contrast, transforming growth factor-β (TGF-β) increases the expression of VSMC contractile genes and reduces VSMC proliferation and migration (ten Dijke & Arthur, 2007). Some vasoconstrictors, such as vasopressin (AVP), also promote increased contractility and induce hypertrophy (Higashita *et al.*, 1997) while others, such as endothelin-1, have been shown to stimulate VSMC proliferation (Komuro *et al.*, 1988).

### 1.2.2. Ion Channels in VSMCs

Phenotypic modulation depends on the ability of VSMCs to display different genetic profiles and readjust cellular activity in response to environmental factors. An intriguing aspect of modulation is switching to different ion transport systems. Coordinate changes in ion channels are an integral component of VSMC plasticity because they can redirect biochemical activity toward new functional responses (Neylon, 2002).

Ion channels are required for controlling basic parameters, such as cell volume and membrane potential ($V_M$). $V_M$ is the net result of the activity of a number of active and passive ion transport mechanisms in the cell membrane. The vascular smooth muscle sarcolemma has at least four types of $K^+$ conducting channels, four types of $Ca^{2+}$ conducting channels, and one type of $Cl^-$ conducting channel (Jackson, 2000). Among $Ca^{2+}$ conducting channels we found voltage-dependent calcium channels (VDCC) that are highly selective for $Ca^{2+}$ and TRP (Transient Receptor Potential) channels, that are $Ca^{2+}$ permeable non-selective cation-conducting channels with very diverse functions and modulation. VDCC, and in particular L-type $Ca^{2+}$ channels are the predominant $Ca^{2+}$ channels in contractile VSMC.

Potassium selective channels are the most diverse group of ion channels, encoded by at least 70 mammalian genes and expressed as more than 100 principal pore forming or principal subunits (α subunits) (Coetzee *et al.*, 1999). $K^+$ channels play a role in the regulation of arterial tone and in the control of cell proliferation. Moreover, changes in $K^+$ channels expression have been described in association with the phenotypic switch of VSMCs (Neylon *et al.*, 1999). $K^+$ channels are gated by different stimuli and have

different structures. Based on their structure and physiological activators and inhibitors, $K^+$ channels are classified into 4 subgroups: voltage gated ($K_V$), calcium activated ($K_{Ca}$), inward rectifier ($K_{IR}$), and two pore domain channels ($K_{2P}$). Nevertheless, Kv and high conductance $K_{Ca}$ ($BK_{Ca}$) channels are present in basically all vascular myocytes, and have an important role in modulating contractile responses (Nelson & Quayle, 1995) and in the regulation of the basal response (figure 1.3.).

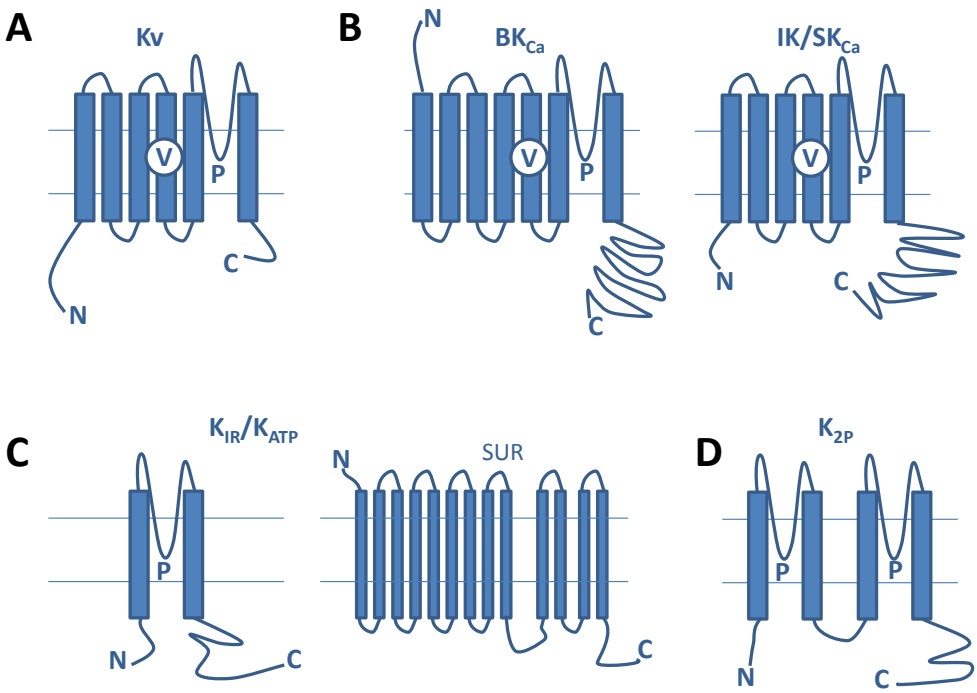


**Figure 1.3. Structure of $K^+$ channels. V: voltage sensor domain; P: pore region; N: N-terminus; C: C-terminus. A) voltage gated potassium channel ($K_V$). B) Large conductance (BKCa) and intermediate and small conductance ($IK/SK_{Ca}$) calcium activated potassium channel. C) Inward rectifier ($K_{IR}$). $K_{IR}$ subunits assemble with sulphonylurea receptors (SUR) to form $K_{ATP}$ (ATP sensitive) potassium channels. D) Two pore domain potassium channels ($K_{2P}$).**

- **Kv channels** activate in response to a depolarizing influence in membrane potential and their main function is to repolarize the $V_M$ to its resting values. They play a key role in regulating contraction of VSMCs through their effects on $V_M$ and on VDCC activity (Cox, 2005). These channels are tetrameric structures consisting of four pore-forming α subunits. Each α subunit is formed by 6 transmembrane and 1 pore domains, **6TM1P**. Kv channels will be further described in greater detail.

- **$K_{ca}$ channels** are activated by elevations in intracellular $Ca^{2+}$, by depolarization or by vasodilators that increase intracellular levels of cAMP or cGMP (Ledoux *et al.*, 2006). The activation of these channels prevent excessive $Ca^{2+}$ entry and promote muscle relaxation. They are classified by their relative conductances into large (BK, $BK_{Ca}$, hSlo or MaxiK channels), intermediate (IK) and small (SK) conductance subfamilies. Excluding $BK_{Ca}$ channels, all $K_{ca}$ channels are formed by 6 transmembrane and 1 pore domains, **6TM1P** α subunits. However $BK_{Ca}$ have an additional T0 transmembrane domain, **7TM1P**, which determines an extracellular topology for N-terminus (Wallner *et al.*, 1996).

### 1.2.3. Ion Channels Involved in the Phenotypic Modulation of VSMCs

The expression of ion channels in the contractile phenotype, for example L-type $Ca^{2+}$ channels, is particularly important for $Ca^{2+}$ entry to activate contraction and regulate the expression of contractile genes (Wamhoff *et al.*, 2006;Gollasch *et al.*, 1998). However, the role of ion channels in the proliferative phenotype is beginning to be appreciated.

Ion channels expressed in contractile VSMCs, which regulate the contractile machinery, are less relevant in the proliferative phenotype and are consequently downregulated. Initial events in the phenotypic switch include a significant loss of $BK_{Ca}$ and L-type $Ca^{2+}$ channels, and gain of the intermediate conductance $K_{ca}$ channels. IK channels enable membrane hyperpolarization, which increases store- and receptor- operated calcium entry through TRPC (transient receptor potential canonical) channels (Kohler *et al.*, 2003;Neylon, 2002). While in the contractile phenotype $Ca^{2+}$ is required mainly for contraction, in the proliferative phenotype it is required to activate proliferation and migration (Beech, 2007).

The expression profile of Kv channels is also altered during the transition of VSMCs from the contractile to the proliferating phenotype. In previous work from our group and in order to elucidate phenotypic modulation-associated changes, the expression pattern of ion channels in VSMCs was studied. A quantitative high-throughput real-time PCR of 87 ion channel genes was performed in mouse femoral artery contractile VSMCs; and two proliferative models: an *in vivo* model of neointimal hyperplasia induced by endoluminal lesion, and an *in vitro* model using cultured VSMCs from arterial explants. The characterization of the changes in expression pattern from the two proliferative models upon phenotypic switch showed a good correlation between both situations. Only two genes, Kv1.3 and its auxiliary subunit Kvβ2.1, showed a concordant upregulation in both models (figure 1.4.). Moreover, Kv1.3 increase paralleled an enormous decrease of Kv1.5, the dominant Kv1 channel in the contractile state. Kv1.3 and Kv1.5 mRNA expression levels correlate with the relative functional expression of channel proteins. Electrophysiological studies in cultured VSMCs and VSMCs from

injured arteries showed an increased functional expression of Kv1.3 currents, and pharmacological (PAP-1 or margatoxin) or genetic Kv1.3 blockade inhibited cultured VSMC migration and proliferation (Cidad *et al.*, 2010). Additionally, the effect of diphenyl phosphine oxide-1 (DPO-1), a selective Kv1.5 blocker, inhibited Kv1.5 currents in freshly dissociated VSMCs from femoral and mesentery arteries (figure 1.5A). The analysis of other vascular beds, such as mesenteric and aorta arteries, confirmed that Kv1.3 upregulation and Kv1.5 downregulation associate with phenotypic switch (Cidad *et al.*, 2012) (figure 1.5B).

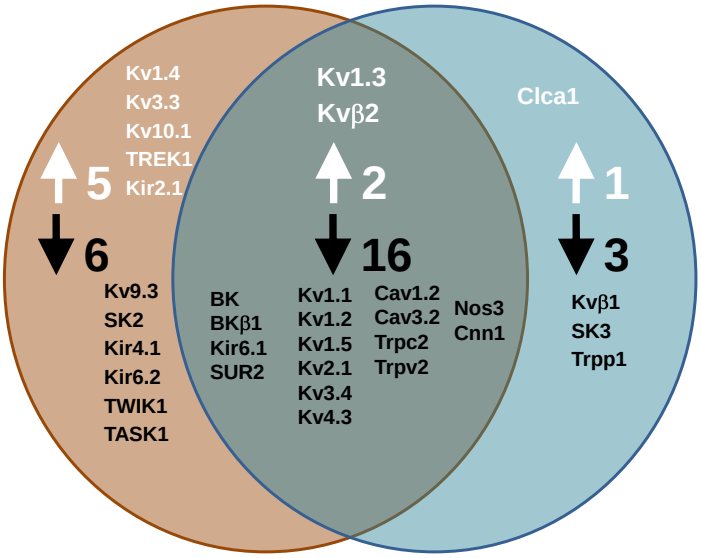


**Figure 1.4. Previous results of our group in two proliferative models of mouse VSMCs. The brown sphere shows expression changes *in vitro*, whilst the blue sphere represents changes *in vivo*. The intersection shows those changes that are common to both models.**

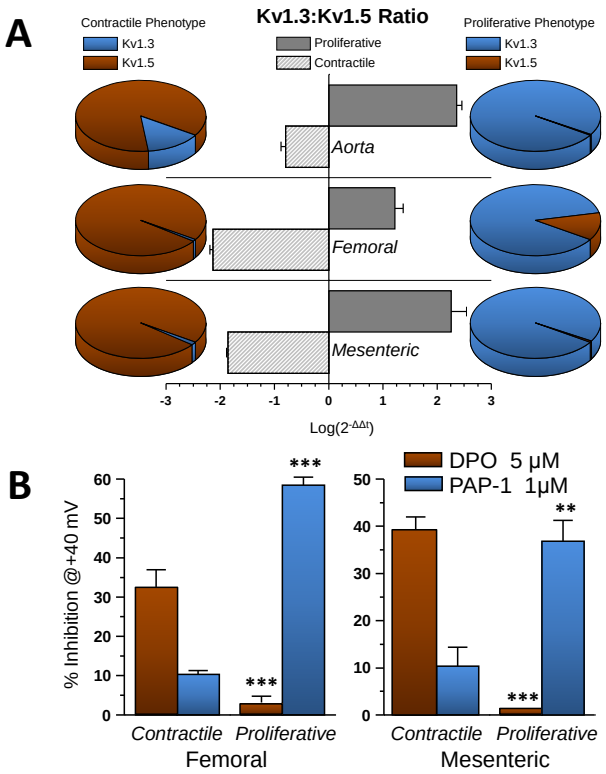


**Figure 1.5. A) Relative abundance of Kv1.3 and Kv1.5 in 3 different vascular beds in both contractile and proliferative phenotypes. The bars plot shows the Kv1.3:Kv1.5 ratio expressed as log (2–ΔΔCt), where ΔΔCt was ΔCtKv1.3–ΔCtKv1.5. A value of 0 indicates a Kv1.3:Kv1.5 ratio of 1, a value of –2 denotes Kv1.5 expression levels 100 times higher than Kv1.3, and a value of +2 Kv1.3 expression levels 100 times higher than Kv1.5. B) Averaged data showing the fraction of the total Kv current represented by Kv1.5 currents (DPO sensitive) and Kv1.3 currents (PAP-1 sensitive) in contractile vs proliferative VSMC from femoral and mesenteric arteries. (Cidad *et al.*, 2012).**

Downregulation of several Kv1 genes (Kv1.5, Kv1.2) has been reported in other preparations (Miguel-Velado *et al.*, 2005;Yuan *et al.*, 1998b;Yuan *et al.*, 1998a). However, the expression profile of ion channels and the phenotypic modulation-induced changes can be vascular bed specific. Although there are several other ion channels, such as TRPC1 (Kumar *et al.*, 2006), T-type calcium channels (Rodman *et al.*, 2005), Kv3.4 channels (Miguel-Velado *et al.*, 2005;Miguel-Velado *et al.*, 2010), and IK1 channels

(Kohler *et al.*, 2003), whose expression and/or function has been linked to VSMC proliferation, the information regarding conservation across different vascular beds and/or species is missed for most of these candidates. Therefore, our finding of Kv1.3 upregulation and Kv1.5 downregulation conserved across different vascular beds may constitute a landmark of phenotypic modulation in VSMCs.

The relevant role of Kv1.3 channels in VSMC proliferation, as well as the changes in Kv1.3 and Kv1.5 mRNA expression upon phenotypic modulation, have been confirmed by our group in four human vascular beds: renal, coronary and uterine arteries, and saphenous veins (Cidad *et al.*, 2014) (figure 1.6.). Our data also indicated that Kv1.3 mRNA expression is constitutive and, on the contrary to IK channels, is not regulated by pro-proliferative signals. Moreover, the changes in Kv1.3/Kv1.5 ratio were shown to be an early event in the process of dedifferentiation, since they were detected before manifest VSMC proliferation. This observation suggested that the changes in Kv channel expression upon phenotypic switch could be a needed and relevant event to facilitate proliferation.

The fact that a pro-proliferative role of Kv1.3 channels was described in VSMCs from several human vessels could reflect an obligatory association of Kv1.3 channels with vascular remodeling, increasing its value as a new therapeutical target. However, further research is needed to elucidate the still unknown molecular mechanisms underlying Kv1.3-induced proliferation, and the main aim of this thesis is to identify them.

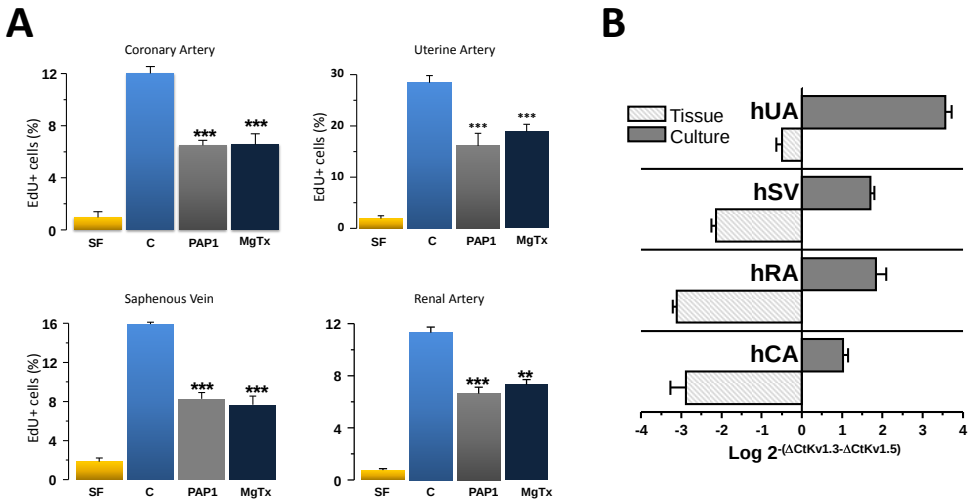


**Figure 1.6. Previous data from our group showing A) Proliferation rate (EdU incorporation) of coronary (hCA), uterine (hUA) and renal (hRA) arteries and saphenous vein (hSV) from human VSMCs. After a 48 h incubation in serum-free (SF) media, cells were kept during 30 h in SF or in the presence of 5 % FBS alone or in combination with 10 nM MgTx (MgTx) or 100 nM PAP-1 (PAP-1). B) Kv1.3:Kv1.5 ratio in the four human vascular beds, both in contractile (striped bars) and proliferative (gray bars) phenotype (Cidad *et al.*, 2014).**

## 1.3. Voltage-gated potassium channels

Kv channels are found in a wide variety of excitable and nonexcitable cells including neurons, lymphocytes, cardiac cells and VSMCs. In nonexcitable cells, their function as feedback regulators of resting $V_M$ has been proposed to participate in many cellular functions ranging from secretion to cell migration, proliferation, and apoptotic death. Functional considerations of all Kv channels include $K^+$ selectivity and the ability to sense and respond to voltage changes across the membrane.

The first cloned potassium channel gene was the *Drosophila* voltage-gated *shaker* channel (mammalian Kv1 subfamily), which was isolated on the

basis of flies' shaking leg response to ether anesthesia (Papazian *et al.*, 1991). This was followed by the identification of other voltage- and ligand-gated potassium channel genes in mammals and many other organisms.

Kv channels are tetrameric structures consisting of four identical or closely related pore-forming Kv alpha subunits (Kvα), which comprise six membrane spanning domains (6TM1P), including the positively charged S4 segment and the ion conduction pathway. Each Kvα subunit may associate with a cytoplasmic modulatory Kvβ subunit, which influences the characteristics of the channel (Bahring *et al.*, 2001). Kvα subunits are grouped into several subfamilies (Kv1-12). However, most of the cloned genes for the alpha-subunits are classified into four subfamilies: Kv1 (Shaker), Kv2 (Shab), Kv3 (Shaw), and Kv4 (Shal).

Kv channel genes can give rise to large number of functional Kv currents via heteromultimerization, association with accessory subunits, alternative splicing, and posttranslational modifications (Coetzee *et al.*, 1999).

### 1.3.1. Structure of Kv channels

Kv channels can functionally exist in three main conformations: open, inactivated and closed (figure 1.7.). The open conformation is a conducting state and it takes places when both the inactivation gates and pore are open. However, in the inactivated and closed states, ion flow is prevented. Some Kv channels, such as Kv1.3 and Kv1.5, preferably undergo inactivation from pre-open states (Hoshi *et al.*, 1990;Zagotta *et al.*, 1990;Kurata *et al.*, 2005), which means that at depolarized membrane

potentials inactivation is couple to channel opening. However, other Kv channels, such as Kv2 and Kv4, preferably inactivate from closed-states, inactivating before opening (Beck & Covarrubias, 2001;Klemic *et al.*, 1998). The three states define channel kinetics, which can be studied by measuring the time constant of activation, deactivation, inactivation and deinactivation. Thus, channel kinetics provide us knowledge of how quickly the channel opens after membrane depolarization (time constant of activation), the rate of channel closure once the voltage stimulus is removed (time constant of deactivation), the rate of channel inactivation (time constant of inactivation) and the rate of channel deinactivation (time constant of deinactivation).

As indicated previously, functional Kv channels are composed of four Kvα subunits that form either homo- or heterotretrameric complexes within the same subfamily members. Each Kvα pore-forming subunit has six transmembrane domains (S1-S6), voltage sensing residues in S4 and two intracellular domains, N- and C-terminus of variable length and composition (Long *et al.*, 2005a).

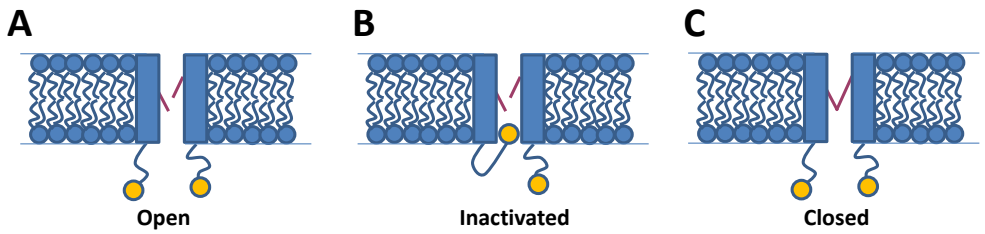


**Figure 1.7. Representation of the three conformations of a Kv channel. Blue boxes represent the transmembrane domains, yellow spheres are the inactivation domains, and red lines represents the pore. A) Kv channel in open state, both the inactivation domains and the pore allow a conducting conformation. B) Kv channel in an inactivated state (N-type inactivation), the inactivation gates occlude the pore preventing conductance. C) Kv channel in a closed state, the pore gate prevents ion flux.**

### 1.3.2. Pore and Selectivity Filter of Kv channels

Once the four Kvα subunits have tetramerized, a highly selective aqueous pore is formed. The central pore is lined by four H5 regions or P regions (pore loops) interconnecting segments S5 and S6 of each subunit (Hartmann *et al.*, 1991), thus subunits are oriented such they allow the four S5-P-S6 regions to face each other forming the central pore (Snyders, 1999b). A large portion of the pore loop is located near the extracellular face of the channel and only a short part extends into the membrane to form the selectivity filter (MacKinnon, 1995) (figure 1.8.).

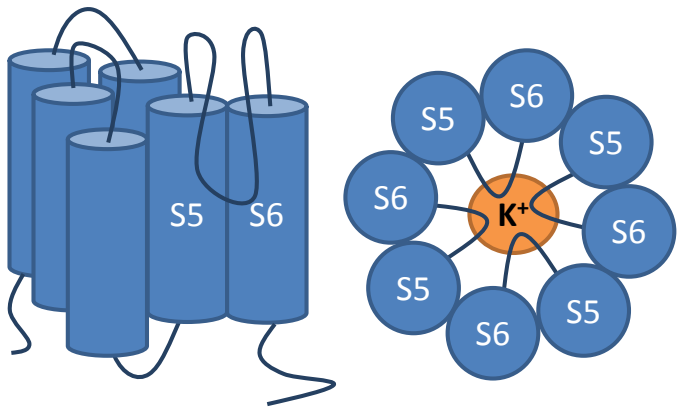


Figure 1. 8. S5-P-S6 regions forming the central pore of a Kv channel. Adapted from (Pardo & Stuhmer, 2014).

The selectivity filter is the narrowest region of the pore and interacts with the permeating ions to ensure ions passing through the channel selectively. It possesses a highly conserved "signature" sequence of amino acid residues, TVGYG, which is necessary for $K^+$ selectivity (Doyle *et al.*, 1998). In particular, mutations in the glycine – tyrosine – glycine (GYG) motif, which is

also conserved in the P- regions of other potassium-selective channels, can alter channel ion-conduction properties (Heginbotham *et al.*, 1994).

Crystallographic studies of KcsA, a baterial $K^+$ channel from *Streptomyces lividan,* provided the first insights into the molecular basis of $K^+$ selectivity and conduction. The affinity of a channel for a given ion depends on the combination of two properties: ionic radius and ion's solvation energy in water.

$K^+$ channel mediates the transfer of a $K^+$ ion from its hydrated state in solution to its dehydrated state in the selectivity filter. The selectivity filter itself consists of four layers each containing rings of four negatively-charged oxygen atoms from the peptide backbone carbonyl groups. The channel recruits $K^+$ ions and eight oxygen atoms surround each ion within the selectivity filter, resembling the arrangement of water oxygen atoms around $K^+$ in the cavity (Zhou *et al.*, 2001) (figure 1.9.). The pore favors dehydrated $K^+$ to dehydrated $Na^+$ ions at a radio 1000:1, since $Na^+$ ions are too small to bind oxygen atoms and their dehydration is not thermodynamically favorable (Heginbotham, 1999).

Conduction gate also regulates selectivity. In absence of $K^+$ and the presence of $Na^+$, the filter adapts a nonconductive state. The binding of dehydrated $K^+$ ions to the selectivity filter is the trigger to induce a conformational change, allowing the channel to adopt a conductive state (Valiyaveetil *et al.*, 2006).

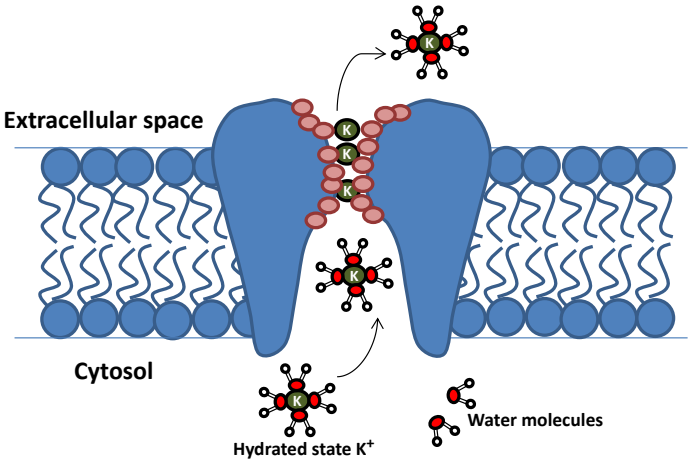


Figure 1.9. Schematic representation of the mechanism of $K^+$ ions (green circles) selectivity and transport in a Kv channel. Hydrated K+ ions are in the water-filled cavity of the channel. Eight carbonyl oxygen atoms (pink circles) mimic the waters of hydration allowing K+ ions to pass through the selectivity filter across the lipid bilayer.

### 1.3.3. Voltage Sensor of Kv channels

Kv channels sense changes in the $V_M$ through the voltage-sensing domain, which is formed by the S1–S4 segments (Seoh *et al.*, 1996). The S4 segment is the main transmembrane voltage-sensing component. It has positively charged amino acids, either arginine or lysine, at every third position, separated by hydrophobic and neutral residues that detect positive electric field. Voltage sensors also have a role in applying positive work to open the pore, which is more stable in its closed than open state (Yifrach & MacKinnon, 2002). Depolarization induces a physical S4 movement that causes a conformational change, opening the channel and allowing $K^+$ permeation (Snyders, 1999c).

The steep voltage dependence of Kv channels is a result of the sensor region moving a large amount of charge across the field. S4 charges move

within the membrane inducing charges in the external and internal solution to move proportionally. Thus, a detectable capacitative current or gating current is generated, which correlates with the opening of the channel. The movement of the gating charge is an electrical marker of conformational changes within the channel, being a useful measurement of intramolecular changes (Bezanilla *et al.*, 1982) (Bezanilla, 2008). Thus, point mutations in which some particular S4 charges have been neutralized are sufficient to modify the voltage-dependence of the gating charge and the conductance (Aggarwal & MacKinnon, 1996;Lecar *et al.*, 2003).

Although it is known that the movement of S4 underlies the coupling between voltage sensing and channel opening, the mechanism has not been fully established. However, several residues of the S6 segment, which are buried in the closed state of the channel, become accessible with depolarization. These data suggest that the pore-lining segment also contributes to the activation gate (Choi *et al.*, 1993;Snyders, 1999a).

### 1.3.4. Inactivation Domains of Kv channels

Inactivation is a process by which an open channel enters a stable non-conducting state after a maintained depolarizing change in membrane potential, thus allowing for cell repolarization. At least two types of inactivation have been identified: N- and C- type, which are associated with different molecular domains. Some Kv channels such as Kv1.4 have fast inactivating currents (A-type currents), which are defined by N-type inactivation. However, other channels such as the delayed rectifier Kv1.3 or Kv1.5 have slowly inactivating or noninactivating currents.

Fast inactivation of Kv channels is voltage-independent, coupled to activation, and involves the intracellular N-terminal region of the channel protein. N-type inactivation can occur as rapidly as a few milliseconds and has been shown to involve a “ball and chain” mechanism, in which an inactivation peptide within the the N-terminus acts as a tethered inactivation particle, binding a receptor site in the pore and occluding it (Hoshi *et al.*, 1990) (figure 1.10.). The inactivation peptide is located at the extreme N-terminus of the channel and through a flexible linker is connected to the rest of the N-terminal domain. Interestingly, Kvβ subunits also play significant roles in modulating N-type inactivation by a similar N-terminal inactivation particle (Rettig *et al.*, 1994).

Removal of this region or point mutations near the N-terminus abolish or slow fast inactivation. Furthermore, the presence or addition of the inactivating “ball” peptide, which is modular in the same way as Kv voltage sensor and pore domains, is sufficient to confer rapid inactivation to channels that do not have endogenous N-type inactivation (Zagotta *et al.*, 1990).

Like N-type inactivation, C-type inactivation is coupled to activation and is voltage independent between -25 and +50 mV. Although C-type inactivation may be studied in the absence of N-type inactivation, it is in fact partially coupled to it and occurs faster from the N-type inactivated state (Hoshi *et al.*, 1991;Baukrowitz & Yellen, 1995).

Despite there exist more than one type of slow inactivation, the mechanisms and domains involved are not so well defined as those of N-type inactivation. C-type inactivation was first described in the Kv1.3 channel as slow

inactivation. This type of inactivation seems to occur by a collection of conformational changes or behaviors instead of displaying the characteristic ball and chain mechanism of N-type inactivation (figure 1.10.). Whereas N-type inactivation involves a cytoplasmic domain of the channel, C-type inactivation is not affected by deletions or mutations in the C-terminal cytoplasmic domain and is instead dramatically altered by a single valine residue change in the transmembrane segment S6 (Hoshi *et al.*, 1991).

C-type inactivation involves a constriction of the outer mouth of the channel, blocking the ion conduction pathway. This rate of inactivation is quite sensitive to permeant ions, and that sensitivity is also disrupted by mutations in the pore region, which alter the interaction of all 4 channel subunits (Ogielska *et al.*, 1995).

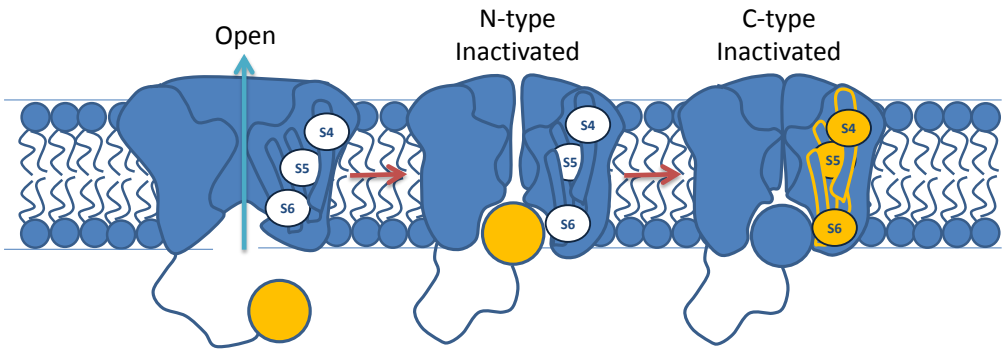


**Figure 1.10. N-type inactivation generally follows activation and involves a cytoplasmic gate on the N-terminal domain of the channel subunit (ball and chain mechanism). The gate or ball occludes the pore and interacts with a receptor that is likely to reside in the S4-S5 loop and vestibule. C-type inactivation can occur from the open state or from the N-type inactivated state. This mechanism involves closure of the extracellular mouth of the channel. Some transmembrane domains or residues are associated with development of the C-type inactivated state: residues in the intracellular mouth of the pore, pore loop, extracellular and intracellular ends of S6 and in the S4 region have been identified to play a role in C-type inactivation. Adapted from (Rasmusson *et al.*, 1998).**

The difference in the regions of the channel taking part in the inactivation conformational changes has also been shown by pharmacological studies, in which external TEA (Tetraethylammonium) competes with C-type inactivation but has no effect on N-type inactivation (Choi *et al.*, 1991).

Some other regions of Kv channels are also involved in inactivation. S4 and the pore domain display a movement and interact during the transitions of voltage sensing and the subsequent closure of the channel's slow inactivation gate. This interaction between S4 and the pore domain represents a substrate for directly coupling voltage sensing to the operation of a channel gate (Gandhi *et al.*, 2000). Moreover, it has been described that S5-P-S6 loop collaborates to open a slow inactivation gate (Larsson & Elinder, 2000). Therefore, in addition to the N-terminal domain, the S4-S5-P-S6 domains also play a role in Kv channel inactivation.

### 1.3.5. T1 domain of Kv channels

The functional heterogeneity of $K^+$ channels in eukaryotic cells comes not only from the multiple $K^+$ channel genes but also from the mixing of different $K^+$ channel polypeptides to form heteromultimeric channels (Xu *et al.*, 1995).

Formation of a functional Kv channel requires the assembly of four Kvα subunits with or without four associated cytoplasmic β-subunit polypeptides (Pongs, 1995). Thus, the number of structurally and functionally Kv channels that could be generated by the combination between Kvα and Kvβ subunits would be very large if there were no restrictions to determine Kv assembly.

One structural element that determines the compatibility of different $K^+$ channel polypeptides in subunit assembly is the cytosolic N-terminal tetramerization domain, also called T1 domain.

T1 is a highly conserved domain involved in Kvα subunit assembly for the Kv1 to the Kv4 subfamilies (Shen *et al.*, 1993). Although T1 is conserved among Kv subfamilies, it confers specificity by limiting Kvα subunit association within a single subfamily (Li *et al.*, 1992) (Shen & Pfaffinger, 1995). T1 encodes molecular determinants for subfamily-specific assembly of α-subunits, in particular a $Zn^{2+}$ binding motif, which is highly conserved among all Kv2, Kv3 and Kv4 subfamily members, but is not found in Kv1 subfamily members (Bixby *et al.*, 1999). This sequence controls the ability of a $K^+$ channel subunit protein to recognize and assemble with another subunit protein.

Kv1.3 channel assembly involves the T1 domain. Nevertheless, multiple interactions between sites in the central core (S1 through S6-COOH) have also been described to play a key role in Kv1.3 assembly. Indeed, these sites seemed to be sufficient for correct assembly of functional Kv1.3 channels in a mutant Kv1.3 that lacked T1 domain (Tu *et al.*, 1996).

Despite the wildest recognized role of the T1 domain in tetramerization, this domain has also been enrolled in channel activity, gating and subcellular localization.

Kv1 channels tetramerize cotranslationally in the ER (Lu *et al.*, 2001), given the fact that T1 start acquiring its secondary structure in the ribosomal tunnel (Kosolapov *et al.*, 2004). In the assembled channels, the T1 domain is close

to the cytoplasmic opening of the pore and attached to S1 through a flexible linker T1-S1 (Long *et al.*, 2005b). Due to its proximity to the pore, alterations in T1 structure can affect pore function (Fan *et al.*, 2012).

Moreover, T1 can interact with proteins, apart from Kvβ subunits, that modulate channel activity by affecting $K^+$ currents. For instance, Kv1.2 channel is modulated by a small GTPase and tyrosine phosphatase that physically interact with its N-terminal T1 domain (Cachero *et al.*, 1998;Tsai *et al.*, 1999).

Some regions of Kv channels, such as the C-terminus of Kv1.2 channels (Yang *et al.*, 2007) or the pore region in Kv1.1 and Kv1.4 channels (Zhu *et al.*, 2001a) can modulate cell surface expression. However, among the regions influencing subcellular localization in Kv channels, T1 is considered one of the main determinants, being able to interact with modulatory proteins that affect cell surface expression.

Kv subunit composition and stoichiometry determine the activity and pharmacology of Kv1 channel and also affect surface expression and membrane localization (Manganas & Trimmer, 2000;Zhu *et al.*, 2003a). For instance, Kv1.3 forms heterotetrameric structures with Kv1.5, and these heterotetramers exhibit different location and targeting than the wild type channels. Whilst Kv1.3 has good surface expression, Kv1.5 shows less membrane localization, being retained in ER (Eldstrom *et al.*, 2002). In fact, increasing concentrations of Kv1.5 impair Kv1.3 surface expression and modulate Kv activity. Thus, different expression of Kv1.3 and Kv1.5 changes the number of channels at the surface, modifying the membrane excitability and signaling (Vicente *et al.*, 2008).

In short, T1 domain plays a role in subcellular localization by adding stability to the formed ion channels, by mediating interactions among α-subunits, and by providing a linkage site for the interactions with modulatory auxiliary proteins.

### 1.3.6. Kvβ subunits

Kvβ subunits are 38-41-kDa cytoplasmic proteins associated to Kv channels. (Scott *et al.*, 1994;Parcej & Dolly, 1989;Parcej *et al.*, 1992). There are four known Kvβ subfamilies: Kvβ1, β2, β3 and β4.

Kvβ subunits associate with the T1 domain of Kvα subunits in a 1:1 ratio (Yu *et al.*, 1996). More than one type of Kvβ subunit can be found in the same Kv channel complex (Rhodes *et al.*, 1996).

In the same way as Kvα-Kvα associations, Kvα and Kvβ coassembly is also subfamily specific. For instance, Kvβ subunits, with the exception of Kvβ4, interact with members of the *Shaker* (Kv1) subfamily. Moreover, Kvβ1 and Kvβ2 do not associate with members of Kv2 or Kv3 (Sewing *et al.*, 1996;Yu *et al.*, 1996;Rhodes *et al.*, 1995;Rhodes *et al.*, 1996;Rhodes *et al.*, 1997;Nakahira *et al.*, 1996;Bekele-Arcuri *et al.*, 1996;Fink *et al.*, 1996;Pérez-García *et al.*, 1999).

Kvβ subunits can modulate the rate of inactivation of Kvα subunits (Rettig *et al.*, 1994;Heinemann *et al.*, 1995;McCormack *et al.*, 1995;Morales *et al.*, 1995). One of the effects of these subunits is inducing fast inactivation on slowly or non-inactivating channels through an N-terminal peptide that

blocks the pore in a similar way as the “ball and chain” mechanism from Kvα subunits (Heinemann *et al.*, 1995).

Kvβ subunits can modify Kv channel electrophysiological properties, such as conductance and open gating. However, even within the same Kvα subfamily, some Kvβ subunits can have specific effects. In fact, the N- and C- terminal domains of Kvβ subunits can affect Kvα channel properties differently (Accili *et al.*, 1997;Accili *et al.*, 1998).

The association of these subunits starts in the ER without affecting Kvα maduration (Nagaya & Papazian, 1997). As a result, Kvβ subunits exert chaperone-like effects on channel biosynthesis, promoting N-glycosylation, and increasing stability and surface expression of Kvα channels (Shi *et al.*, 1996;Campomanes *et al.*, 2002).

### 1.3.7. Post-translational modifications of Kv1 channels

The activity of Kv channels is directly controlled by membrane potential, pH, redox potential, and binding of ligands. However, it can also be modulated indirectly by signal transduction pathways that lead to modifications of Kv channel intracellular domains, either through non-covalent binding of intracellular second messengers or interacting proteins, or through covalent posttranslational modifications mediated by different cytoplasmic modifying enzymes (Levitan, 1994a;Cerda & Trimmer, 2010).

#### *Palmitoylation*

Protein palmitoylation is a reversible posttranslational lipid modification in which a palmitic acid is added to the chain of cysteine residues on proteins,

forming a thioester linkage. This modification is found almost exclusively on membrane proteins, and is a regulatory mechanism to mediate subcellular trafficking of proteins and cell signaling or protein-membrane interaction (Jindal *et al.*, 2008;Mitchell *et al.*, 2006;Mitchell *et al.*, 2006).

Palmitoylation has been reported in several Kv1 channel family members. A consensus sequence for palmitoylation in the cytosolic portion of the S2-S3 linker domain (ACPSKT) has been identified. (Gubitosi-Klug *et al.*, 2005).

### *Glycosylation*

Glycosylation is a common posttranslational modification of membrane proteins that can affect their protein folding, stability, trafficking, localization and functional properties. In the Kv1 channel subfamily, Kv1.1-Kv1.5 members have a N-glycosylation consensus site located in a similar relative position of the extracellular S1-S2 linker (Stuhmer *et al.*, 1989). The relative position of N-glycosylation consensus sites on these linkers may be correlated with the functional effect of N-glycans on some Kv1 potassium channels (Zhu *et al.*, 2003b;Zhu *et al.*, 2012).

Kv1 channels are N-glycosylated in the endoplasmic reticulum when a N-glycan precursor is attached to the asparagines of the N-glycosylation consensus sequence in the S1-S2 linker. The N-glycans are further trimmed and modified into their mature form when passing through the Golgi apparatus before being transported to the cell surface.

Glycosylation can play a key role in the proper folding, targeting and function of Kv1 channels, being able to modify their expression and function. However, the effect of N-glycosylation on surface expression varies between

different glycoproteins even within the Kv1 subfamily. Removal of the N-glycosylation consensus site has little effect on Kv1.1 protein levels, but it considerably reduces surface protein levels of Kv1.2, Kv1.3 and Kv1.4 (Watanabe *et al.*, 2007;Watanabe *et al.*, 2004;Zhu *et al.*, 2012). N-glycosylation also promotes Kv1.5 cell surface expression (Burg *et al.*, 2010a) and modulate its gating properties (Schwetz *et al.*, 2010). The differential effect of N-glycosylation on closely related Kv channels is due to the complexity of the N-glycan structures.

### *Phosphorylation*

Protein phosphorylation is the most common covalent posttranslational modification in signal transduction. Phosphorylation is a reversible and dynamic process involving integrated networks and coordinated actions of protein kinases (PKs) and protein phosphatases (PPs) (Hunter, 1998). It can affect virtually all cellular processes including growth, cell cycle control, differentiation, cell signaling, motility, gene transcription and insulin action. Phosphorylation consists of the transfer of the terminal γ-phosphate group of ATP ($\gamma$-$PO_3^{2-}$) to the hydroxyl group (-OH) on the side chains of serine, threonine or tyrosine residues of target proteins in a motif dependent context. This phosphoryl transfer reaction is enzymatically mediated by PKs, whilst the enzymatic hydrolytic removal of phosphate from proteins is mediated by PPs.

A wide variety of Kv channels are targets of covalent modification by several PKs and PPs, whose activity is regulated by diverse signaling pathways and can result in dynamic and reversible changes in Kv channel expression,

localization, and function (Park *et al.*, 2008). Nevertheless, different Kv channels can exhibit distinct sensitivities to modulation by phosphorylation.

Many putative phosphorylation sites are found in the N- and C-terminal domains of Kv channels, although it is the C-terminal domain the target of most of the known phosphorylation-dependent modulatory events. Phosphorylation sites are substrates for tyrosine, serine or threonine kinases, and their location determines how and when the properties of the channel are modulated (Jonas & Kaczmarek, 1996).

Phosphorylation can dynamically modulate the biophysical properties of Kv channels. For example, Mammalian Shaker subfamily channels (Kv1.1-Kv1.7) have a consensus site for phosphorylation by PKA on the C-terminal domain, located in close proximity to the S6 segment. Serine/threonine phosphorylation by PKA in some of these channels, such as Kv1.1, can alter inactivation kinetics, levels of channel protein at the plasma membrane and potassium current amplitude (Levin *et al.*, 1995;Drain *et al.*, 1994).

Besides the modulation and phosphorylation of Kv1 channels by serine and threonine protein kinases (Cai & Douglass, 1993), Kv1 channels are also a target for tyrosine phosphorylation. In particular, the heterologous coexpression of the nonreceptor tyrosine kinase v-src, or the epidermal growth factor receptor (EGFr) tyrosine kinase together with Kv1.3, increased channel phoshorylation. Additionally, a basal tyrosine phosphorylation of Kv1.3 was detected after treatment with pervanadate, a tyrosine phosphatase inhibitor, indicating that there are constitutively active tyrosine kinases that recognize and phosphorylate Kv1.3 (Holmes *et al.*, 1996).

Tyrosine phosphorylation of Kv1 channels has a variety of physiological effects on channels, including both potentiation and inhibition of channel activity. For instance, pervanadate-induced tyrosine phosphorylation of Kv1.3 decreased channel current in a heterologous system, while current was not altered in a tyrosine point mutant Kv1.3 channel (Y449F). Another finding demonstrated that insulin stimulation of insulin receptor kinase caused multiple phosphorylation of Kv1.3 at discreet tyrosine residues in the N- and C- terminal domains to induce current suppression of the channel (Fadool *et al.*, 2000). Similar results were obtained in tyrosine phosphorylated Kv1.2 channels, whose current was suppressed by the tyrosine kinase PYK2 and EGFr (Lev *et al.*, 1995); and Kv1.5, which was suppressed by Src-mediated tyrosine phosphorylation and growth factor receptor activation by increasing phospholipase C and PKC activity (Holmes *et al.*, 1996;Timpe & Fantl, 1994).

Once Kv1 channels tyrosine residues have been phosphorylated, they can serve as recognition sites for Src homology 2 domain (SH2) containing proteins. Moreover, Kv1 channels also contain proline-rich ligand sequences for protein-protein interactions with Src homology 3 (SH3) containing protein kinases (Holmes *et al.*, 1996). The recruitment of specific proteins containing SH2 domains initiates downstream signaling cascades that affect diverse cellular targets via both tyrosine and serine/threonine kinases. For example, the activation of EGFr and the insulin receptor tyrosine kinases induce activation of PLCγ, $PLA_2$, PI-3 kinase and the Ras/ MAPK signaling cascade (Bowlby *et al.*, 1997).

## 1.4. Voltage-Dependent $K^+$ Channels Kv1.3 and Kv1.5

Kv1.3 and Kv1.5 are voltage dependent $K^+$ channels from the *Shaker* Kv1 subfamily. Both channels are widely expressed throughout the body and are involved in a variety of physiological processes, proliferation, tissue differentiation and immune system physiology (Bielanska *et al.*, 2009;Felipe *et al.*, 2006;Bielanska *et al.*, 2010).

As described before, Kv1.5 to Kv1.3 switch on proliferation is conserved in VSMCs from several vascular beds, suggesting that the ratio Kv1.3:Kv1.5 is a representative parameter of the VSMC phenotype.

Kv1.3 and Kv1.5 are inhibited by 4-aminopyridine (4-AP), which is a general $K^+$ channel blocker (Grissmer et al., 1994). There is also another potent chemical inhibitor of both channels, 5-(4-phenylbutoxy) psoralen or Psora-4, which has a smaller effect on the rest of Kv isoforms (Vennekamp *et al.*, 2004).

**Kv1.3** channels were first cloned from brain tissue. Although they are ubiquitous in the body, they are highly expressed in lymphocytes and the olfactory bulb (Stuhmer *et al.*, 1989), and several studies have shown expression of Kv1.3 in both skeletal and smooth muscle (Swanson *et al.*, 1990;Villalonga *et al.*, 2008;Bielanska *et al.*, 2012b;Bielanska *et al.*, 2012a).

Kv1.3 currents display cumulative inactivation and a marked C-type inactivation. The single channel conductance of Kv1.3 is 13 pS, and the $V_{1/2}$ for activation is −35 mV (Comes *et al.*, 2013).

Two highly specific toxins have been proved to be effective for Kv1.3, Charybdotoxin and Margatoxin (MgTx) (Leonard *et al.*, 1992;Garcia-Calvo *et*

*al.*, 1993) as well as the anemone peptide ShK and their derivatives (Cahalan & Chandy, 1997) and the small molecule (Kd 2 nM) selective blocker 5-(4-phenoxybutoxy) psoralen (PAP-1) (Schmitz *et al.*, 2005).

**Kv1.5** channel was first isolated from the human ventricle (Tamkun *et al.*, 1991) and it is also ubiquitously expressed (Swanson *et al.*, 1990;Bielanska *et al.*, 2009;Bielanska *et al.*, 2010). This channel is expressed in the immune system, the kidney, skeletal and smooth muscle and, to a lower extent, the brain (Vicente *et al.*, 2003b;Vicente *et al.*, 2006;Villalonga *et al.*, 2007a;Villalonga *et al.*, 2008;Bielanska *et al.*, 2012b;Coma *et al.*, 2003).

The conductance of the Kv1.5 channel is 8 pS, and the $V_{1/2}$ for activation is approximately -14 mV. Contrary to Kv1.3, Kv1.5 inactivates very slowly ($\tau$ > 5 s) and lacks cumulative inactivation (Comes *et al.*, 2013).

Kv1.5 is highly insensitive to Kv1.3 blockers and has no known specific pharmacology. However, new chemicals such as S0100176 (Decher *et al.*, 2004) or diphenyl phosphine oxide-1 (DPO-1) have been discovered to potently inhibit Kv1.5 (Du *et al.*, 2010).

Kv1.3 and Kv1.5 channels are subject to modulation by Kvβ subunits. The heterologous expression of Kv1.3 and Kv1.5 with Kvβ subunits in mammalian cells, can modify the rate of $K^+$ current density (McCormack *et al.*, 1999) and inactivation (Sewing *et al.*, 1996), respectively. In fact, Kvβ2 subunit acts as a chaperone of Kv1.3, being able to accelerate the functional assembly of Kv1.3 channels and enhance Kv1.3 current levels (McCormack *et al.*, 1999).

Differences in Kv1.3 and Kv1.5 biophysical features may explain their distinct regulation in a number of cell types. Moreover, as previously stated, Kv1.5 and Kv1.3 subunits can form heteromeric channels. Depending on the stoichiometry of these heterotetramers, the new generated channels can display different pharmacological and biophysical properties and different activation of specific cellular responses (Vicente *et al.*, 2003a;Vicente *et al.*, 2006;Vicente *et al.*, 2008;Villalonga *et al.*, 2007a;Villalonga *et al.*, 2007b). The expression level of both subunits can influence the degree of cell proliferation, differentiation or activation.

## 1.5. Mechanisms involved in the pro-proliferative effect of Kv1.3

The contribution to migration and proliferation of Kv channels, including Kv10.1 (ether-à-go-go, EAG), Kv11.1 (HERG, human ether-à-go-go related gene) and Kv1.3, has been well documented in different cellular systems (Pardo, 2004;Wulff *et al.*, 2009). Association between Kv1.3 expression and cell proliferation has been postulated in many cell types, including several cancer cell lines, endothelial cells (Erdogan *et al.*, 2005), microglia (Kotecha & Schlichter, 1999), T-lymphocytes (Cahalan & Chandy, 2009), macrophages (Villalonga *et al.*, 2010), oligodendrocyte progenitors (Chittajallu *et al.*, 2002) and VSMCs (Cidad *et al.*, 2010), but the underlying mechanisms linking Kv1.3 upregulation to proliferation remain controversial.

Several mechanisms, which may not be mutually exclusive, can be controlled by Kv1.3 channels during cell proliferation. Some of these events are membrane potential, $Ca^{2+}$ signaling and cell volume (figure 1.11.).

During G1/S phase progression of cell cycle, cells undergo a transient hyperpolarization which involves channel activity (Wonderlin & Strobl, 1996). Nevertheless, it is well known that cancer cells are on average more depolarized than terminally differentiated cells (Wonderlin & Strobl, 1996;Pardo, 2004). Changes in membrane potential can affect $Ca^{2+}$ influx, which is crucial for cell proliferation, the driving force for $Na^{+}$-dependent nutrient transport and intracellular pH. However, if the only action of Kv channels was related to membrane potential variations, blockade of $K^{+}$ flux would need to induce depolarization of the cells to inhibit transient hyperpolarization and proliferation. Furthermore, induced depolarization should also be expected to inhibit proliferation, and Kv blockers should affect intracellular $Ca^{2+}$ levels (Pardo, 2004).

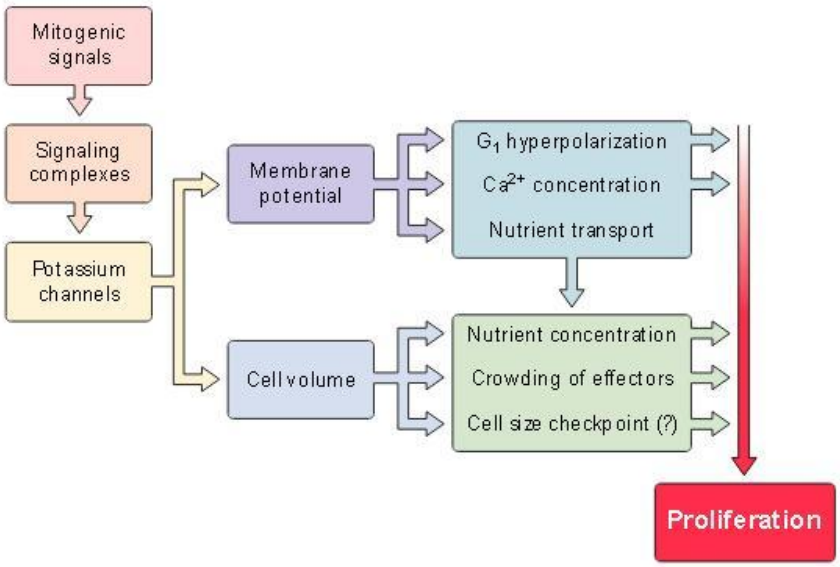


**Figure 1.11. The combination of effects related to changes in membrane potential and cell volume regulation are necessary for cell cycle progression and require the action of $K^{+}$ channels (Pardo, 2004).**

Kv channels can also be important for proliferation because they influence cell volume. Kv channels along with $Cl^-$ channels are necessary for regulatory volume changes. Proliferation is associated with volume increase along the $G_1$ phase of the cell cycle. Cell volume needs to be controlled so that crucial solutes, and cell cycle-regulating proteins themselves, maintain an appropriate concentration to support proliferation.

Both changes in membrane potential and cell volume are necessary for progression of the cell cycle and both require the action of Kv channels. However, there are several studies suggesting that Kv1.3 channels could also participate in the control of cell cycle through other mechanisms, including the dynamic interaction of Kv1.3 with integrin receptors (Levite *et al.*, 2000;Artym & Petty, 2002;Welschoff *et al.*, 2014), or the modulation of intracellular calcium that can determine the phosphorylation of several proliferation-related signaling processes (Hu *et al.*, 2012;Robbins *et al.*, 2005).

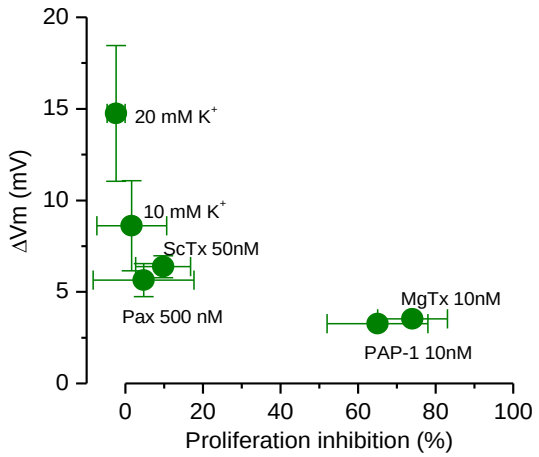


**Figure 1. 12. Previous data showing the effects of $K^+$ channel blockers or high $[K^+]e$ on resting $V_M$ (current-clamp experiments) and on proliferation inhibition (EdU incorporation). (Cidad *et al.*, 2010).**

In T-lymphocytes, genetic or pharmacological Kv1.3 blockade has an antiproliferative effect due to membrane depolarization and consequent reduced calcium entry (Cahalan & Chandy, 2009). However, this may not be the case in VSMCs, because even though Kv1.3 inhibition leads to VSMC depolarization, proliferation was not affected if depolarization was induced with other channel blockers or with high $[K^+]_e$ (Cidad *et al.*, 2010) (figure 1.12.) This intriguing observation suggests that the pro-proliferative effect of Kv1.3 upregulation may not be related to its role as a $K^+$ channel.

There are some studies indicating that the effects of $K^+$ channels on cell proliferation rely on non-conducting properties of the channel proteins. EAG channel cytoplasmic domains have a key role mediating cell proliferation, its N- and C- terminal domains have putative binding sites and domains that regulate protein kinase activity (Sun *et al.*, 2004). Moreover, the voltage-dependent gating of EAG channels is involved in controlling the MAPK signalling pathway and cell proliferation by a mechanism that is independent of $K^+$ flux through the channel (Hegle *et al.*, 2006). Another case related with non-conducting properties are IK1 channels, which are upregulated in proliferating VSMCs and whose blockade is well stablished to inhibit VSMC proliferation (Kohler *et al.*, 2003;Cheong *et al.*, 2005). It has been shown that IK1-induced proliferation occurs by a direct interaction with ERK1/2 and JNK (c-Jun N-terminal kinase) signaling pathways and independently of $K^+$ conductance, hyperpolarization and enhanced $Ca^{2+}$ entry (Millership *et al.*, 2011).

When exploring the effects of Kv1.3 blockers on the signaling pathways that mediated PDGF-induced proliferation in human VSCMs, Kv1.3 blockade did

not sum up the effect of IK1 blockade, suggesting that Kv1.3 and IK1 channels promote proliferation through a common signaling pathway. Kv1.3 blocker effects were occluded in the presence of PLCγ and MEK/ERK blockers (U73122 and PD98059 respectively), but they were unaffected upon blockade of PI3K/mTOR pathway (LY294002/Rapamycin), suggesting that Kv1.3 mediates proliferation through PLCγ and MEK/ERK cascades (Cidad *et al.*, 2014) (figure 1.13.).

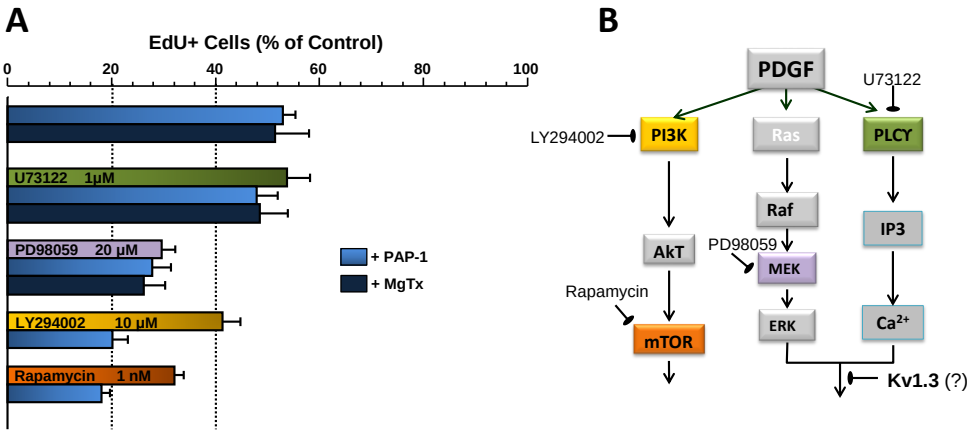


**Figure 1.13. Previous results from our group where the effects of different treatments on the PDGF-induced proliferation of hCA VSMCs is studied. The combined effect of these blockers with 10 nM MgTx (dark blue) or 100 nM PAP-1 (light blue) was also explored. Data were normalized to EdU incorporation in control conditions. B) Diagram showing the pathways explored and the targets of the blockers used. The putative location of Kv1.3 in the proliferative response is also indicated. (Cidad *et al.*, 2014).**

However, while the effects of several growth factors on Kv1.3 expression have been characterized in several preparations, the modulation of mitogen-induced signalling cascades by Kv1.3 is yet to be studied. In this work, we sought to explore in more detail the functional meaning of the Kv1.5 to Kv1.3 channel switch associated with VSMC proliferation and the mechanisms through which Kv1.3 induces proliferation. Thereby, an important question

regarding the mechanisms linking Kv1.3 expression to proliferation refers to whether this association depends on the ion-conducting properties of the channel or not. Overexpression of Kv1.3 in a heterologous system can enable us to answer this question, characterizing and reproducing the role of Kv1.3 in this system. Moreover, the use of channel mutants may be advantageous to assess the molecular determinants involved in Kv1.3-induced proliferation and to identify Kv1.3 domains, regions and residues that are required for its pro-proliferative effect.

# 2

# OBJECTIVES

The overall goal of this work is the characterization of the role of Kv1.3 channels in cell proliferation. For that purpose, we will study the molecular determinants of Kv1.3 –induced proliferation and the mechanisms and signaling pathways involved. Specifically we will try to answer the following questions:

1. **Are the voltage-dependent gating and/or the ion flux through Kv1.3 channels required for proliferation?** To explore this we will:
    - Validate the use of a heterologous expression system (HEK293 cells) to determine if there is an effect of Kv1.3 and Kv1.5 channels on cell proliferation.
    - Explore the involvement of pore and voltage sensor domains on Kv1.3-induced proliferation, by designing and studying mutant Kv1.3 channels.

2. **What are the regions of Kv1.3 channels that are relevant for its effect on proliferation?** To answer this question we will take advantage of the opposite effect of Kv1.3 and Kv1.5 on cell proliferation and we will:
    - Design Kv1.3/Kv1.5 chimeric channels to identify Kv1.3 and Kv1.5 intracellular domains that could be relevant for proliferation.
    - Explore the effects of point mutations in the relevant regions of Kv1.3 identified with the above strategy.
    - Validate the role of these regions or residues in proliferation by testing several refined mutant channels.

- Identify potential signaling cascades that could be using these regions of the channels as docking sites for the induction of cell proliferation.

3. **Can we extrapolate the effects observed with Kv1.3 and Kv1.5 in the heterologous system to the proliferation of native tissues such as VSMCs?** To explore this first we need to be able of manipulate Kv1.3 and Kv1.5 expression in these tissues, and as an initial step, we will
    - Generate Kv1.3 and Kv1.5 lentiviral vectors and determine optimum culture conditions for transducing primary VSMCs.

# 3

# Materials and Methods

## 3.1. Plasmid construction

Plasmids serve as important tools to clone or express particular genes thanks to their multiple cloning site or polylinker, which has several restriction sites to which DNA inserts may be ligated.

Polymerase Chain Reaction (PCR) was performed in a Veriti® 96-Well thermal cycler (Applied Biosystems, Waltham, USA). *Phusion® Hot Start* High-Fidelity DNA Polymerase (Finnzymes, Espoo, Finland) was used to generate flanked sites (shown in bold in the tables below) and to delete the STOP codon when necessary. The resulting PCR fragment or plasmid insert was digested with restriction enzymes (Thermo Fisher, Waltham, USA; or New England Biolabs, Ipswich, USA) following the manufacturer's instructions and run in an agarose gel to cut out the band containing the digest DNA. DNA was gel purified away from the agarose with a QIAquick® Gel Extraction Kit (Qiagen, Venlo, The Netherlands) and ligated to the pre-digested vector using T4 deoxyribonucleic acid (DNA) Ligase (Thermo Fisher).

The ligated reaction was transformed into DH5α chemically competent cells (Invitrogen, Waltham, USA), and the transformed cells were plated onto lysogeny broth (LB) plates supplemented with 25 µg/ml Kanamycin or 100 µg/ml Ampicilin (*Sigma*-Aldrich, St. Louis, USA) . After overnight incubation at 37 ºC single colonies were cultured in LB with Kanamycin or Ampicilin overnight. Plasmid DNA was obtained using QIAprep® Spin Miniprep (Qiagen) and analyzed by restriction digest to confirm presence of the insert. Further amplification of plasmid DNA was done using HiSpeed® Plasmid

Midi Kit (Qiagen). The resulting plasmid was verified for DNA purity and accuracy by DNA quantification, gel analysis, and sequencing analysis.

The plasmid constructs used in this thesis were the following:

### pCR4-TOPO-mKv1.3

pCR4-TOPO-mKv1.3 (figure 3.1.), which has the complete mouse Kv1.3 coding sequence into pCR4-TOPO plasmid, was purchased from Geneservice Ltd. The full Kv1.3 cDNA sequence was subcloned into different vectors to generate plasmids in which Kv1.3 was either coexpressed with reporter genes or expressed as a fusion protein.

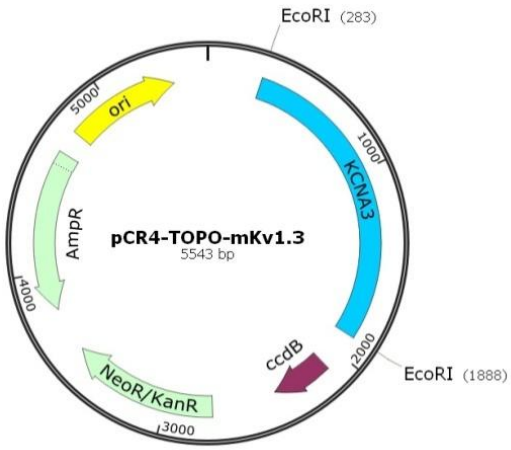


Figure 3.1. pCR4-TOPO-mKv1.3.

### pcDNA3-Kvβ2.1

pcDNA3-Kvβ2.1vector (figure 3.2.) was provided by Dr. WC Cole (University of Calgary, Canada). The Kvβ2.1 gene was subcloned into EcoRI/EcoRV sites.

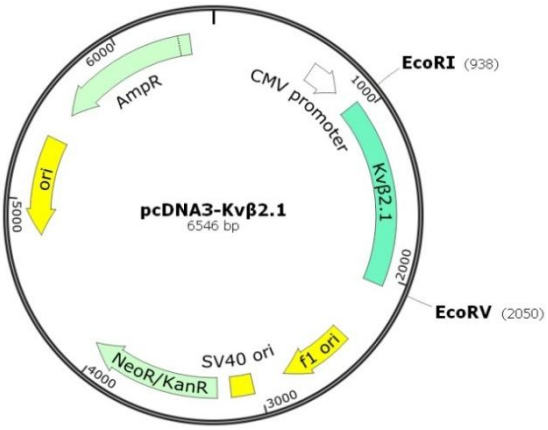


Figure 3.2. pcDNA3-Kvβ2.1.

### 3.1.1. Reporter Gene Vectors

#### dsRED2-IRES

The red fluorescent protein dsRED2 (drFP583) is a GFP homolog protein isolated from Discosoma coral (Matz et al., 1999). DsRed monomers show similar topology to GFP, but additional chemical modification to the chromophore account for the red-shifted spectra (558nm/583nm). This vector (figure 3.3.) was provided by Dr. Kääb (LMU, Munchen), and was made by switching the EGFP in the pEGFP-C3 vector (Clontech) to dsRED2 protein and adding an internal ribosomal entry site (IRES) to allow the bicistronic or simultaneous expression of two proteins separately by one promoter.

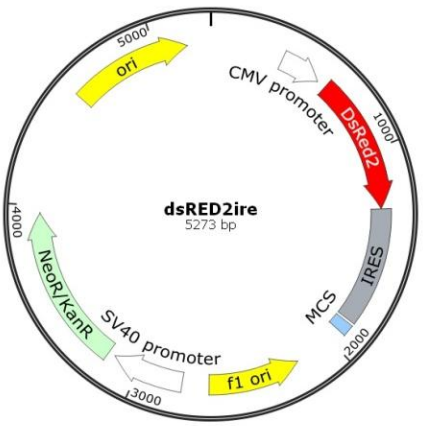


Figure 3.3. dsRED2ire.

## pEGFP-N1 and pEGFP-N3

pEGFP-N1 and pEGFP-N3 vectors (addgene) (figure 3.4.) allowed us the generation of fusion proteins in the N-terminus of EGFP. They encode a red-shifted variant of wild-type GFP which has been optimized for brighter fluorescence and higher expression in mammalian cells (488 nm / 507 nm). These plasmids were also used to express EGFP as control vectors for our experiments.

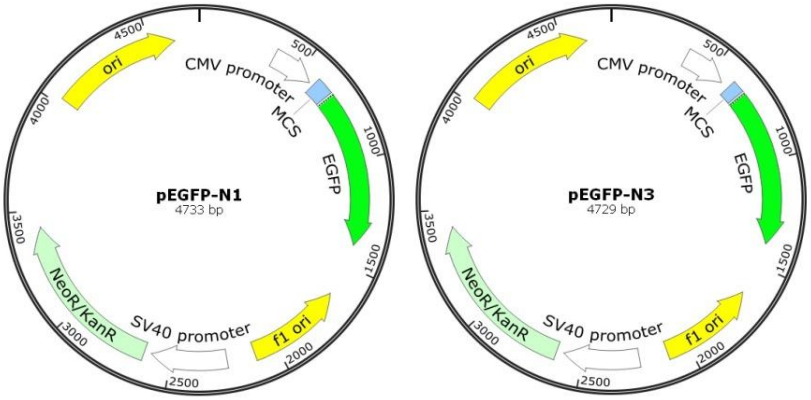


Figure 3.4. pEGFP-N1 and pEGFP-N3.

## pmCherry-N1

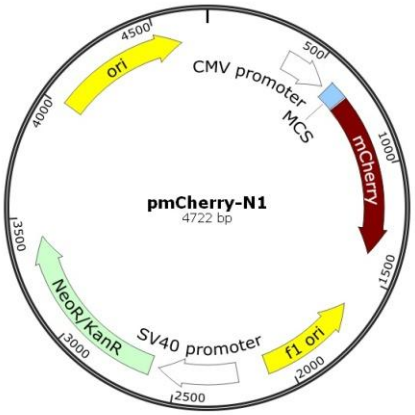


Figure 3.5. pmCherry-N1.

pmCherry-N1 (Clontech) (figure 3.5.) is a mammalian expression vector designed to express a protein of interest fused to the N-terminus of mCherry. mCherry is a mutant fluorescent protein derived from the tetrameric Discosoma sp. red fluorescent protein, DsRed. The excitation and emission maxima of the native mCherry protein are 587 nm and 610 nm, respectively.

### 3.1.2. Bicistronic Vectors

#### dsRED2-IRES-mK1.3

The dsRED2-IRES-mKv1.3 bicistronic vector (figure 3.6.) expresses both dsRED2 and mKv1.3 proteins. To make the construct, a gel purified EcoRI-EcoRI fragment of the pCR4-TOPO-mKv1.3 construct containing the coding region of the mouse KCNA3 gene was subcloned into the dsRED2-IRES vector. Because dsRED2 is expressed separately from the mKv1.3 protein, it serves only as a marker of cell transfection without interfering in the folding or function of Kv1.3.

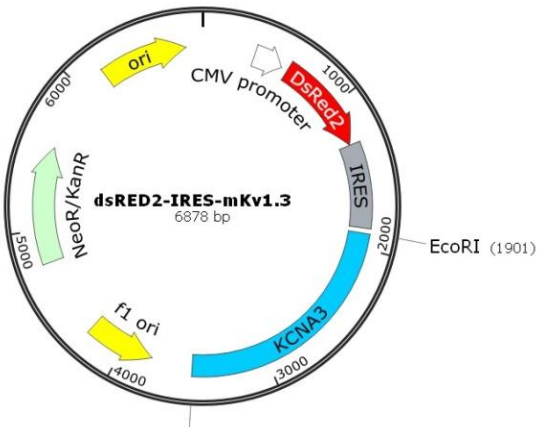


Figure 3.6. dsRED2-IRES-mKv1.3.

#### pCMS-EGFP-hKv1.5

The pCMS-EGFP-Kv1.5 vector (figure 3.7.) was provided by Dr. JX Yuan (UCSD). In this vector, the coding sequence of the human Kv1.5 gene was subcloned into EcoRI and XbaI sites of the pCMS-EGFP mammalian expression vector (Clontech). In the pCMS-EGFP vector, the EGFP gene is expressed separately from the gene of interest and is used as a transfection marker.

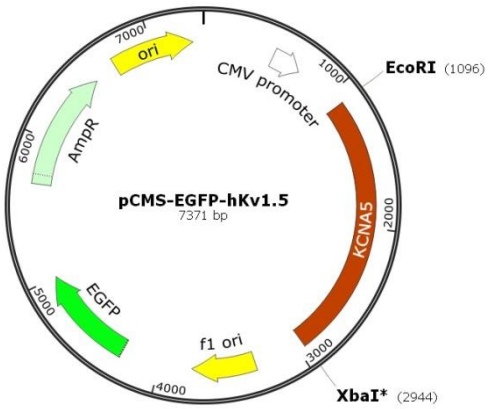


Figure 3.7. pCMS-EGFP-hKv1.5.

### 3.1.3. Fusion Protein Vectors

#### pEGFP-N3-mKv1.3

A mKv1.3 cDNA flanked by EcoRI sites and without the STOP codon was produced by PCR. Then it was cloned into the MCS of the pEGFP-N3 vector (figure 3.8.), between the CMV promoter and the EGFP coding sequence, allowing the EGFP to be in frame with the channel. Thus, a C-terminal EGFP-tagged channel (Kv1.3-GFP) was generated and sequence-verified.

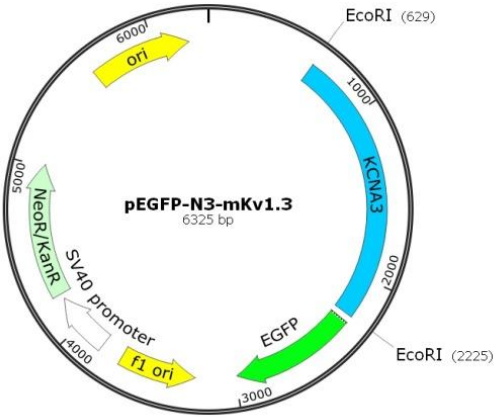


Figure 3.8. pEGFP-N3-mKv1.3.

| | Primer Sequence (5' to 3') (forward and reverse) |
|---|---|
| **pEGFP-N3-mKv1.3** | 5'-ATC**GAATTC**AGACATGACCGTGGTG-3'<br>5'-CA**GAATTC**TGGACATCAGTGAATATCTTCTTGA-3' |

Table 3.1. Primer pair used to generate pEGFP-N3-mKv1.3.

#### pEGFP-N1-hKv1.5

Kv1.5 cDNA was subcloned into the pEGFP-N1 vector via 5'-EcoRI and 3'-KpnI (figure 3.9.). PCR was performed to generate the full-length Kv1.5 fragment without the STOP codon as an EGFP fusion protein. The resulting vector was also sequenced.

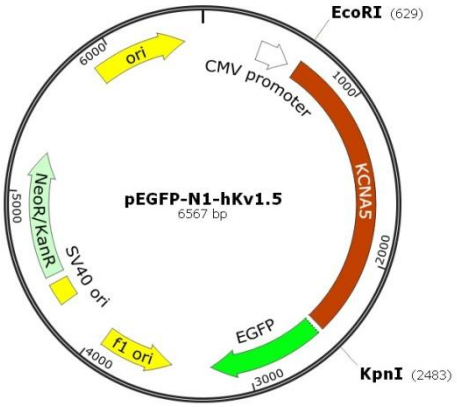


Figure 3.9. pEGFP-N1-hKv1.5.

| | Primer Sequence (5' to 3') (forward and reverse) |
|---|---|
| **pEGFP-N1-mKv1.5** | 5'-ATT**GAATTC**CCGCGCCATGGAGATC-3'<br>5'-ATT**GGTACC**AAATCTGTTTCCCGGCTGG-3' |

Table 3.2. Primer pair used to generate pEGFP-N1-mKv1.5.

## pmCherry-N1-hKv1.3

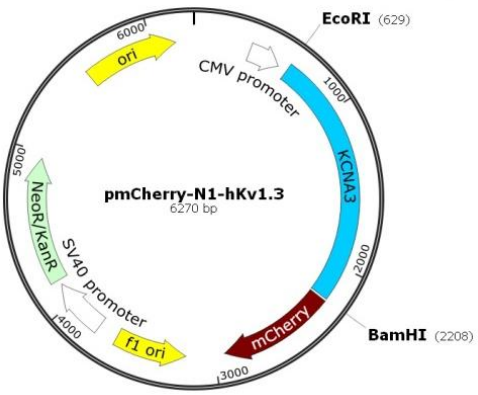


Figure 3.10. pmCherry-N1-hKv1.3.

EcoRI/BamHI flanked Kv1.3 was generated by PCR from genomic uterine artery VSMC DNA (MagNA Pure Systems, Roche). Once digested, it was ligated to the pmCherry-N1 vector as a C-terminal Cherry fusion protein (figure 3.10.). The vector was sequenced afterwards.

| | Primer Sequence (5' to 3') (forward and reverse) |
|---|---|
| **pmCherry-N1-hKv1.3** | 5'-AAT**GAATTC**CCGACATGACCGTGGTGCC-3'<br>5'- ATT**GGATCC**ACATCGGTGAATATCTTTTTGATG -3' |

Table 3.3. Primer pair used to generate pmCherry-N1-hKv1.3.

### 3.1.4. Mutant Kv1.3 Vectors

#### Pore and voltage sensor mutants

The pore and sensor Kv1.3 mutants we used were: a dominant-negative pore mutant Kv1.3AYA (G399A/G401A) (Pérez-García et al., 2000), a non-conducting point mutant with intact gating properties Kv1.3WF (W389F) (Perozo et al., 1993) and a voltage-insensitive KV1.3WF channel generated by means of a triple mutation in the S4 region, Kv1.3WF3X (R320N/L321A/R326I). This triple mutation shifts channel activation to potentials bellow -170 mV, so that the channel remains inactivated along the physiological range of voltages, behaving as an inward rectifier (Miller & Aldrich, 1996). As in the case of pEGFP-N3-mKv1.3, all these mutants were fusion proteins with a C-terminal EGFP tag (figure 3.11.).

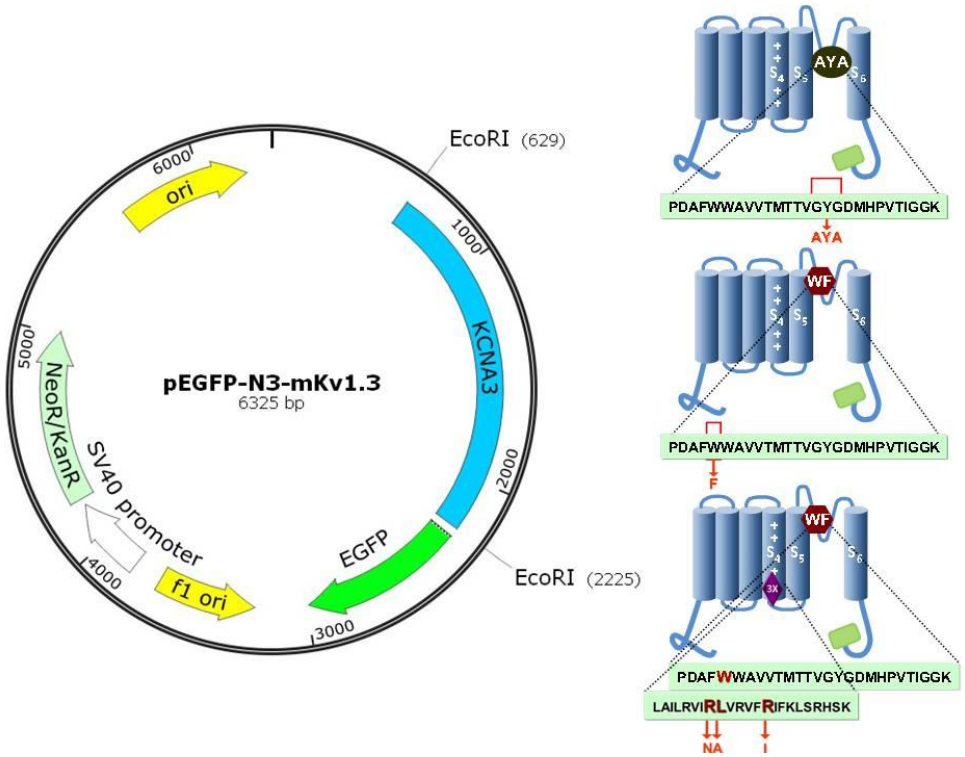


Figure 3.11. Kv1.3 pore and voltage sensor mutants. Mutated residues are shown in pictures.

Mutagenesis was performed with Stratagene's commercially available QuikChange II Site-Directed Mutagenesis Kits as follows. pEGFP-N3-mKv1.3 dsDNA template was incubated with both of the mutant primer pairs (table 3.4), dNTP, reaction buffer, and water. *Phusion Hot Start* High-Fidelity DNA polymerase was added and the reactions were subject to the following cycling parameters:

| Step | Temperature | Time |
|---|---|---|
| **Initial Denaturation** | 95 ºC | 20 sec |
| **20 Cycles** | 95 ºC / 55 ºC/ 64 ºC | 20 sec / 10 sec / 12 min |
| **Final Extension** | 64 ºC | 5 min |

Methylated parental DNA was digested with DpnI and the PCR product was used to transform DH5α E.coli competent cells. DNA purified from transformed colonies was sent for sequencing to verify the presence of the mutation and the integrity of the insert.

| | | **Primer Sequence (5' to 3') (forward and reverse)** |
|---|---|---|
| **pEGFP-N3-mKv1.3AYA** | G399A_G401A | 5'-AACCATGACAACTGTT**GCT**TAT**GCT**GATATGCACCCAGTGA-3'<br>5'-TCACTGGGTGCATATC**AGC**ATA**AGC**AACAGTTGTCATGGTT-3' |
| **pEGFP-N3-mKv1.3WF** | W389F | 5'-TTTAACAGTATCCCGGATGCCTTC**TTC**TGGGCAGTAGTAA-3'<br>5'-TTACTACTGCCCA**GAA**GAAGGCATCCGGGATACTGTTAAA-3' |
| **pEGFP-N3-mKv1.3WF3X** | R320N | 5'-TGGCCATTCTGAGAGTCATC**AAC**GCAGTAAGGGTTTTCCGCATCTT-3'<br>5'-AAGATGCGGAAAACCCTTACTGC**GTT**GATGACTCTCAGGATGGCCAG-3' |
| | L321A | 5'-CCTGAGAGTCATCCGC**GCA**GTAAGGGTTTTCCGC -3'<br>5'-GCGGAAAACCCTTAC**TGC**GCGGATGACTCTCAGG -3' |
| | R326I | 5'-CGCCTAGTAAGGGTTTTC**ATC**ATCTTCAAGCTCTCCCG-3'<br>5'-CGGGAGAGCTTGAAGAT**GAT**GAAAACCCTTACTAGGCG -3' |

**Table 3.4. Primer pairs used for site directed mutagenesis of Kv1.3 pore and voltage sensor mutants. Base pairs from mutated residues are shown in bold.**

## Kv1.3 COOH point mutants

Alanine substitutions were introduced at any of the potential phosphorylation residues Ser, Thr and Tyr of the C-terminal Kv1.3 that were not in the consensus amino acid sequence C-terminal Kv1.3-Kv1.5, with the exception of the T439 that was used as a negative control. The alignments of the C-terminal domains of Kv1.3 and Kv1.5 were performed using ClustalW software (figure 3.12.).

```
Kv1.3 -NFNYFYHRETEGEEQSQYMH-VGSCQHLSSSAEELRKARSNS--TLSKSEYMVIEEGGM 485
Kv1.5 SNFNYFYHRETDHEEPAVLKEEQGTQSQGPGLDRGVQRKVSGSRGSFCKAGGTLENADSA 576
       **********: ** :   .  *: .: ..  . :::  *.*  ::.*:   : : ..

Kv1.3 NHSAFPQTPFKTGNSTATCTTNNNPNSCVNIKKIFTDV 523
Kv1.5 RRGSCPLEKCNVKAKSNVDLRRSLYALCLDTSR-ETDL 613
       . . *    .    .           *..  .  **.
```

Figure 3.12. Clustal alignment of Kv1.3 and Kv1.5 C-terminal domains.

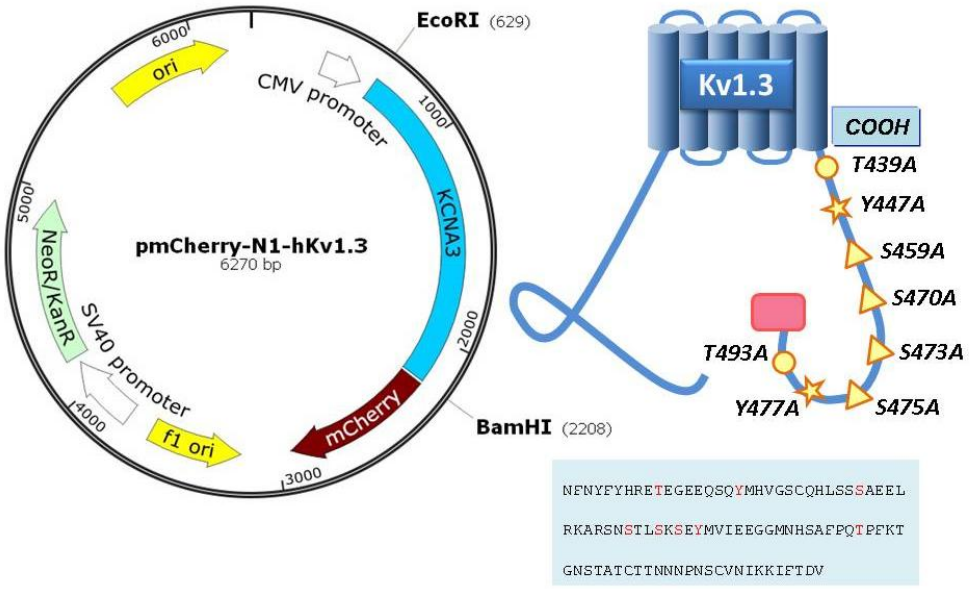


Figure 3.13. Kv1.3 COOH mutants. Mutated residues and their nomenclature are shown in picture.

Phosphorylation sites were predicted by NetPhos 2.0 Server (figure 3.13.) and confirmed with Scansite. This last program identifies protein sequence motifs that are recognized by modular signaling domains, phosphorylated by

protein Ser/Thr- or Tyr-kinases or mediate specific interactions with protein or phospholipid ligands (Obenauer *et al.*, 2003).

pmCherry-N1-hKv1.3 dsDNA plasmid was used as template. Mutagenesis was performed with Stratagene's QuikChange II Site-Directed Mutagenesis Kits as indicated previously. The primer pairs used to design Kv1.3-COOH mutants are shown in table 3.5.

| pmCherry-N1-hKv1.3 | Primer Sequence (5' to 3') (forward and reverse) |
|---|---|
| **T439A** | 5'-TCTACCACCGGGAG**GCA**GAAGGGGAAGAG-3'<br>5'-CTCTTCCCCTTCT**GC**CTCCCGGTGGTAGA-3' |
| **Y447A** | 5'-GGGAAGAGCAATCCCAG**GCC**ATGCACGTGGGAAGTT-3'<br>5'-AACTTCCCACGTGCAT**GGC**CTGGGATTGCTCTTCCC-3' |
| **S459A** | 5'-GCACCTCTCCTCT**GCA**GCCGAGGAGCT-3'<br>5'- AGCTCCTCGGC**TGC**AGAGGAGAGGTGC -3' |
| **S470A** | 5'-GAAAAGCAAGGAGTAAC**GCG**ACTCTGAGTAAGTCG-3'<br>5'- CGACTTACTCAGAGT**CGC**GTTACTCCTTGCTTTTC-3' |
| **S473A** | 5'-AAGGAGTAACTCGACTCTG**GCT**AAGTCGGAGTATATGGTG-3'<br>5'-CACCATATACTCCGACTTAGCCAGAGTCGAGTTACTCCTT-3' |
| **S475A** | 5'-ACTCGACTCTGAGTAAG**GCG**GAGTATATGGTGATC-3'<br>5'-GATCACCATATACTC**CGC**CTTACTCAGAGTCGAGT-3' |
| **Y477A** | 5'-GACTCTGAGTAAGTCGGAG**GCT**ATGGTGATCGAAGAGGGG-3'<br>5'-CCCCTCTTCGATCACCAT**AGC**CTCCGACTTACTCAGAGTC-3' |
| **T493A** | 5'-GCGCTTTCCCCCAG**GCC**CCTTTCAAAACG-3'<br>5'-CGTTTTGAAAGG**GGC**CTGGGGGAAAGCGC-3' |

**Table 3.5. Primer pairs designed to generate Kv1.3 COOH mutants. Base pairs from mutated residues are shown in bold.**

### 3.1.5. Chimeric Kv1.3-Kv1.5 Vectors

#### NH2-COOH Chimeric Vectors

Chimeric Kv1.3-Kv1.5 channels were made by substituting either NH2- or COOH- terminal domain on the Kv1.5 backbone with the corresponding domains of Kv1.3, creating the K5N3 and the K5C3 sequences. These

chimeras were expressed as Cherry- or EGFP-fusion proteins: pmCherry-N1-K5N3 and pEGFP-N1-K5C3 (figure 3.14.).

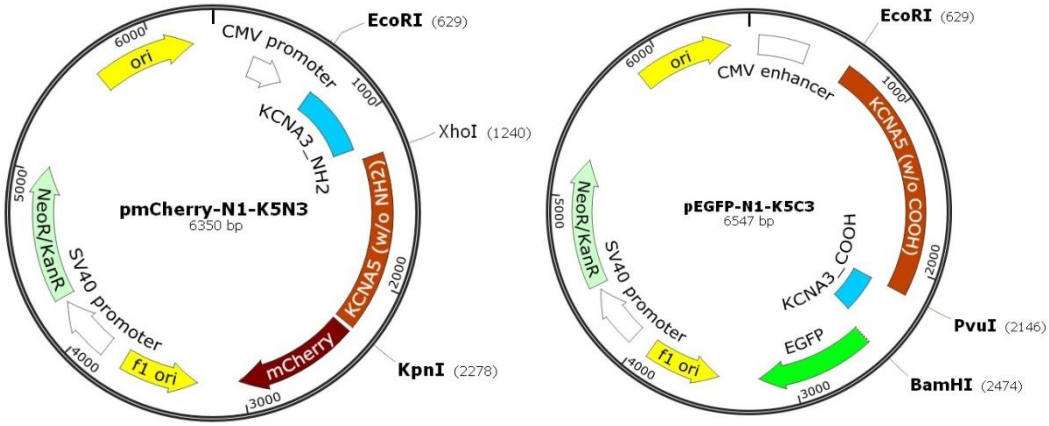


Figure 3.14. NH2-COOH chimeric plasmids.

- pmCherry-N1-K5N3: N-terminal Kv1.3 fragment flanked by EcoRI/XhoI and Kv1.5 backbone without N-terminus flanked by XhoI/KpnI were generated by PCR. Both fragments were subcloned into EcoRI/KpnI digested pmCherry-N1 following a T4 DNA ligase triple ligation.
- pEGFP-N1-K5C3: EcoRI/PvuI Kv1.5 backbone with no C-terminal domain and C-terminal Kv1.3 flanked by PvuI and BamHI were also made by PCR and ligated to the digested pEGFP-N1 vector.

| | | **Primer Sequence (5' to 3')<br>(forward and reverse)** |
|---|---|---|
| **pmCherry-N1-K5N3** | NH2- Kv1.3 | 5'-AAT**GAATTC**CCGACATGACCGTGGTGCC-3'<br>5'- CGT**CTCGAG**GCAGAAGATGACAATGGAG-3' |
| | Kv1.5 Backbone (w/o NH2-) | 5'- TGC**CTCGAG**ACCCTGCCTGAGTTCAG-3'<br>5'- ATT**GGTACC**AAATCTGTTTCCCGGCTGG -3' |
| **pEGFP-N1-K5C3** | Kv1.5 Backbone (w/o COOH-) | 5'-ATT**GAATTC**CCGCGCCATGGAGATC-3'<br>5'- CGG**CGATCG**CACACAGCGAGCC-3' |
| | COOH- Kv1.3 | 5'-GTG**CGATCG**CCGGTGTCTTGACC-3'<br>5'- ATT**GGATCC**ACATCGGTGAATATCTTTTTGATG -3' |

Table 3.6. Primer pairs designed to generate NH2-COOH chimeras.

## YS Fragment Chimeric Vectors

YS Fragment is a 16-amino-acid-residue fragment from hKv1.3 that comprises Y447 and S459 (figure 3.15.). It is located at the beginning of the C-terminus and right after the consensus sequence between Kv1.3-Kv1.5 C-terminal domains. This fragment was inserted in the C-terminal domain of the hKv1.5 at two different positions to generate two chimeras, K5-532YS and K5-613YS. The third construct of this series, K3YS, is not really a chimeric vector but a truncated form of hKv1.3 with a short C-terminus consisting only on the YS fragment.


Figure 3.15. Kv1.3 YS fragment inserted (or maintained) to generate YS chimeras.

- pmCherry-N1-K3YS

pmCherry-N1-K3YS (figure 3.16.) was made from the pmCherry-N1-hKv1.3 vector by deleting the Kv1.3 sequence of amino acids 461-523, corresponding to the end of the C-terminus. Thus, the fragment YS was kept as the only sequence in the C-terminus of this chimera. Due to the difficulty in finding restriction sites to achieve the deletion mutation, we made a short double stranded DNA region by designing overlapping oligos. Once these oligos had been annealed, they were cloned directly into the overhangs generated by restriction digest of the existing sites in the original vector.

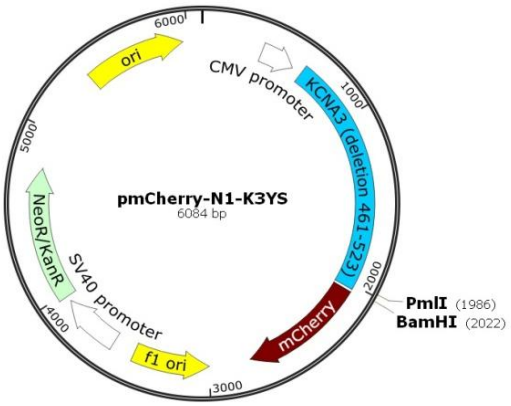


Figure 3.16. pmCherry-N1-K3YS.

Oligos designed containing the YS fragment were flanked by a 5'- blunt end PmlI, restriction site located right before the YS region in the template vector, and a 3'- sticky end BamHI, located at the end of the C-terminus (table 3.7.).

| | Primer Sequence (5' to 3')<br>(forward and reverse) |
|---|---|
| **pmCherry-N1-K3YS** | 5'-**GTG**GGAAGTTGCCAGCACCTCTCCTCTTCAGCCGTG-3'<br>5'-**GATCC**ACGGCTGAAGAGGAGAGGTGCTGGCAACTTCCCAC-3' |

Table 3.7. Primer pair used to generate pmCherry-N1-K3YS. PmlI and BamHI ends shown in bold.

For the annealing, the oligos were subjected to a cycle of heating for denaturation followed by cooling to allow the two oligos to base pair together. Oligos must be also phosphorylated in their 5'OH end for ligation into the vector cut with the appropriate enzymes (figure 3.17.).

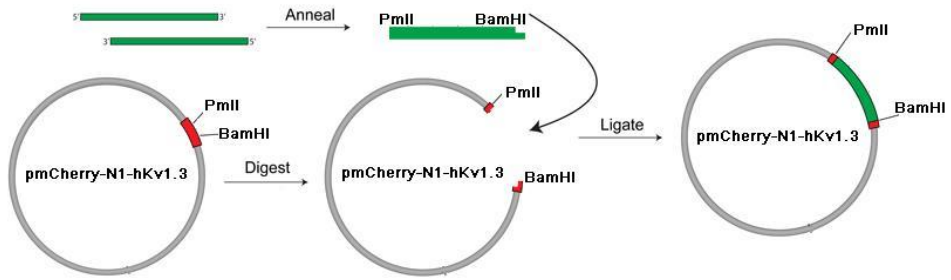


Figure 3.17. Schematic representation to generate pmCherry-N1-K3YS.

Both oligos were mixed in equimolar concentration in a PCR tube. Then, T4 Polynucleotide Kinase (PNK) was added together with its commercial buffer (Thermo Fisher, Waltham, USA) and nuclease-free water. The tube was placed in a thermocycler programmed, beginning with an incubation of 30 minutes at 37 ºC to let the PNK work. Afterwards, the following program was performed: 95°C for 5 minutes and a ramp cool to 23 °C over a period of 45 minutes. Annealed oligos were diluted 1:100 in nuclease-free water and the

concentration was quantified to be mixed with the PmlI/BamHI digest pmCherry-N1-hKv1.3 in a standard ligation reaction (2 ng annealed oligos and 40 ng plasmid). To verify mutant deletion, DNA was sequenced.

- pEGFP-N1-K5-613YS

pEGFP-N1-K5-613YS (figure 3.18.) was made from the pEGFP-N1-hKv1.5 vector by inserting overlapping oligos with the YS fragment of hKv1.3 at the end of the Kv1.5 C-terminus. Oligos were designed containing the YS fragment flanked by a 5'-KpnI and a 3'- AgeI sticky ends, both sites are located just after the end of the C-terminal Kv1.5 (table 3.8.).

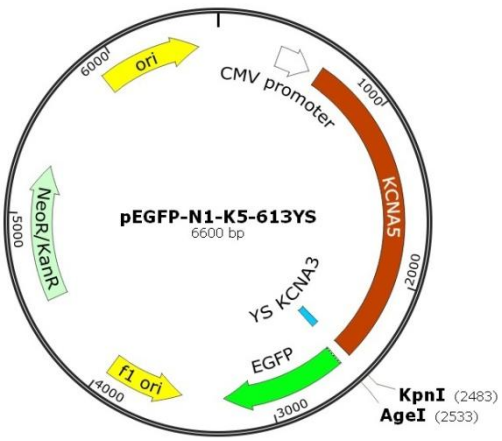


Figure 3.18. pEGFP-N1-K5-613YS.

| | Primer Sequence (5' to 3')<br>(forward and reverse) |
|---|---|
| **pEGFP-N1-K5-613YS** | 5'-**C**GCAGTACATGCACGTGGGAAGTTGCCAGCACCTCTCCTCTTCAGCCGAA -3'<br>5'- **CCGGT**TCGGCTGAAGAGGAGAGGTGCTGGCAACTTCCCACGTGCATGTACTGCGGTAC-3' |

Table 3.8. Oligos with KpnI and AgeI ends (shown in bold) used to generate pEGFP-N1-K5-613YS

Annealing and cloning (figure 3.19.) was performed as indicated previously.

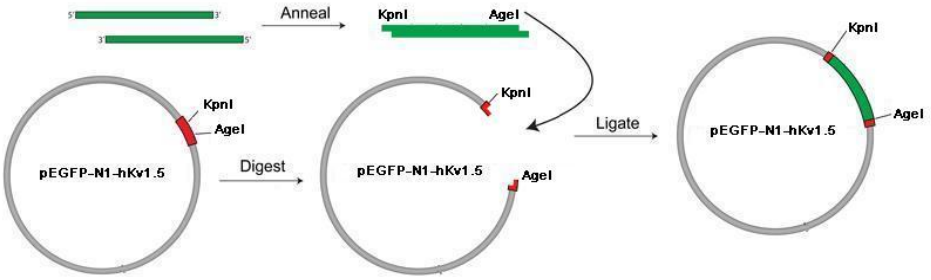


Figure 3.19. Schematic representation to generate pEGFP-N1-K5-613YS.

- pEGFP-N1-K5-532YS

The following chimeric vector (figure 3.20.) was made by overlap extension PCR cloning. This method is conceptually similar to the QuikChange site directed mutagenesis procedure, and it is used to clone any DNA insert into a plasmid of choice without the use of restriction endonucleases or T4 DNA ligase (Bryksin & Matsumura, 2010).

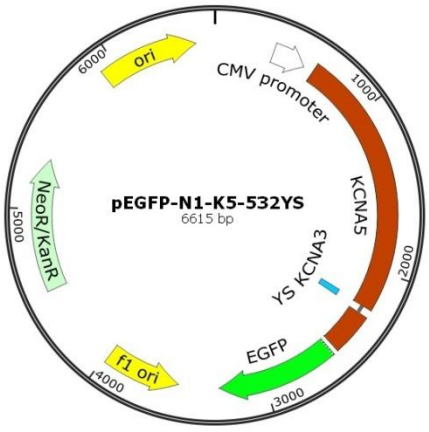


Figure 3.20. pEGFP-N1-K5-532YS.

Kv1.3 YS fragment was inserted into pEGFP-N1-Kv1.5, amino acid 532 of Kv1.5, which corresponds to Kv1.3 analog position (downstream from the consensus C-terminal Kv1.3-Kv1.5 sequence).

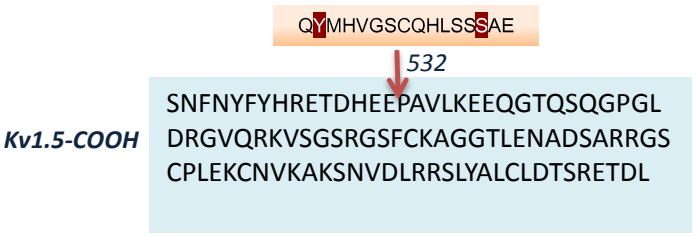


To accomplish this, a pair of hybrid primers (table 3.9.) were designed containing complementary sequence to both the desired insert, YS fragment, and the target plasmid, pEGFP-N1-hKv1.5 (shown in bold).

| | Primer Sequence (5' to 3') (forward and reverse) |
|---|---|
| **pEGFP-N1-K5-532YS** | 5'-**ACTACTTCTACCACCGGGAAACGGATCACGAGGAG**CAGTACATGCACGT GGGAAGTTGCCAGCACCTCTCCTCTTCAGCCGAG-3' 5'-**CTCTGAGTGCCCTGCTCTTCCTTAAGGACTGCCGG**CTCGGCTGAAGAG GAGAGGTGCTGGCAACTTCCCACGTGCATGTACTG-3' |

Table 3.9. Primer pair for overlapping extension PCR cloning to generate pEGFP-N1-K5-532YS. Target plasmid complementary sequence is shown in bold.

These primers were used to amplify the insert (YS fragment) using *Phusion Hot Start* High-Fidelity DNA Polymerase and the following parameters: 100ºC for 2 minutes, followed by 30-32 cycles of 94 ºC for 30 seconds, 60 ºC for 30 seconds, and 68 ºC for 10 minutes and by a final extension of 68 ºC for 10 minutes. The resulting product was purified and used as a 'mega-primer' in a secondary PCR reaction, with the target plasmid (pEGFP-N1-hKv1.5) acting as template. PCR profile was:

| Step | Temperature | Time |
|---|---|---|
| **Initial Denaturation** | 100 ºC | 1 min |
| **18-22 Cycles** | 95 ºC / 60 ºC/ 68 ºC | 50 sec / 50 sec / 12 min |
| **Final Extension** | 68 ºC | 12 min |

The plasmid is amplified in both directions, and the mega-primers act as long single-stranded overhangs that allow the complementary strands of the plasmid to anneal, forming a nicked hybrid molecule. DpnI was used to degrade any parental plasmid (based on its methylation), and the final product was used to transform DH5α competent cells. This process is depicted below (figure 3.21.).

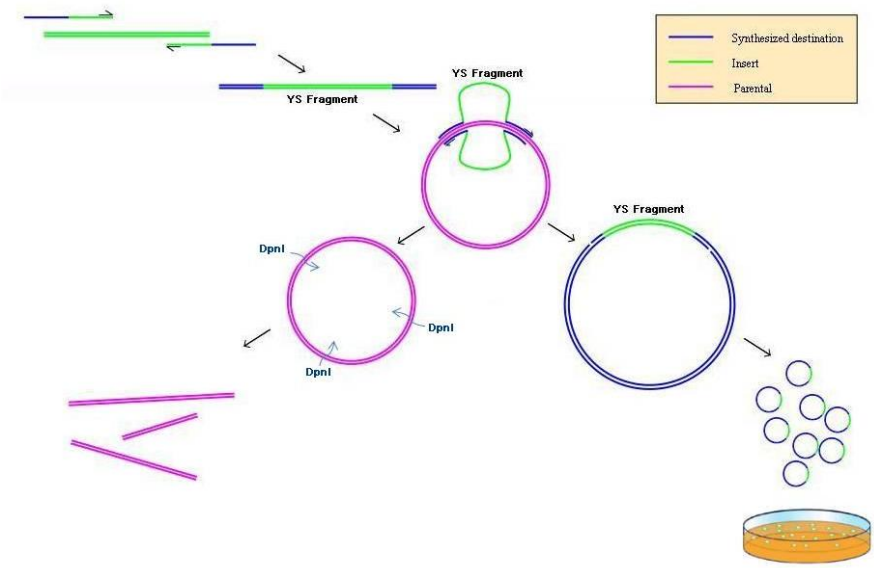


Figure 3.21. Simplified schematic procedure of overlap extension PCR cloning used for pEGFP-N1-K5-532YS chimeric vector.

### 3.1.6. Lentiviral Vectors

For producing lentiviral particles is necessary to use three different lentivirus plasmids: 1) the packaging plasmid psPAX2, which contains all the important packaging components: Gag, Pol, Rev, and Tat; 2) the enveloping plasmid pMD2.G, an envelope vector that encodes for VSV-G (figure 3.22.), and 3) the transcription factor plasmid pSin-EF2-Sox2-Pur (or transfer vector), which contains the cDNA and the flanking long terminal repeats

(LTRs). pSin-EF2-Sox2-Pur plasmid has a large deletion in the 3'LTR that makes the virus replication incompetent. These three plasmids were purchased from Addgene Inc. (Cambridge, USA).

EGFP and the fusion proteins hKv1.5EGFP and hKv1.3Cherry were subcloned from their respective plasmids into pSin-EF2-Sox2-Pur to generate lentivirus expression plasmids (figure 3.23.).

Oligonucleotides containing EcoRI-SpeI restriction sites were designed (table 3.10.).

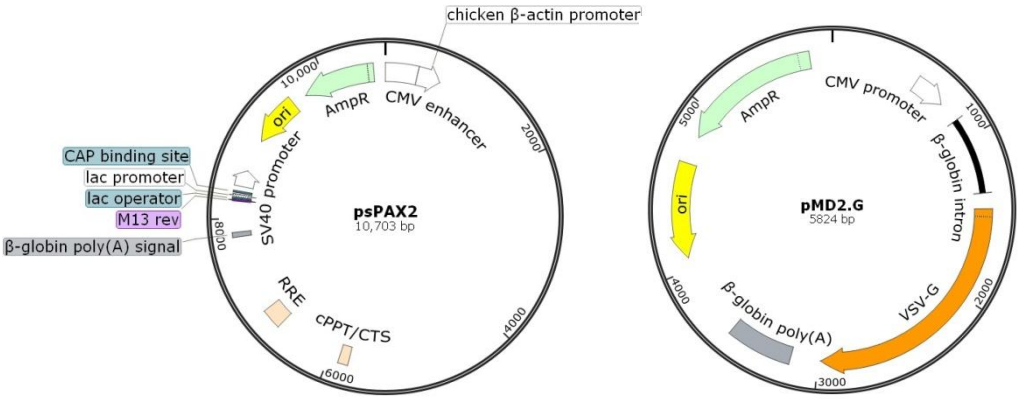


Figure 3.22. psPAX2 and pMD2.G plasmids used to produce lentivirus.

| | Primer Sequence (5' to 3') (forward and reverse) |
|---|---|
| **pSin-EF2-Sox2-Pur-EGFP** | 5'-AAT**GAATTC**CACCATGGTGAGCAAGGG-3'<br>5'-ATA**ACTAGT**TACTTGTACAGCTCGTCCATG -3' |
| **pSin-EF2-Sox2-Pur-hKv1.5EGFP** | 5'-ATT**GAATTC**CCGCGCCATGGAGATC -3'<br>5'-ATA**ACTAGT**TACTTGTACAGCTCGTCCATG-3' |
| **pSin-EF2-Sox2-Pur-hKv1.3Cherry** | 5'-AAT**GAATTC**CCGACATGACCGTGGTGCC-3'<br>5'-ATC**ACTAGT**GCTACTTGTACAGCTCGTCC-3' |

Table 3.10. Primer pairs used to subcloned EGFP, hKv1.5EGFP and hKv1.3Cherry into EcoRI-SpeI sites (shown in bold) of pSin-EF2-Sox2-Pur plasmid.

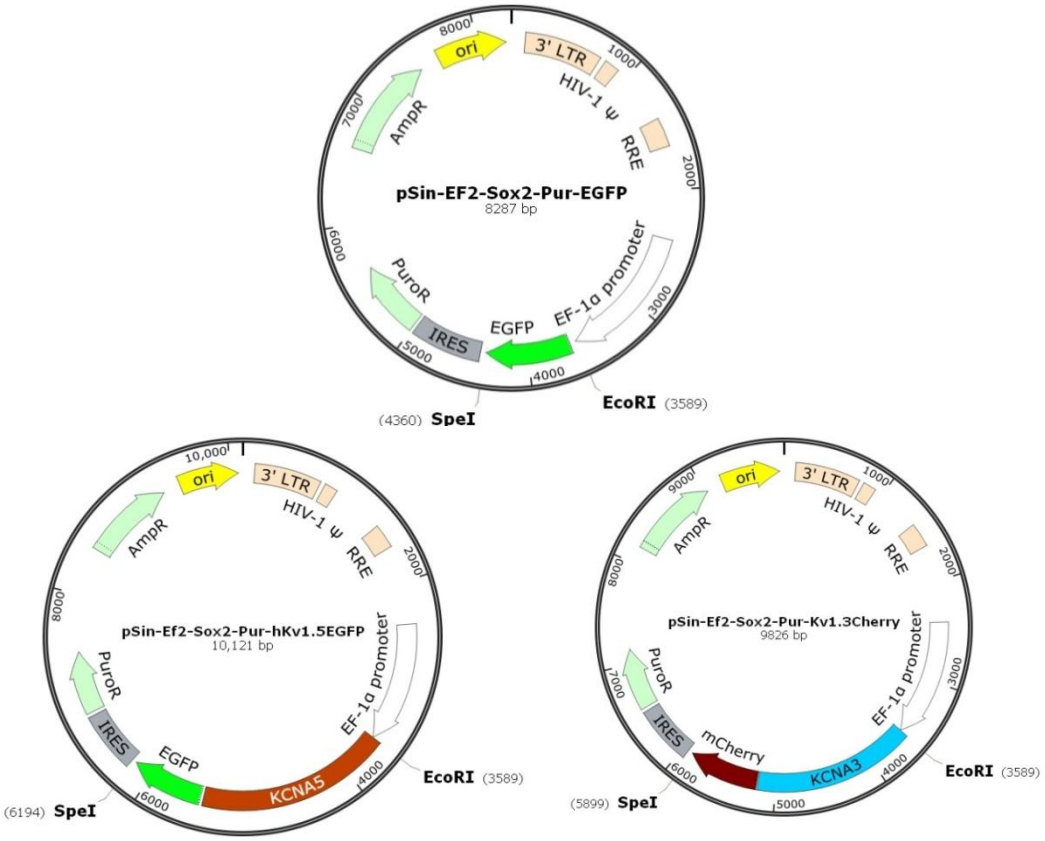


Figure 3.23. pSin-EF2-Sox2-Pur lentiviral plasmids expressing EGFP, hKv1.5EGFP and hKv1.3Cherry.

## 3.2. Cells and Culture

In this thesis we used an immortalized cell line, human embryonic kidney 293 (HEK293), for most of the experiments. We also used a variant of this cell line, 293FT, and primary cell lines (human vascular smooth muscle cells) for some specific studies.

HEK293 cells were used as a heterologous expression system for the overexpression of our genes of interest, due to the low expression level of endogenous ion channels. The 293FT cell line (Invitrogen) was employed as

a host for lentiviral production while VSMCs were used to be infected by lentiviral transduction.

Renal and uterine artery samples from human donors were obtained through the Collection of Human Arterial samples (COLMAH), an initiative of the HERACLES Network for Cardiovascular Research. Samples arrived in our lab within the next 24 h following extraction at the hospitals and were processed as previously described (Cidad 2014). Briefly, VSMCs were isolated from the medial layer of the vessel kept in DMEM (Dulbecco's Modified Eagle's Medium) after manual removal of both adventitia and endothelial layers under a dissection microscope. Once isolated, the muscle layer was cut in 1 $mm^2$ pieces that were seeded in 35 mm Petri dishes treated with 2 % gelatin (Type B from bovine skin, Sigma) or collagen (6 well multidish collagen, Thermo Scientific), in DMEM supplemented with 20 % SFB, penicillin-streptomycin (100 U/ml each), 5 µg/ml fungizone, and 2 mM L-glutamine (Lonza) at 37 ºC in a 5% $CO_2$ humidified atmosphere. Migration and proliferation of VSMCs from the explants was evident within 10-15 days.

Cell culture media and supplements were purchased from Lonza. Unless otherwise noted, all solution reagents were from Sigma. HEK293, VSMCs and 239FT cells were cultured in DMEM with different supplements (table 3.11.).

All cells were incubated in a humidified environment at 37 ºC and 5 % $CO_2$. Media was changed 24 hours after initial seeding and every 48 hours subsequently. When cells reached 80-90 % confluency, cells were gently washed with phosphate buffered saline (PBS), incubated with trypsin/EDTA solution until detachment and then incubated with medium with FBS to

neutralize trypsin. The cell suspension was then transferred to a sterile 10-ml tube, centrifuged at room temperature for 4 minutes at 1000 rpm, and then resuspended in appropriate growth media, counted with a hemocytometer and seeded. HEK293 and 293FT cells were used up to passage 20 while VSMCs were used between passages 3 and 8.

| | HEK293 cells | VSMCs (P-STIM) | 239FT Cell Line |
|---|---|---|---|
| **bFGF** | | 2 ng/ml | |
| **EGF** | | 0,5 ng/ml | |
| **Insulin** | | 5 µg/ml | |
| **FBS** | 5 % | 10 % | 10 % |
| **Penicillin** | 100 U/ml | 100 U/ml | 100 U/ml |
| **Streptomycin** | 100 U/ml | 100 U/ml | 100 U/ml |
| **Fungizone** | 0.25 µg/ml | 0.25 µg/ml | 0.25 µg/ml |
| **L-glutamine** | 2 mM | 2 mM | 6mM |
| **Non-Essential Amino Acids (NEAA)** | | | 0.1 mM |
| **Geneticin** | | | 500 µg/ml |

**Table 3.11. Different media supplements used for HEK293, VSMCs and 293FT cells.**

## 3.3. Drugs

- DPO. Diphenyl phosphine oxide-1 (Tocris Bioscience): Kv1.5 selective blocker. Reconstituted in ethanol at 1 µM, stored at -20 ºC, used at 100nM in proliferation assays and from 10 nM to 5 µM for electrophysiological experiments.
- rMargatoxin or MgTx (Alomone Labs): Kv1.3 selective blocker. Reconstituted in PBS at 2 µM, stored at -20 ºC and used at 10nM.

- PAP-1. 5-(4-Phenoxybutoxy) psoralen (Sigma): Kv1.3 selective blocker. Reconstituted in DMSO at 10 mM, stored at -20 ºC, used at 100 nM.
- PD98059. 2-(2-Amino-3-methoxyphenyl)-4*H*-1-bonzopyran-4-one (Tocris Bioscience): inhibitor of mitogen-activated protein kinase kinase (MKK/MEK). Reconstituted at 25 mM in DMSO, stored at -20 ºC, used at 20 µM.
- Pervanadate: tyrosine phosphatase inhibitor vanadyl hydroperoxide. Reconstituted in cell culture media from a solution of sodium orthovanadate and hydrogen peroxide, used at 250 µM.

## 3.4. Transfection

Two or three days after seeding in 35 mm petri dishes, HEK293 cells were transiently transfected at 80-90 % confluency with Lipofectamine 2000 (Invitrogen). Transfection reagent (in µl) and DNA (in µg) was added directly to cells in growth media in a 3:1 ratio. Transfections were made with 1 µg of plasmid DNA unless otherwise noted. Mock transfected cells underwent the same protocol in the absence of plasmid DNA. Kv1.3:Kvβ2 ratio in cotransfections ranged from 1:10 to 1:100, to ensure maximal functional effect of Kvβ2.

Opti-MEM Reduced Serum Media (Gibco) was used to dilute DNA and transfection reagents. DNA and Lipofectamine 2000 were separately diluted in Opti-MEM, incubated at room temperature for 5 minutes before combined, incubated at room temperature for 20 minutes and then added to cells. The complexes were removed from cells after an overnight incubation in a humidified environment at 37 ºC and 5 % $CO_2$. Cells were then harvested, counted with hemocytometer and reseeded at the adequate density in fresh

growth media for experimentation 24-48 hours after transfection. Under these conditions, transfection rate was between 35-60 %. This rate was quantified in each experiment by fluorescence microscopy.

## 3.5. Lentivirus Production and Titering

### 3.5.1. Production

Recombinant lentiviruses were produced by co-transfecting 293FT cells in 150 mm dishes with 10 µg of the lentivirus expression plasmid pSin-EF2-Sox2-Pur-(EGFP, hKv1.5EGFP or hKv1.3Cherry), 5 µg of the envelope plasmid pMD2.G and 7.5 µg of the packing vector psPAX2 using Lipofectamine 2000 method (described before). After overnight transfection, medium was changed to the complete 293FT culture medium. Infectious lentiviruses released to the medium were harvested at 48 and 72 h post-transfection, centrifuged at room temperature for 5 minutes at 1500 rpm to eliminate cell debris, and then filtered through 0.45-µm filters. The filtered supernatant was centrifuged at 13 ºC for 2 hours at 22000 rpm in a Optima™ L-100XP ultra centrifuge, Rotor JA 25.50 (Beckman Coulter, Pasadena, USA). Supernatant was discarded and the pellet was dried at room temperature for 1 hour. 500 µl of previously filtered 1 % Human serum albumin (HSA) was added and kept at 4 ºC overnight. The following day, pellet was resuspended to make aliquots and stored them at -80 ºC until use.

### 3.5.2. Titering

#### RNA Isolation

Determination of the lentiviral titer allowed us to estimate the multiplicity of infection (MOI) and thus to deduce the infectious activity of the viral stocks. In order to do this, viral nucleic acids were first isolated from RNA using The PureLink® Viral Mini Kit (Invitrogen). The viral particles were lysed using Proteinase K and Lysis Buffer containing Carrier RNA at 56°C. Ethanol was added to the lysate to a final concentration of 37 % and the sample was loaded onto a silica spin column. The viral RNA molecules bound to the silica column and impurities such as proteins and nucleases were removed by thorough washing with Wash Buffer. The RNA was then eluted in sterile, RNase free water. After quantification with a nanodrop, RNA was either stored at -80 ºC or used to make cDNA.

#### RT and real time quantitative PCR (qPCR)

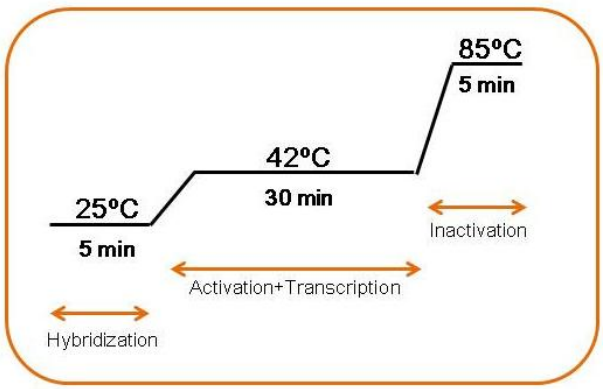


Figure 3.24. RT protocol.

Reverse Transcriptase (RT) was performed with 500 ng of viral RNA in a thermal cycler Rotor-Gene 3000 (Corbett Research) programmed with the

protocol indicated in figure 3.24., using MultiScribe ™ Reverse Transcriptase Mu-LvRT (2.5 u/µl), Random Hexamers (2.5 µM), Oligo dT (2.5 µM), RNAse inhibitor (1 u/µl), PCR buffer (1X), $MgCl_2$ (5 mM) and a mixture of dNTPs (4 mM). All reagents were purchased from Applied Biosystems.

Once the cDNA was synthetized, it was diluted 1:10 and used as a template to determine the infectious titer by real time qPCR and SYBR Green I (Thermo Fisher). SYBR Green I is a commonly used fluorescent DNA binding dye that binds all double–stranded DNA and can be detected by measuring the increase in fluorescence throughout the cycles.

Analysis of the PCR results requires the setting of a detection threshold $C_t$ (cycle threshold) within the exponential phase of all amplification curves. $C_t$ is defined as the number of cycles required for the fluorescent signal to cross the threshold and it is inversely proportional to the initial amount of cDNA molecules.

Serially diluted standards of pSin-EF2-Sox2-Pur-(EGFP, hKv1.5EGFP or hKv1.3Cherry) with known concentration and length were used to produce a standard curve (figure 3.25.).

The standard curve revealed a linear relationship ($R^2 > 0.99$) between $C_t$ and initial amount of total DNA. The copy numbers of plasmid DNA (from $10^9$ to $10^4$ copies/µl) were calculated using the online calculator provided by the URI Genomics & Sequencing Center. The formula used is: (amount × $6.022\times10^{23}$) / (length × $1\times10^9\times$ 650), in which amount, is concentration of plasmid in nanogram/microliter, $6.022\times10^{23}$ (molecule/mole) is Avogadro's number, length is full length of plasmid in base pair, 650 (gram/mole) is the

average molecular weight of a base pair and $1\times10^9$ is used for conversion gram to nanogram.

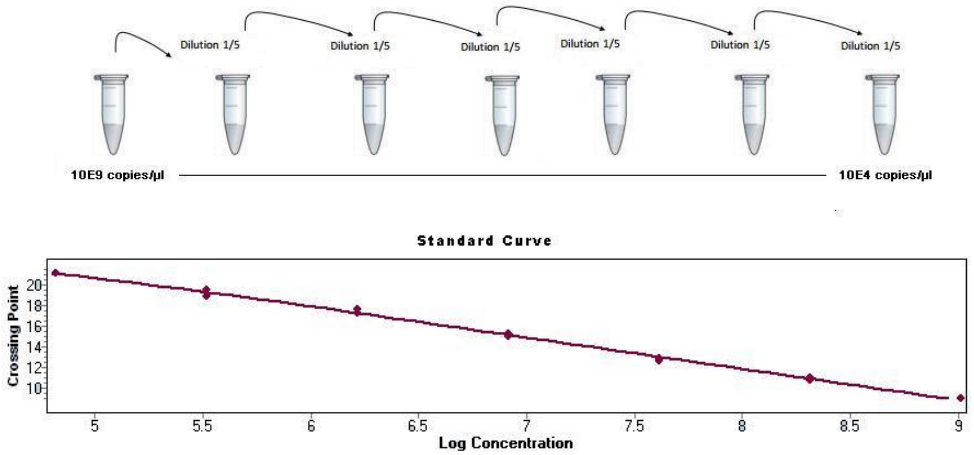


**Figure 3.25. Seven 5-fold dilutions fom $10^9$ to $10^4$ copies/µl of pSin-EF2-Sox2-Pur plasmids were prepared for plotting the standard curve.**

For the real time qPCR reaction, 1X SYBR Green I Master Mix was mixed with both oligos (0.5 µM), cDNA sample (1:10) or plasmid DNA (for the standard curve) and nuclease-free water up to 20 µl. Oligos were designed containing part of the LTRs sequences, lentiviral genes present in pSin-EF2-Sox2-Pur construct (table 3.12.).

| | **Primer Sequence (5' to 3')<br>(forward and reverse)** |
|---|---|
| **LTRs Oligos** | 5'-TGGGAGCTCTCTGGCTAACT-3'<br>5'-GACGGGCACACACTACTTGA-3' |

**Table 3.12. Oligos used to determine lentiviral titer.**

The real time qPCR procedure included appropriate negative controls (no template controls).

The parameters used in LightCycler 480 (Roche) were: 10 minutes at 95 ºC followed by 40 cycles of 95 ºC for 15 seconds, 60 ºC for 30 seconds and 72 ºC for 40 seconds. To verify the absence of primer-dimers and nonspecific amplification, a melting curve was performed after amplification. This was generated by increasing the temperature from 65 ºC to 95 ºC in small increments (0.11 ºC/second) and monitoring the fluorescent signal at each step.

As shown before, average $C_t$ values for each pair of duplicate control template amplifications were determined and plotted versus concentration on a log scale to generate a standard curve. Thus, the average $C_t$ of each pair of duplicate cDNA sample amplifications was interpolated and used to read the absolute copy number equivalent from its plasmid DNA standard curve. Virus titers were at the range of $10^6$-$10^8$ virions/µL.

## 3.6. Lentiviral Vector Transduction

In order to optimize the MOI for each cell line: HEK293 cells and Uterine and Renal VSMCs were seeded at $5x10^3$ cells/well in 96-well plates two days before transduction. Infection was performed at different MOIs (from 20 to 200 virions per cell) in Opti-MEM containing 5 µg/mL protamine sulfate, a polycation used as an alternative to polybrene due to its higher infection efficiency and lower toxicity (Cornetta & Anderson, 1989). After overnight incubation at 37 ºC and 5 % $CO_2$, medium was replaced to complete growth

medium and, 48 hours post-transduction, reporter gene expression was examined using fluorescent microscopy. Mock transductions were made following the same protocol in the absence of viral particles.

Afterwards, transduced cells were selected by adding 2 µg/ml puromycine, an aminonucleoside antibiotic, into the medium for 5 days. Infected cells could be selected due to puromycin antibiotic resistance conferred by the pac gene in the lentiviral vector pSin-EF2-Sox2-Pur.

## 3.7. Coating coverslips with Poly-L-Lysine

Poly-L-Lysine (Sigma) facilitates cell adhesion and it was used for coating the coverslips used for electrophysiology, proliferation assays and immunocytochemistry. For electrophysiological recordings, cells were seeded in coverslips small enough to fit the recording chamber, while for proliferation assays and immunocytochemistry we used 12 mm diameter coverslips.

Autoclaved coverslips were coated with poly-L-Lysine in a laminar flow cabinet by submerging them in 0.01 mg/ml poly-L-Lysine for 30 minutes. Then, they were rinsed several times with distilled autoclaved water and dried against the wall of a Petri dish to prevent adhesion between them. Once dry, they were stored until use.

The coverslips were then placed on a Petri plate and a droplet of cell-containing medium was placed on top of them.

## 3.8. Proliferation assays

The rate of proliferation of HEK293 cells transfected with different plasmids was determined in all cases by two alternative, complementary methods: Cell counting and EdU incorporation assays.

Proliferation assays were always designed with parallel intra-experimental controls, using HEK293 cells transfected with the corresponding empty vector (dsRED2-IRES, pEGFP-N3, pmCherry-N1) at the same concentration that channel-expressing vectors. For cell counting assays, transfected cells were harvested, and seeded in 24-well-plates at a density of 40000 cells/well. In all cases, each data point was the mean of 3 independent determinations in each experiment. Cells were allowed to attach during five hours; after that, triplicate wells for each condition were harvested and the averaged number of cell counted was taken as the t=0 for each condition. Cells were harvested and counted at the indicated times, up to 96 h in some experiments. When the effect of drugs was explored, they were added to the media when seeding the cells (for the Kv1.3 specific blockers: MgTx or PAP-1) or 4 hours before performing the experiment (for the MEK blocker, PD98059).

The percentage of cells entering the S-phase of the cell cycle was determined by means of EdU incorporation assays using a commercial kit Click-iT® EdU Imaging Cell proliferation assay (Invitrogen) following manufacturer specifications. Transfected cells were harvested and plated onto poly-L-Lysine coated 12 mm coverslips at a density of 40000 cells/coverslip, and incubated for 24-48 hours in 5 % FBS supplemented DMEM media with or without additional treatment. At the end of these

periods, cells were incubated with the thymidine analog-5-ethynyl-2´-deoxyuridine (EdU), that is incorporated into DNA during active DNA synthesis, for 45 minutes at 37 ºC in a 5 % $CO_2$ humidified atmosphere, fixed with 3.7 % formaldehyde in PBS and permeabilized with Triton X-100 0.5 %. Incorporated EdU was detected by incubation with a reaction buffer containing Alexa fluor reagent for fluorescence detection of EdU-incorporating cells (figure 3.26.). Cells were incubated with Hoechst 33342 (1:2000 in PBS) for 30 minutes at room temperature, for counting nuclei. Coverslips were mounted in Vectashield and proliferation rate was estimated as the percentage of EdU positive cells (EdU+) from the total cell number stained with Hoechst. In each experiment, EdU incorporation was obtained from the average of at least 10 different fields for each condition taken with the 20x objective of a Nikon Eclipse 90i microscope (Nikon Corp., Tokyo, Japan).

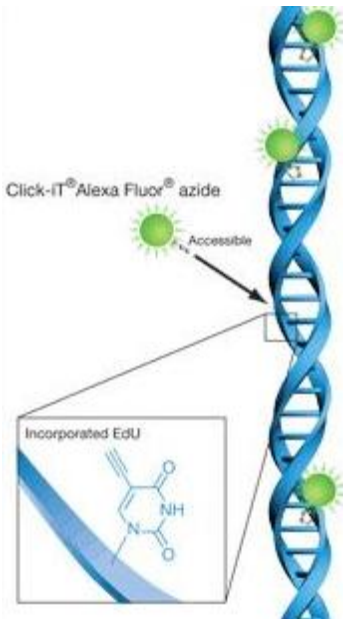


**Figure 3.26. Detection of the incorporated EdU with the Alexa Fluor azide.**

## 3.9. Apoptosis assays

Transfected HEK293 cells were plated on poly-L-Lysine coated 12 mm glass coverslips at a density of 40000 cells/well and incubated for 24-48h. After this time, apoptosis was detected by TUNEL method (*In Situ Cell Death Detection Kit,* Roche Applied Science, Germany), that identifies DNA strand breaks by enzymatic labelling with terminal deoxynucleotidyl transferase (TdT). This enzyme catalyzes polymerization of labelled nucleotides (fluorescein –dUTP) to the free 3'-OH termini. The assay was performed following manufacturer instructions. The positive and negative controls were cells treated with DNAse I (3000 U/ml, Ambion) before labelling and cells incubated without TdT respectively. Cells were incubated with Hoechst 33342 as described previously and mounted with Vectashield. Positive (apoptotic) cells were expressed as the percentage of the total cell number. In each experiment, at least 10 different fields were averaged for each condition.

## 3.10. Immunocytochemistry

Once transfected, HEK293 cells were seeded in 12 mm coverslips placed in the bottom of petri dishes 24 hours before the immunofluorescence assay. Then, they were fixed with 3.7 % formaldehyde in PBS for 10 minutes and blocked in 2 % of normal goat serum with PBS (nonpermeabilized cells) or Triton X-100, 0.1 % (permeabilized cells) for 15 minutes. Primary antibody was diluted in blocking solution and incubated with cells for 60 minutes. Nonpermeabilized cells were incubated with extracellular binding antibodies. Afterwards, cells were exposed to fluorescently labelled secondary antibody

in the respective blocking solution for another 60 minutes. Nuclei were stained with Hoechst 33342 (1:2000 in PBS) for 30 minutes. All incubations were made at room temperature, and several washes with PBS were made after each incubation. Coverslips were mounted onto glass slides using Vectashield (Vector Labs), and visualized under appropriate filters on a LEICA SP5 confocal microscope.

Primary and secondary antibodies are listed in table 3.13.

| Primary Antibody | | | Secondary Antibody | | |
|---|---|---|---|---|---|
| **Antibody** | **Company and Cat. No** | **Dilution** | **Antibody** | **Company and Cat. No** | **Dilution** |
| rabbit anti-Kv1.3 extracellular | Alomone Labs APC101 | 1:50 | Goat anti-rabbit 488 | Molecular Probes A-11008 | 1:1000 |
| rabbit anti-Kv1.5 extracellular | Alomone Labs APC150 | 1:50 | Goat anti-rabbit 532 | Molecular Probes A-11009 | 1:1000 |
| mouse anti-Kv1.3 COOH | NeuroMab 75-009 | 1:50 | Goat anti-mouse 532 | Molecular Probes A-11002 | 1:1000 |
| rabbit anti-Kv1.5 COOH | Alomone Labs APC004 | 1:50 | Goat anti-rabbit 594 | Molecular Probes A11012 | 1:1000 |

**Table 3.13. Primary and secondary antibodies used for immunocytochemistry assays.**

## Image analysis

Confocal images obtained from HEK293 cells transfected with different Kv1.3-Kv1.5 constructs were used to assess the relative expression of Kv1.3 and Kv1.5 constructs at the plasma membrane. 40x (1.25NA) or 63x (1.4NA) objectives were used to capture Z-stacks with a pinhole aperture of 1 Airy

and a voxel size compatible with the Nyquist criterion. EGFP (488ex/507em) or mCherry fluorescence (587ex/610em) were taken as a measure of total expression of the fusion proteins, whilst secondary antibody fluorescences: Alexa Fluor 594 (590ex/617em), 532 (531ex/554em) or 488 (495ex/519em) were taken as a measure of membrane expression, since extracellular primary anti-Kv1.3 and anti-Kv1-5 antibodies recognize an extracellular epitope and the immunocytochemical staining was performed in nonpermeabilized cells. Both images were binarized using a threshold automatically defined with the ImageJ software (http://rsb.info.nih.gov/ij/), and the number of pixels with a value of 1 was taken as an estimation of the image area filled with the Kv1.3-construct or Kv1.5-construct labelling: EGFP or mCherry images define the total area ($A_{Total}$), anti-Kv1.3 or anti-Kv1.5 images define the membrane area ($A_{Membrane}$). Both values are used to compute the % of membrane expression.

## 3.11. Inmunoblot

Total protein from HEK293 cells transfected with vectors expressing pEGFP-N3-mKv1.3 and the different pore and voltage sensor Kv1.3 mutants, was isolated using RIPA buffer (150 mM NaCl, 1 % NP-40, 0.5 % sodium deoxycholate, 0.1 % SDS, 50 mM Tris pH 8) and 1x protease inhibitor cocktail (Roche). Protein content was determined by using the BCA Protein Assay Kit (Pierce). Samples containing 50 µg of protein were heated for 5 minutes at 95 ºC and the proteins were separated by SDS-PAGE in 10 % Bis-Tris precast gels (Criterion XT precast gel, BioRad) and transferred to PVDF membranes. After blockade of the membranes with 5 % non-fat dry

milk in PBST (PBS with 0.1 % Tween 20), they were incubated with either mouse monoclonal anti-Kv1.3 (clone 23/27,Antibody Inc., USA) or mouse monoclonal anti-β-actin (ab8226, Abcam, Cambridge, UK) in blocking solution at a final concentration of 1:1000 for 1 hour. Then the membranes were washed with PBST, incubated with horseradish peroxidase (HRP) conjugated secondary antibody (donkey anti-mouse, BioRad) at final concentration 1:10000 for 1 hour and developed with VersaDoc 4000 Image System (BioRad) using chemiluminescence reagents (SuperSignal West Femto Chemiluminescent Substrate, Pierce Biotechnology).

### Digestion of glycoproteins with N-glycosidase F

HEK293 cells transfected with pEGFP-N3-mKv1.3, were resuspended in N-Glycosidase F incubation buffer (12.5 mM Na2HPO4, 1 % Triton X-100, 0.1 % SDS, 2 mM EDTA, 150 mM NaCl, 1 % (w/v) 2-mercaptoethanol and protease inhibitor cocktail). 40-50 µg of total protein were incubated with or without 0.7 units of N-glycosidase F (Roche) at 37 ºC for 18 hours with shaking. The digested samples were resolved by SDS-PAGE and subjected to anti-Kv1.3 western blotting as described above.

## 3.12. Immunoprecipitation

HEK293 cells platted onto 35 mm dishes were transfected with 0.4 µg of the selected plasmids. Afterwards, they were incubated with the corresponding treatments during the indicated times (see results) at 37 ºC in a 5% $CO_2$ humidified atmosphere. During the last 5 minutes of incubation, all cells were treated with pervanadate, an irreversible protein-tyrosine phosphatase

inhibitor. Pervanadate was prepared using a 30-minutes incubation at room temperature of 100 mM sodium orthovanadate and 0,3% hydrogen peroxide in distilled water, followed by dilution to 250 µM in cell culture media.

### RFP/GFP-TRAP®_A and Immunoblotting

After incubation and treatment, transfected cells were harvested in cold PBS and transferred to a precooled tube. They were centrifuged at 300x g for 4 minutes at 4 ºC and washed twice with cold PBS. Pellet was resuspended in Modified RIPA Buffer (MRB) (150 mM NaCl, 1 % NP-40, 0.2 % sodium deoxycholate, 50 mM Tris pH 8) with 1x protease inhibitor cocktail (Roche) and 1 mM of the phosphatase inhibitors sodium fluoride and sodium orthovanadate; and incubated for 15 minutes on ice. Samples were centrifufed at 12000x g for 10 minutes at 4 ºC and supernatant was stored at -20 ºC until used.

RFP/GFP-TRAP®_A contains small alpaca antibody fragments covalently coupled to the surface of agarose beads. 5-10 µl bead slurry were equilibrated in 500 µl ice cold MRB and spin down at 4000x g for 2 minutes at 4°C. Then, supernatant was discarded and beads were washed 2 more times.

In order to immunoprecipitate RFP/GFP fusion proteins, cell lysates (in MRB) were incubated 2 hours at 4°C under constant mixing with the already equilibrated RFP/GFP-Trap_A beads. The immunoprecipitates were centrifuged for 2 min at 8000x g and washed four times in MRB followed by 3 washing steps in 750 mM NaCl MBR. Finally, pellet was resuspended in MRB and used for immunoblotting.

Samples with XT Reducing Agent and XT Sample Buffer (BioRad) were heated for 10 minutes at 95 ºC and proteins were separated by SDS-PAGE in 10 % polyacrylamide gels and transferred to nitrocellulose membranes. After blockade of membranes with 3% BSA (Bovine Serum Albumin) or 5 % non-fat dry milk in PBST, they were incubated with either mouse monoclonal anti-Phosphotyrosine antibody, clone 4G10 (Milipore, MA, USA) or rat monoclonal anti-RFP antibody (5F8) or rat monoclonal anti-GFP (3H9) (ChromoTek, NY, USA) in blocking solution at a final concentration of 1:1000 at 4 ºC and overnight. Membranes were then washed with PBST, incubated with HRP-Goat anti-Mouse (Dako) or HRP-Goat anti-Rat (Abcam) secondary antibodies at final concentration 1:20000 for 1 hour and developed as previously indicated.

## 3.13. Electrophysiological recordings

Patch clamp techniques were used for the analysis of the currents expressed by the wild-type channels and the different mutants and chimeras constructed. In addition, we also use these techniques for the determination of the resting membrane potential (resting $V_M$) of transfected or mock-transfected cells. The different configurations of this technique allow us to study ion channels at different levels: either whole-cell (activity of all ion channels) or individual ion channels; and to manipulate the composition of the solutions bathing the extracellular or the intracellular side of the membrane during a recording.

In order to study ion channel behavior and record the membrane current, it is necessary to control membrane potential. This situation is called voltage

clamp and occurs usually through an electronic feedback system where a measured potential is compared with a potential set by the experimenter. The current needed to maintain the selected potential is the parameter we measure. In the other extreme, we can measure the changes in resting membrane potential in response to current injection or pharmacological stimuli, in a configuration called current clamp.

The patch clamp configurations (figure 3.27.) used in this thesis were:

### Cell-attached patch mode

The principle of this method is to record current flowing through an isolate patch of membrane. The patch is achieved by pressing a polished glass pipette against the cell membrane and applying light suction. This results in a high resistance seal (1 gigaseal). The cell-attached patch mode is therefore a single-channel configuration. Because the pipette is on the extracellular side of the membrane, it is usually filled with a solution with a composition close to extracellular media. As the patch resistance $R_{patch}$ is high compared with the resistance of the rest of the cell ($R_m$) and the pipette resistance ($R_{pipette}$), he circuit is going to monitor current flow through ion channels in the patch.

### Whole-cell mode

Whole-cell is obtained after gigaseal formation in cell-attached mode by breaking the patch of membrane under the pipette tip. To do so, an additional suction pulse is applied through the pipette pressure tubing. The pipette solution and the electrode are in direct contact with the cytoplasm. This solution resembles the ionic composition of the cytoplasm and will replace it.

As a consequence of the disruption of the patch, $R_{patch}$ becomes very low and is renamed the access resistance $R_{access}$. This configuration allows the observation of currents through membrane resistance $R_{m,}$ being this one the largest one. Because these currents are the sum of currents through all activated single channels of the cell, they are named whole-cell currents.

### Perforated-patch mode

Perforated patch recording allows us having a good electrical access without losing the preservation of the intracellular milieu. This configuration is gained from cell-attached mode and relies on the action of drugs to create holes in membranes of a very distinct size, permeable to ions but not larger molecules, most critically second messenger molecules. The pipette was filled with the same solution used in whole-cell containing amphotericin B (300 µg/ml). The perforate-patch configuration was used for the recording of membrane potential changes in the current-clamp configuration.

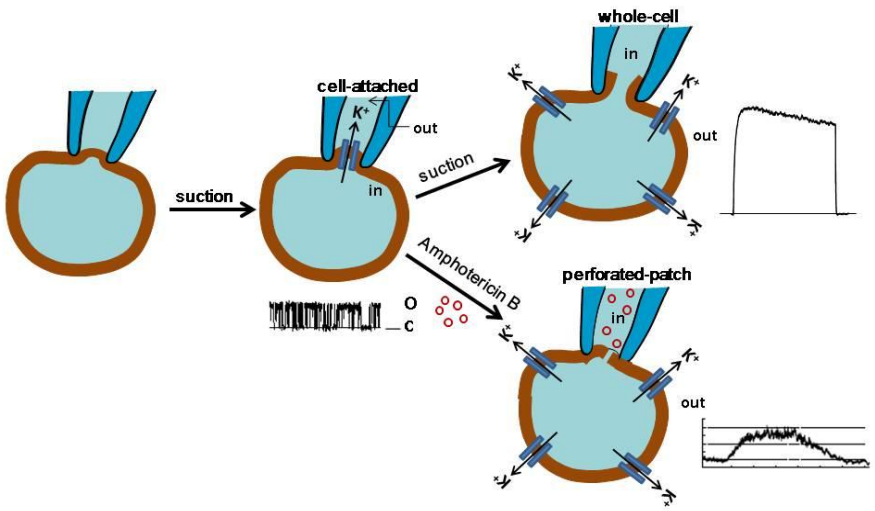


**Figure 3.27. Illustration of Cell-Attached, Whole-Cell and Perforated-Patch configurations. Once a Gigaohm seal is achieved between the patch pipette and the cell, single channel recordings are made in the cell-attached mode. If additional suction is applied to the seal, whole-cell is gained. Perforated-patch configuration was obtained by adding amphotericin B to the internal solution.**

Transfected HEK293 cells were seeded onto converslips and used for eletrophysiological recordings. Coverslips were placed into the recording chamber (0.2 ml) of a IX70 (Olympus, Tokyo, Japan) inverted microscope and superfused with external solution by gravity perfusion. All experiments were performed at room temperature on a vibration isolation table (TMC, Peabody, MA, USA).

Some of the ionic currents were recorded using the **whole-cell** configuration of the patch-clamp technique as previously described (Cidad et al 2012) Patch pipettes were made from borosilicate glass (2.0 mm O.D., WPI) and double pulled (Narishige PP-83) to resistances ranging from 4 to 8 MΩ when filled with an internal solution (high-$K_i$). The composition of the solutions is shown in table 3.14.. Outward $K^+$ currents were elicited by 200-800 ms depolarizing pulses from a holding potential of -80 mV to +40 mV applied in 10 seconds intervals. In some cells, full current/voltage curves were constructed from potentials ranging from -60 to +100mV in 10 mV steps. Kv1.3 component was defined as the PAP-1 (100 nM) or Margatoxin (10 nM) –sensitive current and Kv1.5 currents were dissected with their sensitivity to DPO (10 nM - 5 μM). In all cases, the effects of the drugs were calculated taken as control the averaged current amplitude before and after drug application.

**Cell-attached** recordings were used for the kinetic characterization of the currents. Internal and external solutions are shown in table 3.14. Current was elicited by 500 ms depolarizing pulses to +40 mV from a holding potential of -80mV. IV curves were constructed with 800 ms depolarizing pulses from -80 to +100 mV in 20 mV steps applied every 10 seconds.

Conductance curves were obtained from the amplitude of the fit to a mono-exponential function of the tail currents upon repolarization to -80 mV. After normalization to the maximal conductance ($G_{max}$) the data was fitted to a boltzmann function to obtain the $V_{1/2}$ of activation and the slope of the curve: $G/G_{max}=[1/(1+\exp\{(V-V_{1/2})/k\})]$, where V represents the pre-pulse potential and k the slope factor indicating the steepness of the relationship between voltage and current.

The steady-state inactivation was studied with a two-pulse protocol, in which a 200ms pulse to +40mV was preceded by a family 1,8 seconds depolarizing pulses from -100 to +40 mV in 20 mV intervals applied every 20 seconds. The peak current amplitude of the +40 mV pulse was normalized to the maximal amplitude (obtained with the -100 mV prepulse), plotted as a function of the prepulse potential, and fitted to a Boltzmann function: $I/I_{max}=[1/(1+\exp\{(V_{1/2}-V)/k\})]$, where $I_{max}$ represents the maximal current amplitude.

In order to determine the membrane potential in the cell-attached patch, we assumed that in the ***High-$K_e$*** there was no voltage difference across the cell membrane. This was confirmed with the measurement of the $[K^+]_i$ from an instantaneous IV curve. 100 ms depolarizing prepulses to +60 mV were followed by repolarization to potentials from -100 to +60 mV. The IV curve obtained allowed to determine the reversal potential of the current and to calculate $[K^+]_i$, so that we could correct the estimated transmembrane potentials.

Membrane potential measurements were performed with the **perforated-patch** configuration to avoid dialysis of intracellular medium. For these

experiments, recordings were obtained with an Axopatch 700A patch-clamp amplifier. The solution, which contains amphotericin B, used to filled pipette tips is shown in table 3.14. After obtaining a high-resistance seal, electrical access to cell cytoplasm was assessed by monitoring the increase in cell capacitance. At this point, the amplifier was switched to current-clamp mode and membrane potential was continuously recorded.. The composition of the bath solution was the same as the indicated for the voltage-clamp experiments.

The solutions and protocols used for gating current recordings are a modification of previous reports describing the gating charge movement in Kv channels (Bezanilla *et al.*, 1991;Perozo *et al.*, 1993;Wang *et al.*, 2007). The composition of the internal and external solutions is shown in table 3.14. Patch pipettes had resistances ranging from 1 to 3 MΩ when filling with the internal solution. Capacity compensation was routinely used, and series resistance was between 2 and 8 MΩ for all recordings. For some experiments, currents were recording using 60-75% series resistance compensation.

The voltage-dependence of $Q_{on}$, was studied with a series of depolarizing pulses of 10 ms duration from a holding potential of -120, ranging from -100 to +100 mV in 10 mV intervals. For the study of the voltage dependence of $Q_{off}$, after a 10 ms pulse from -100 to +40 mV to activate the channels, repolarizing pulses of 30 ms from -40 to -200 mV in 10 mV intervals were applied.

Charge measures ($Q_{on}$, and $Q_{off}$) were obtained by integrating the on and off gating currents over sufficient time to allow the currents to return to baseline.

Charge-Voltage (Q/V) relationships were constructed from the $Q_{on}$, or $Q_{off}$ elicited to variable test potentials with the above detailed protocols, and normalized to the maximum $Q_{on}$, or $Q_{off}$ respectively. The voltage dependence of gating charge movement was obtained from the fit of the normalized Q/V curves to Boltzmann functions.

Electrophysiological analyses were performed with both the CLAMPFIT subroutine of the PCLAMP software (Axon) and ORIGIN 7.5 software.

| | Whole Cell | | Perf-patch | Gating currents recordings | | Cell-attached | |
|---|---|---|---|---|---|---|---|
| mM | Int. Solution | Ext. Solution | Int. Solution | Int. Solution | Ext. Solution | Int. Solution | Ext. Solution |
| KCl | 125 | 4.7 | 40 | | | 30 | 150 |
| MgCl2-6H20 | 4 | 1.2 | | 1 | 1 | | 0.5 |
| HEPES | 10 | 10 | 10 | 10 | 10 | 10 | 10 |
| MgATP | 5 | | | | | | |
| EGTA | 10 | | | | | | 1 |
| Glucose | | 10 | | | 10 | | |
| CaCl2-2H20 | | 1.8 | 8 | | 1 | 2 | |
| NaCl | | 141 | | | | 120 | |
| K-Glutamate | | | 95 | | | | |
| Amphotericin B | | | 480 µg/ml | | | | |
| NMDG | | | | 140 | 140 | | |
| | pH 7.2 (KOH) | pH 7.4 (NaOH) | pH 7.2 (KOH) | pH 7.2 (ClH) | pH 7.4 (ClH) | pH 7.4 (KOH) | pH 7.4 (KOH) |

**Table 3.14. Internal and external solutions used for electrophysiology.**

## 3.14. Statistical Analysis

The composite data are expressed as means ± standard error of the mean (SEM). Statistical analysis was performed using paired or unpaired Student's t-test for comparison of two groups. Comparison of three or more groups

was conducted using One-Way Anova (Sigma Plot software). Differences were considered to be significant when $p<0.05$ (*), $p<0.01$ (**) and $p<0.001$ (***).

Correlation between membrane expression or proliferation and current amplitude (functional expression) was performed by regression analysis. Data was fitted to lineal regression plots, thus obtaining the p-value and R-Squared value.

# 4

# RESULTS

In this thesis, we proposed to continue our previous work on the characterization of Kv1 channels as markers of the phenotypic switch, by studing the functional contribution of Kv1.5 and Kv1.3 to phenotypic modulation and the mechanisms linking their expression to celll proliferation.

## Chapter 4.1. Molecular mechanisms involved in Kv1.3-induced proliferation

In previous work we characterized the ion channels expression profile associated with the phenotypic switch of mice femoral VSMC, finding an upregulation of Kv1.3 channels, whose functional expression was related to proliferation. However, Kv1.5 was the predominant channel in contractile VSMC, being almost absent in cultured VSMC (Cidad *et al.*, 2010). The analysis of other murine vascular beds confirmed these results. Moreover, Kv1.3 (MgTx- or PAP-1-sensitive currents) represented the largest fraction of Kv currents in both femoral and mesenteric cultured VSMC, while Kv1.5 currents (DPO-sensitive) were predominantly expressedin freshly dissociated VSMC (contractile phenotype) (Cidad *et al.*, 2012)

Similar results regarding functional expression of Kv1.3 and Kv1.5 were obtained in several vascular beds from human VSMC (Cidad *et al.*, 2014) suggesting that the ratio Kv1.3:Kv1.5 could represent a landmark of the phenotypic modulation.

However, the molecular mechanisms through which Kv1.3 and Kv1.5 could be enrolled in proliferation remain unknown. Our previous work discard the possibility of Kv1.3 being involved in proliferation through its role in

controlling $V_M$ (Cidad *et al.*, 2010). Therefore, our studies have been focused on determine other possible mechanisms linking Kv1.3 and Kv1.5 to proliferation. The easiest approach to these studies was the use of an heterologous expression in which we could manipulate the expression of the channels or use mutant channels, but first we needed to determine if Kv1.3 and Kv1.5 behaved in this system as in native VSMCs with regards to proliferation.

### 4.1.1. Validation of the heterologous system HEK293 cells to overexpress Kv1.3 and Kv1.5

Since VSMC are difficult to obtain in large amounts and hard to transfect efficiently, we first explored if our hypothesis held true in a system more amenable to modify Kv channels expression and thus to study the molecular mechanisms involved in their effects on cell proliferation. With this idea, we studied the effect of Kv1.3 and Kv1.5 overexpression on the proliferation rate of HEK293 cells, using 2 alternative methods: cell counting and determination of the percentage of cells entering S-phase of the cell cycle using Click-iT EdU.

First of all, we explored whether Lipofectamine, a cationic liposome reagent used to transfect cells, or the process of introducing foreign nucleic acids could have cell toxicity or any effect on normal proliferation rate of HEK293 cells. Figure 4.1. showed no differences in proliferation among untransfected, mock transfected, and cells transfected with an empty vector. Taking this into consideration, further experiments were made using the latter condition as control.

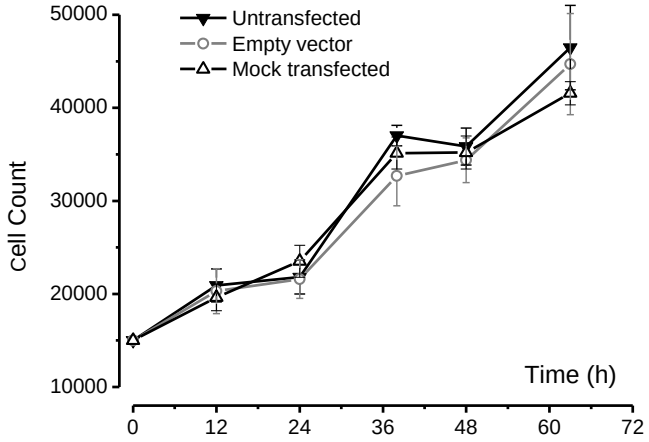


**Figure 4.1. Proliferation time course of HEK293 cells explored in untransfected, mock transfected or cells transfected with an empty vector. Each point is the mean±SEM of 5 to 8 experiments, with 4 to 8 different data points each.**

In order to explore the effects on proliferation of Kv1.3 and Kv1.5, we started by analyzing the temporal course of the effects by cell counting (figure 4.2A). Cells were counted at different times up to 4 days after transfecting HEK293 cells with 1 µg of the bicistronic vectors expressing Kv1.3 or Kv1.5 (dsRED2-IRES-mKv1.3 and pCMS-EGFP-hKv1.5). Kv1.3 overexpression significantly increased proliferation rate up to 60 hours after transfection, with a loss of this effect at longer times probably due to plasmid dilution with cell divisions. On the contrary, the expression of Kv1.5 had an anti-proliferative effect at all times explored. Further analysis of these cell counting experiments allowed us to define the duplication time and compare it between HEK293 cells transfected with the empty vector dsRED2-IRES versus those transfected with dsRED2-IRES-mKv1.3. Figure 4.2B shows that the increase cell number in cells overexpressing Kv1.3 correlates with a significantly

decreased duplication time, from 15 hours in control cells to 10 hours in Kv1.3-transfected ones.

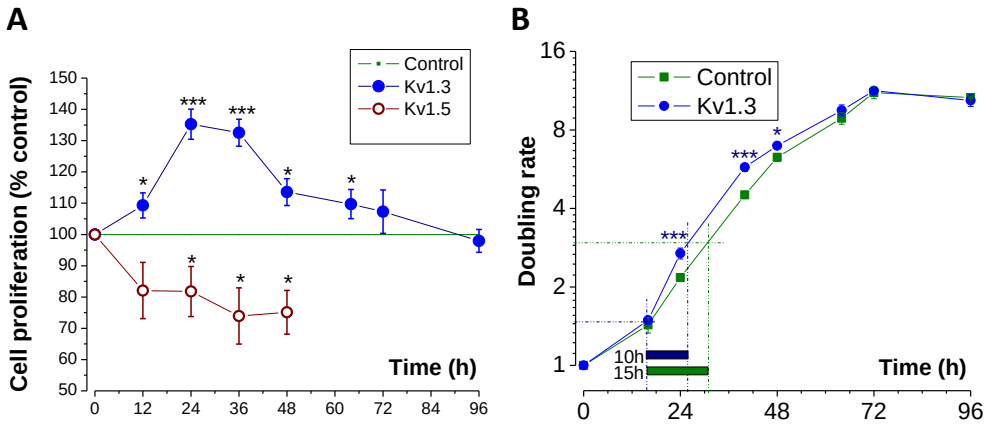


**Figure 4.2.A) Proliferation time course of HEK293 cells explored in cells transfected with plasmids expressing voltage-dependent potassium channel (Kv)1.3 (dsRED2ires-Kv1.3) or Kv1.5 (Kv1.5-EGFP). Data are normalized for the proliferation of dsRED2ires-transfected HEK293 cells (control; empty vector). B) Time course of the doubling rate of HEK293 cells transfected with dsRED2-ires-Kv1.3 and dsRED2-ires (control; empty vector). Each point is the mean±SEM of 5 to 8 experiments, with 4 to 8 different data points each.**

Due to the anti-proliferative effect shown in HEK293 cells overexpressing Kv1.5 and previous reports suggesting a pro-apoptotic role of Kv1.5 channels in some VSMC preparations (Remillard & Yuan, 2004) (Moudgil *et al.*, 2006), we examined whether Kv1.5 could be inducing apoptosis. Figure 4.3 represents average data of TUNEL assays in HEK293 transfected with pCMS-EGFP-hKv1.5, dsRED2-IRES-mKv1.3 or an empty vector (dsRED2-IRES). No evidence of increased apoptosis was observed in any condition in comparison with the empty vector.

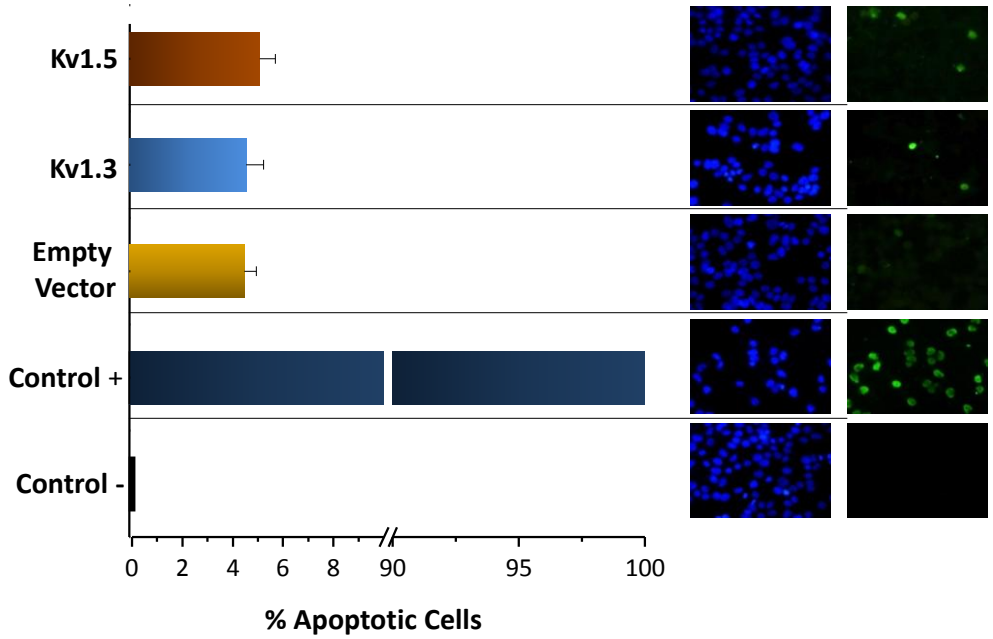


**Figure 4.3. TUNEL assays in HEK293 cells transfected with the maximal dose of the plasmid used in our studies (1 µg in a 35 mm petri dish). The positive and negative controls were cells treated with DNAse and untreated with the terminal deoxynucleotidyl transferase, respectively. Each bar is the mean ± SEM of 3-5 independent experiments.**

Next we explored if the induction of proliferation by Kv1.3 overexpression was "dose-dependent". When transfection of HEK293 cells was carried out with decreased amounts of Kv1.3 plasmid (to tritate down the current density) we found a good correlation between the rate of proliferation and the amplitude of the Kv currents recorded in the transfected cells (figure 4.4A, blue symbols), that saturated when higher amounts of plasmid (and higher currents) were obtained. In femoral VSMC, phenotypic switch associates with the increased expression of both Kv1.3 and Kvβ2.1. Because Kvβ2.1 has a chaperone effect increasing the functional expression of Kv1.3 channels (McCormack *et al.*, 1999) we have explored if Kvβ2.1

coexpression could affect HEK293 proliferation. Using different amounts of Kv1.3 plasmid alone or in combination with excess Kvβ2.1 plasmid we have confirmed the chaperone effect of Kvβ2.1 in electrophysiological studies (figure 4.4A, inset). However, Kvβ2.1 coexpression (figure 4.4A, pink symbols) did not elicit a proliferative effect different from the maximal effect obtained with Kv1.3 alone, suggesting that Kvβ2.1 effect on proliferation simply relates to its chaperon effect. Accordingly, Kvβ2.1 coexpression was able to significantly increase proliferation at low concentrations of Kv1.3 plasmid (figure 4.4B), but no additional effect was observed at saturating expression levels of Kv1.3 plasmid.

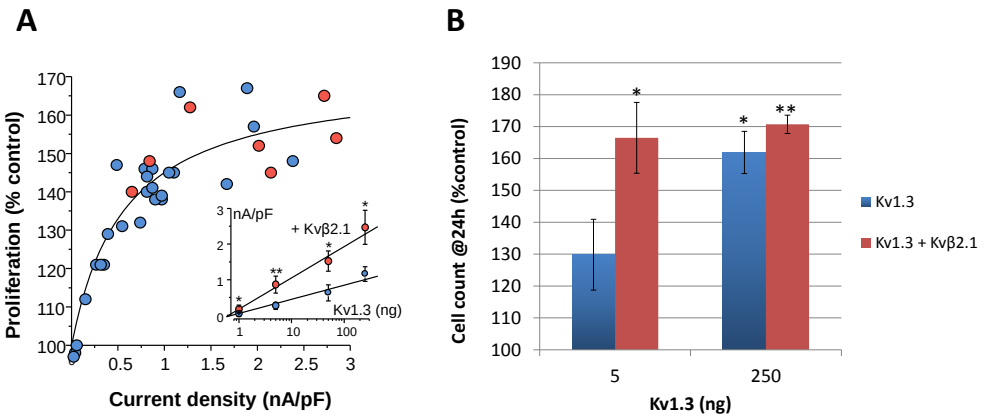


**Figure 4.4. A) HEK293 cells were transfected with increasing amounts (from 1–250 ng/35 mm dish) of Kv1.3 alone (blue symbols) or together with Kvβ2.1 (pink symbols), and both proliferation rate (determined by cell counting at 24 hours after transfection) and current density of the transfected cells (obtained from the current amplitude elicited in depolarizing pulses to +40mV) were monitored. Each current density data point is the average of 3 to 6 cells/culture. The line shows the fit of the data to a hyperbolic function (Pmax 170.6%, P0.5 0.57 nA/pF). The inset shows the current density obtained in HEK293 cells transfected with different amounts of Kv1.3 without (blue dots) or with (fpink dots) Kvβ2.1 subunit. Both groups of data were fitted to linear functions. Each point is mean±SEM of 6 to 12 determinations. B) The proliferation rate of HEK293 cells transfected with low (5 ng) and high (250 ng) amounts of Kv1.3 alone or in combination with excess of Kvβ2.1 are represented in the bars plot.**

The specificity of the effect of Kv1.3 on proliferation rate was confirmed by Kv1.3 pharmacological blockade. 24 and 40 hours after seeding transfected

dsRED2-IRES-mKv1.3 cells in presence or absence of MgTx 10 nmol/L, cell counting assays were performed. dsRED2-IRES cells in presence of MgTx 10 nmol/L were used as control. Figure 4.5A plots the pro-proliferative effect induced by Kv1.3 overexpression and its specific blockade in presence of MgTx 10 nmol/L at both times.

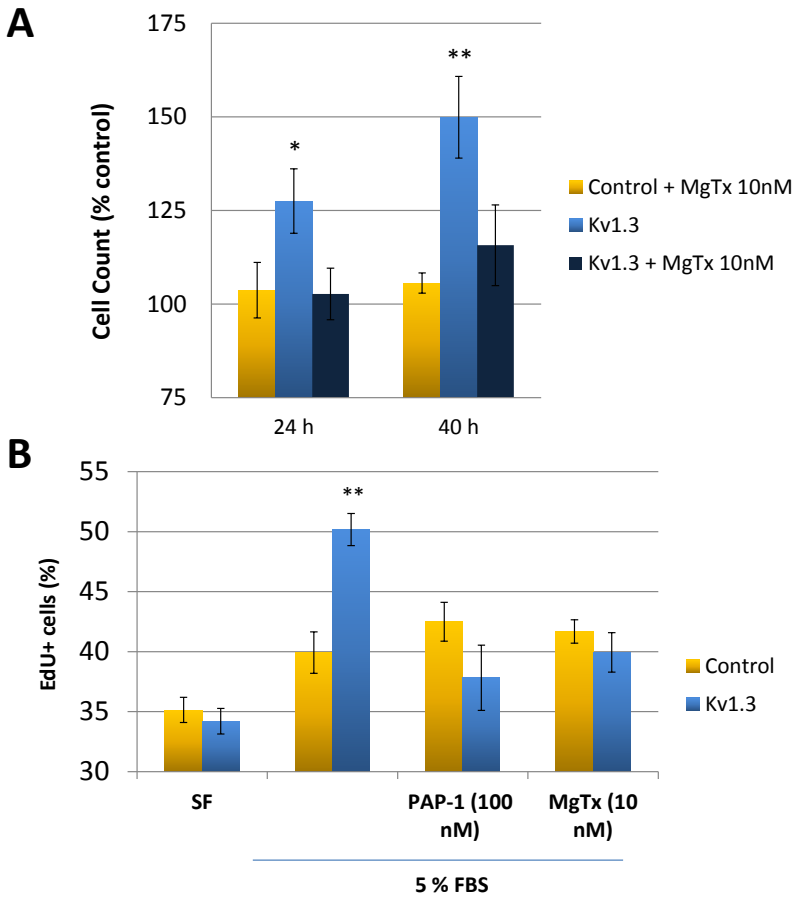


**Figure 4.5. A) The effect of treatment with 10 nmol/L MgTx on the proliferation rate was explored by cell counting at two different times after transfection (mean±SEM, n=4). B) Proliferation rate of HEK cell transfected with dsRED2-ires vector (control) or dsRED2-ires-Kv1.3 was determined by measuring the fraction of cells incorporating EdU reagent after 24 h incubation in serum-free media (SF) or with 5% FBS, alone or in the presence of MgTx or 5-(4-phenoxybutoxy) psoralen (PAP-1) (mean±SEM, n=4–10). Statistical significance was determined against control cells incubated with 5% FBS.**

Similar results were obtained using Click-iT EdU assay. Figure 4.5B, represents the summary data of the proliferation rate of control or dsRED2-IRES-mKv1.3 transfected cells. Serum-induced proliferation of HEK293 cells was significantly augmented in Kv1.3 transfected cells and could be abolished in the presence of MgTx (10 nmol/L) or PAP-1 (100 nmol/L). At these concentrations (within the range of complete blockade of Kv1.3 currents (Schmitz *et al.*, 2005;Garcia Calvo *et al.*, 1993)) the drugs had no effect on the proliferation rate of control cells.

### 4.1.2. Kv1.3EGFP fusion proteins as tools to generate Kv1.3 mutant channels

In order to explore the mechanisms through which Kv1.3 increases proliferation in HEK293 cells, we decided to generate Kv1.3 mutant channels. To start with, we fused enhanced green fluorescent protein (EGFP) or Cherry protein to the C-terminal of Kv1.3. Fusion proteins enabled us to determine subcellular distribution of all the mutants channels generated.

It has been observed that fusing fluorescent proteins to either the N- or the C-terminal of another proteins does not interfere with the localization and functional properties of the fusion partner (Stauber *et al.*, 1998;Ludin & Matus, 1998). In fact, green fluorescent protein (GFP) has been fused to Kv1.3 to transiently transfect HEK293 cells. The subcellular localization patterns, whole-cell voltage clamp recordings and kinetic analysis demonstrated that Kv1.3GFP fusion protein localized to the plasma membrane, formed functional potassium channels and displayed gating

kinetics indistinguishable from the wild-type channel (Kupper, 1998).Nevertheless, we compared proliferation rates in HEK293 cells transfected with Kv1.3 subcloned in bicistronic and fusion proteins vectors (figure 4.6) and found no differences when comparing Kv1.3 fusion protein to the corresponding bicistronic vector.

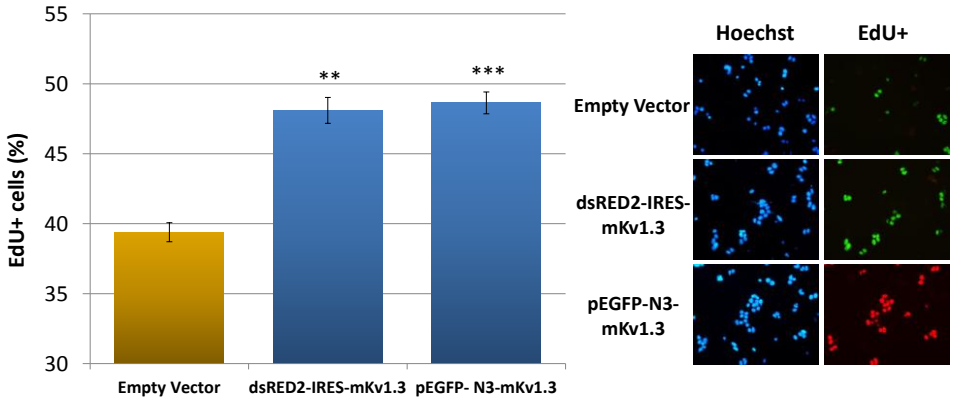


**Figure 4.6. Proliferation assay of HEK293 cells transfected with pEGFP-N3 (empty vector), the bicistronic vector dsRED2-IRES-mKv1.3 and the fusion protein vector pEGFP-N3-mKv1.3. Pictures represent a random field of each condition, showing the total number of cells in that field (Hoechst) versus proliferating cells (EdU+). Each point is mean±SEM of 4 determinations.**

### 4.1.3. Characterization of WT-Kv1.3 channel and Kv1.3-AYA, Kv1.3-W389F, and Kv1.3-WF3x mutant channels

#### *Protein expression characterization*

Voltage-dependent ion channels sense changes in membrane potential and catalyze ion fluxes that modulate those changes. Theoretically, the channel pro-proliferative effect could require the voltage-sensing, the $V_M$ modulation, or both. To distinguish between these options, we designed some Kv1.3 mutant channels in which one or the two functions were lost. We created 2 pore mutants and 1 voltage sensor and pore mutant: pEGFP-N3-Kv1.3AYA

(dominant-negative pore mutant), pEGFP-N3-Kv1.3W389F (nonconducting point mutant with intact gating properties) and pEGFP-N3-Kv1.3WF3x (nonconducting and voltage-insensitive channel).

Kv1.3 is a surface membrane protein which has a glycosylation site on its extracellular loop between S1 and S2. Oligosaccharides are modified in the biosynthetic pathway from the ER to the Golgi apparatus (Zhu *et al.*, 2001b;Zhu *et al.*, 2012). Thus, Kv1.3 can appear as a doublet on immunoblot with the upper band representing the mature sialylated form (present in the Golgi and on the cell surface), while the lower band represents the immature high mannose N-linked oligosaccharide form (present in the ER).

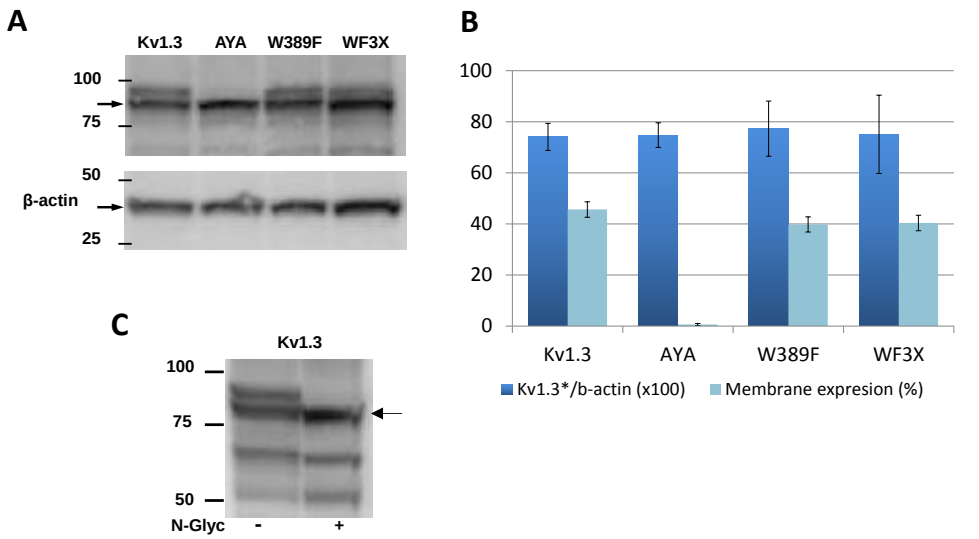


**Figure 4. 7. A) Immunoblot of cell lysates from cultures with anti-Kv1.3 antibody shows a band (upper arrow) of the expected molecular weight (in kDa, for the Kv1.3-EGFP fusion protein) and a band of higher molecular weight in all cases but in the Kv1.3-AYA expressing cells. Loading control (β-actin) of the same membrane is also shown. B) Dark blue bars show average data of Kv1.3 protein expression normalized to β-actin protein from several inmunoblots as the one shown in A. The light blue bars represent averaged fraction of extracellular anti-Kv1.3 labeling obtained from confocal images of nonpermeabilized cells as in figure 4.8. C) Immunoblot of cell lysates of Kv1.3 transfected cells treated overnight with N-glycosidase F.**

Whole cell protein lysates from HEK293 cells transfected with WT-Kv1.3, Kv1.3AYA, Kv1.3-W389F and Kv1.3WF3x channels were separated by SDS-PAGE and transferred to PVDF membranes which were probed with anti-Kv1.3 antibody. No differences in protein expression were observed for all Kv1.3 constructs, and the percentage of membrane expression was similar for Kv1.3, W389F, and WF3X. Moreover, immunoblot using anti-Kv1.3 revealed a band of the expected molecular size and an extra band of slightly higher molecular weight in all constructs but Kv1.3AYA (figure 4.7A, B). This extra band that reflects the N-glycosilation of the channel located at the plasma membrane, disappeared on treatment of the samples with N-glycosidase (figure 4.7C).

To examine the effects of AYA, W389F and WF3x mutations on Kv1.3 subcellular localization, transfected nonpermeabilized HEK293 cells were subject to standard immunocytochemical staining using the extracellular Kv1.3 antibody (figure 4.8.).

As the constructs were EGFP-fusion proteins, GFP fluorescence was used to detect Kv1.3 expression and location. HEK293 cells transfected with WT-Kv1.3 demonstrated two distinct patterns of staining: cell surface and perinuclear staining. Cell surface Kv1.3 staining was visible as positive antibody staining around the perimeter of the cell in all the constructs but Kv1.3AYA. Additionally, perinuclear staining was also visible in all conditions, being exclusive in Kv1.3AYA (indicative of intracellular retention), in agreement with the immunoblot data showing the absence of the N-glycosilated form for this mutant.

The confocal images obtained with the immunocytochemical staining of the different channels were analyzed in order to be able to quantify membrane expression of all the constructs. Membrane expression (%) was estimated by binarizing the images as described in materials and methods (figure 4.9.). Images were also taken as z-stacks through the cell to verify that the perimeter staining of Kv1.3 in fact represented cell surface staining.

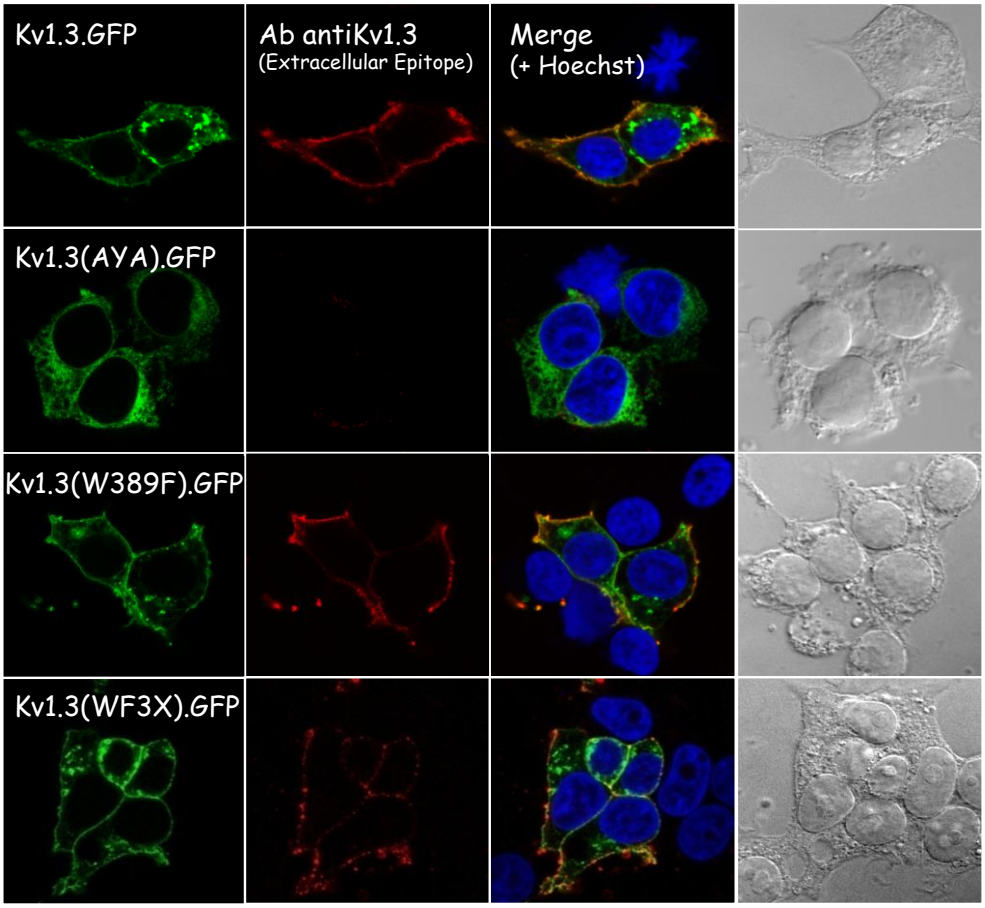


**Figure 4.8. Confocal images obtained in HEK293 cells transfected with vectors expressing GFP fusion proteins of voltage-dependent potassium channel (Kv)1.3 or the different Kv1.3 mutants. The panels show GFP fluorescence (green), labeling of nonpermeabilized cells with an extracellular anti-Kv1.3 channel (red), the nuclear staining with Hoechst (blue) and the bright field image.**

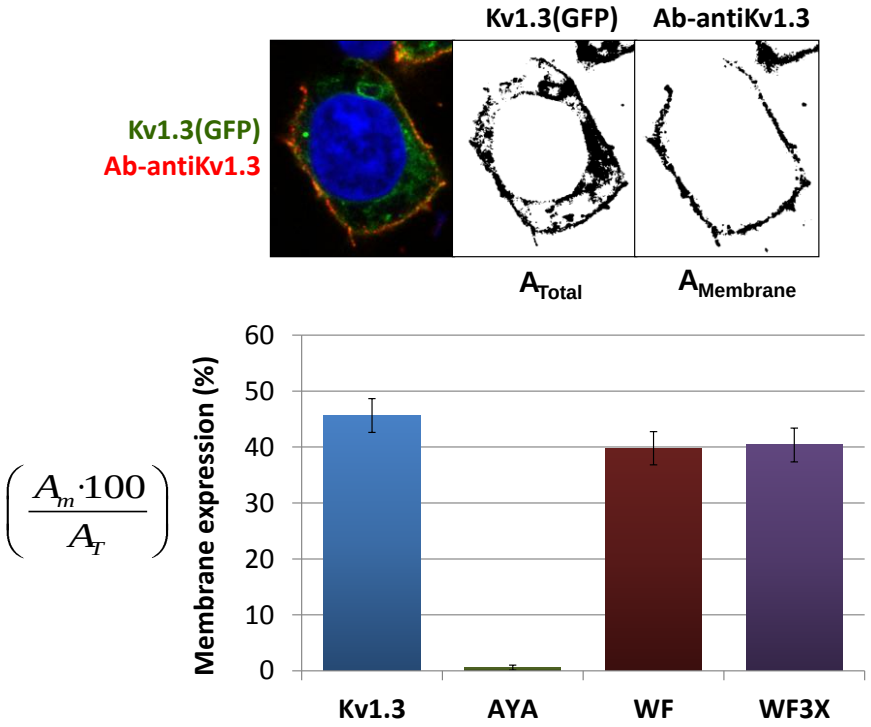


Figure 4.9. Protocol of image analysis carried out to estimate the membrane expression (%) of the different Kv1.3-GFP constructs used in this work. Color image illustrates a HEK293 cell transfected with Kv1.3-GFP (green) and labelled with anti-Kv1.3 (red). The nucleus was stained with Hoechst and appears in blue. Binary images are depicted in the right. Bars represent the average results (mean ± SEM) obtained in different experiments. Each value was obtained by averaging data from several confocal planes of 4 to 7 different cells in each condition.

### *Functional characterization*

Functional characterization of the channels was carried out with the patch-clamp technique (figure 4.10.). Although large voltage-dependent outward currents were recorded in WT-Kv1.3 channel-expressing cells (Figure 4.10 B), only gating currents could be recorded at the onset and the end of the pulse when cells expressed Kv1.3W389F mutant. Moreover, gating currents were absent in the Kv1.3WF3X mutant, as there are not conformational

changes along the range of voltages explored (figure 4.10A). Gating currents similar to the Kv1.3W389F mutant were disclosed in WT-Kv1.3 transfected cells when $K^+$ fluxes were almost completely blocked by replacing intra- and extracellular $K^+$ with N-methyl–D-glucamide (figure 4.10B).

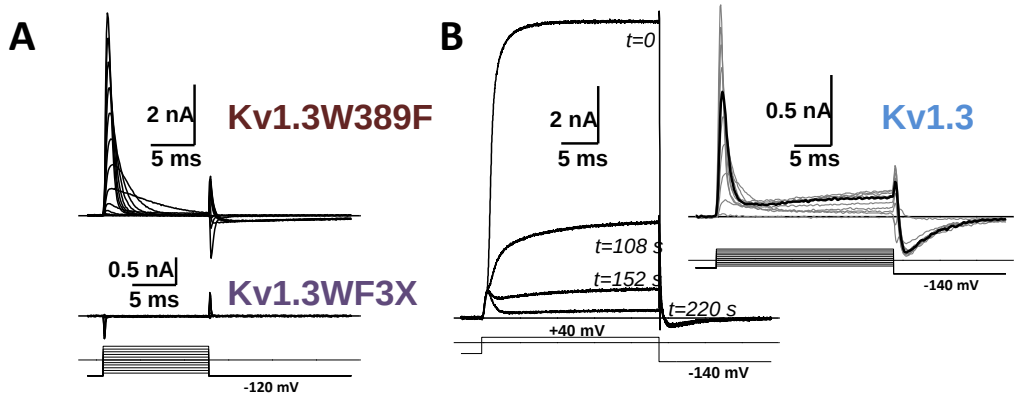


**Figure 4.10. A) Representative current traces obtained from the indicated constructs with external and internal high-$K_i$ solutions (bath and pipette, respectively) with the voltage protocol shown at the bottom. B) Whole-cell current traces from a Kv1.3-transfected cell illustrating K+ currents washout on intracellular dialysis with a solution free of K+ (replaced by N-methyl-D-glucamide). Trace labeled as t=0 was obtained immediately after breaking the patch. A family of current traces after complete dialysis is shown on the right panel (the thicker trace corresponds to the pulse to +40 mV). Recording solutions for gating currents.**

Additional confirmation of the behavior of the channels was obtained in current-clamp experiments, as only cell transfected with WT channels (Kv1.3 or Kv1.5) showed a significant hyperpolarization that in the case of Kv1.3 was sensitive to the selective blocker PAP-1 (100nM) (figure 4.11A and 4.11B).

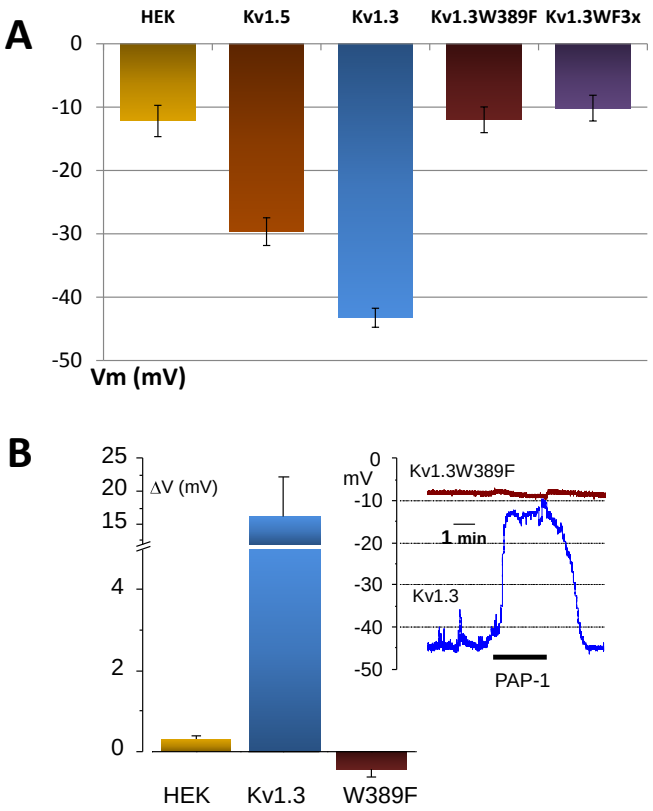


**Figure 4.11. A) Resting membrane potential ($V_M$) was measured with the perforated-patch configuration in all the conditions studied, including nontransfected HEK293 cells (HEK). Data are mean±SEM,n=8-15 cells. B) Effect of voltage-dependent potassium channel (Kv)1.3 blockers on $V_M$. The bars plot shows the change in $V_M$ (mean±SEM) on application of PAP-1, in control cells or cells transfected with Kv1.3 or Kv1.3W389F channels (n=8–10). Sample traces are shown in the inset.**

### 4.1.4. Modulation of proliferation by Kv1.3-pore and gating mutant channels

The effect of these Kv1.3 mutants on proliferation was assessed by cell counting and by Click-iT EdU assays with comparable results. HEK293 cells were transfected with pEGFP-N3-mKv1.3 and the mutants: Kv1.3AYA, Kv1.3W389F and Kv1.3WF3x. Cell counting experiments were made at different times up to 48 hours. Among the mutant channels, only Kv1.3W389F was able to induce proliferation, being the magnitude and the

time course of the effect indistinguishable from WT-Kv1.3 channels (figure 4.12A).

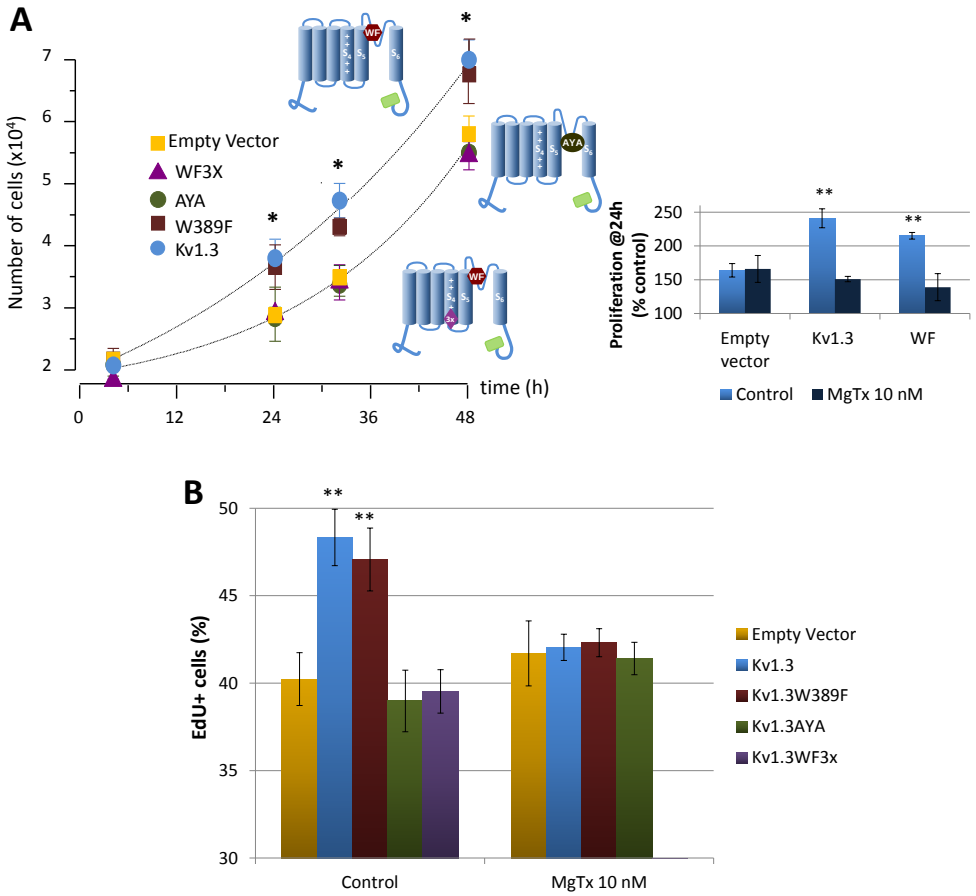


**Figure 4.12. A) Cell counting was used to determine proliferation rate of the different voltage-dependent potassium channel (Kv)1.3 mutants in parallel with proliferation of HEK293 cells transfected with the empty vector (control) and with the wild-type Kv1.3 channel (positive control). Each data point is the mean±SEM of 3 to 5 independent experiments. The inset shows the effect of 10 nmol/L MgTx treatment on proliferation (measured also by cell counting) of control cells or cells expressing Kv1.3 or Kv1.3W389F mutant at 24 hours post transfection. B) Percentage of cells incorporating EdU at 24 h posttransfection when transfected with the indicated constructs. Cells were maintained in 5% FBS (control) or in control media containing 10 nmol/L MgTx. Data are mean±SEM of 4 independent experiments with internal controls in all cases (empty vector and Kv1.3 transfected cells).**

Additionally, cell counting and Click-iT assays at 24 hours post-transfection were made to test the effect of Kv1.3 blockers. Both WT-Kv1.3 and Kv1.3W389F pro-proliferative effects were sensitive to MgTx 10 nmol/L (figure 4.12A, B). These results strongly suggest that modulation of proliferation by Kv1.3 channels requires gating movement but not $K^+$ permeation. Thus, the presence of the voltage sensor in the membrane is a requirement for Kv1.3-induced proliferation.

### 4.1.5. Effects of Kv1.3 pore blockers on Kv1.3W389F-induced proliferation

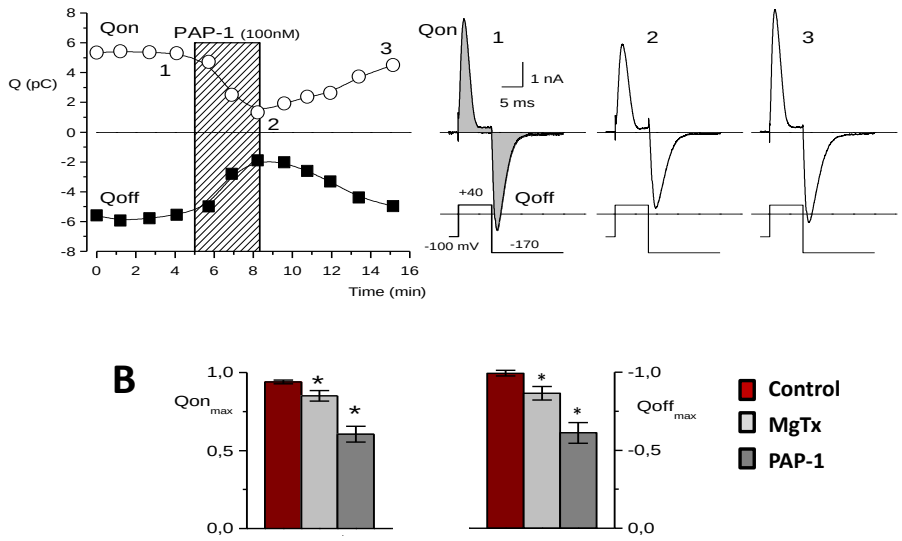


**Figure 4.13. A) Time course of the effect of PAP-1 100 nmol/L on gating charge movement of voltage-dependent potassium channel (Kv)1.3-W389F transfected cells on depolarization to +40 mV (Qon, grey dots) and repolarization to –170 mV (Qoff, black squares). Representative gating current traces at the indicated times 1,2,3 are shown on the right, with the voltage protocol depicted below the current traces. Shaded areas in the control trace represent the gating charge movement (current integral) elicited on depolarization (Qon) and repolarization (Qoff). B) Qon and Qoff voltage dependence of Kv1.3W389F mutants. Qon was obtained with the voltage protocol depicted in figure 4.10A in gating current external solution alone or with 10 nmol/L MgTx or 100 nmol/L PAP-1. Qoff was obtained with a family of pulses like that shown in panel A with repolarization from –40 to –200 mV. Data are mean±SEM of 4 to 6 different cells. Bar plots represent the average±SEM of the parameters fit to a Boltzmann function (Normalized Qon(max) and Qoff(max).**

The previous data were difficult to reconcile with our observation that Kv1.3 induced proliferation could be abolished by MgTx or PAP-1, because these two drugs are described as open channel blockers (Wulff *et al.*, 2009;Aiyar *et al.*, 1995;Garcia-Calvo *et al.*, 1993), which then suggest that ion fluxes through the channels are required. The characterization of the effects of MgTx and PAP-1 on Kv1.3W389F gating currents (figure 4.13.) indicated that these 2 blockers are able to interfere with the conformational changes associated with the movement of the voltage sensor. Figure 4.13A shows an example of the reversible effect of PAP-1 on the gating currents of a Kv1.3W389F transfected cell. MgTx and PAP-1 significantly reduced the maximal charge movement for the $Q_{on}$ and the $Q_{off}$ (figure 4.13B). Therefore, MgTx and PAP-1 may inhibit Kv1.3 by producing some charge immobilization, in addition to their effects blocking $K^+$ fluxes.

## Chapter 4.2. Identification of Kv1.3 and Kv1.5 intracellular domains involved in cell proliferation

Our results determine that Kv1.5 and Kv1.3 had opposite effects on proliferation and that Kv1.3 can modulate cell proliferation by an ion-flux independent mechanism. Additionally, previous work from our group in human VSMC from different vascular beds suggest that Kv1.3 induces proliferation acting through MEK/ERK and PLCγ signaling pathways (Cidad *et al.*, 2014). To confirm this hypothesis, hKv1.3 domains or residues that might directly interact with signaling proteins need to be identified. With the aim of gainning further understanding of the channel domains involved in proliferation, hKv1.3/hKv1.5 chimeric and mutant channels were generated.

The effect on proliferation of hKv1.3 overexpression was first studied to exclude functional differences between murine and human Kv1.3 in transfected HEK293 cells. As seen in figure 4.14., HEK293 cells overexpressing mKv1.3 or hKv1.3 had similar proliferation rates.

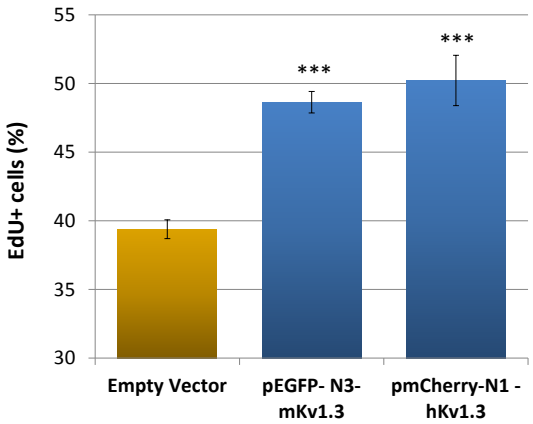


**Figure 4.14. Proliferation assay of HEK293 cells transfected with pEGFP-N3 (empty vector), pEGFP-N3-mKv1.3 or pmCherry-N1-hKv1.3. Each point is mean±SEM of 4 determinations.**

### 4.2.1. Characterization of K5C3 and K5N3 chimeric constructs

#### *Protein expression characterization*

We hypothesize that the different role of Kv1.3 and Kv1.5 channels modulating proliferation could reflect the specific association of those channels with intracellular proteins involved in different signaling pathways. To test that hypothesis we proposed to construct Kv1.3/Kv1.5 chimeras by switching the intracellular Kv1.3 C- or N-terminus into Kv1.5 backbone to pinpoint the relevant region of the channel, and creating K5C3 and K5N3 chimeras respectively. These constructs were created as fusion proteins with either GFP of Cherry and were transfected in HEK293 cells to check

their biophysical and pharmacological properties, and to characterize their effects on proliferation.

Immunocytochemical assays were performed in HEK293 cells overexpressing pmCherry-N1-K5N3 or pEGFP-N1-K5C3 (figure 4.15). The expression of either mCherry or EGFP were used as markers of chimeric channel transfection and location.

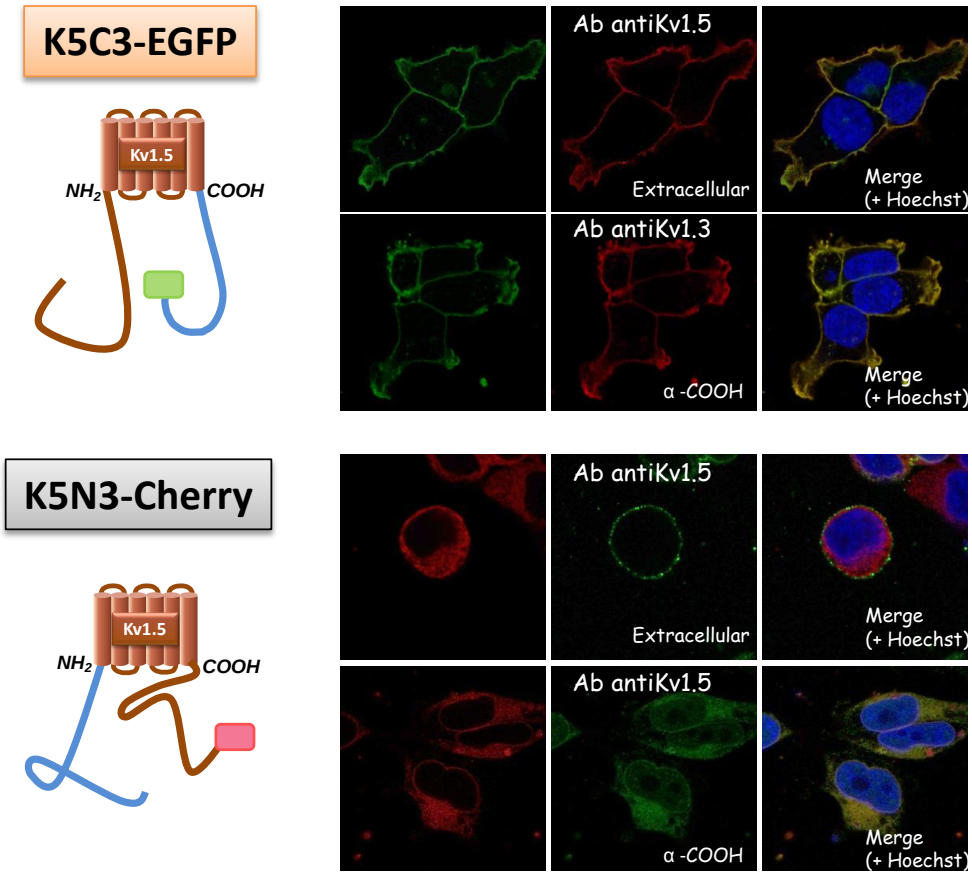


**Figure 4.15. Confocal images obtained in HEK293 cells transfected with vectors expressing K5C3-EGFP and K5N3-Cherry chimeric vectors. Membrane expression was determined in nonpermeabilized cells by labelling cells with an extracellular anti-Kv1.5 antibody (shown in red for K5C3 and in green for K5N3). Subcellular expression of K5C3-GFP and K5N3-Cherry was determined in permeabilized cells by using an anti-Kv1.3COOH antibody (red) and an anti-Kv1.5COOH antibody (green) respectively. Hoechst shows the nuclear staining (blue).**

Both chimeras showed cell surface Kv1.5 stainning, indicating that these chimeric channels are trafficking to the membrane. However, image quantitative analysis showed K5N3 had a much smaller ratio of cell surface/ER staining than K5C3 chimeric channel and WT-Kv1.5 (table 4.1.).

| | Kv1.5 | K5-532YS | K5-613YS | K5N3 | K5N3+β | K5C3 |
|---|---|---|---|---|---|---|
| **Mean % Cell surface expression** | **39,59** | **46,75** | **40,58** | **21,03**** | **25,74*** | **96,11***** |
| **SEM** | **3,03** | **5,70** | **4,45** | **1,66** | **2,47** | **4,01** |

**Table 4.1. Percentage of membrane expression of chimeric channels containing Kv1.5 backbone versus wild-type Kv1.5. Average data and SEM are represented (n=10-45). (*) Values significantly different ($p<0.05$) from WT-Kv1.5.**

### *Functional characterization*

Electrophysiological characterization of K5N3 and K5C3 chimeric channels was first made by studying their pharmacological properties. Since both chimeras comprise Kv1.5 backbone, DPO blockade was studied in whole-cell measurements. As seen in the representative traces in figure 4.16., DPO was applied at different concentrations, from 10 nM to 5 μM. Currents were elicited during a series of pulses to +40 mV. The initial current dimished in the presence of DPO in both K5C3 and K5N3 (figure 4.16A) chimeric channels. The dose-dependency and the IC50 of the effect of DPO on the currents was not different in the two cases,and was similar to the reported sensitivity of cloned Kv1.5 channels (Lagrutta *et al.*, 2006) (figure 4.16B).

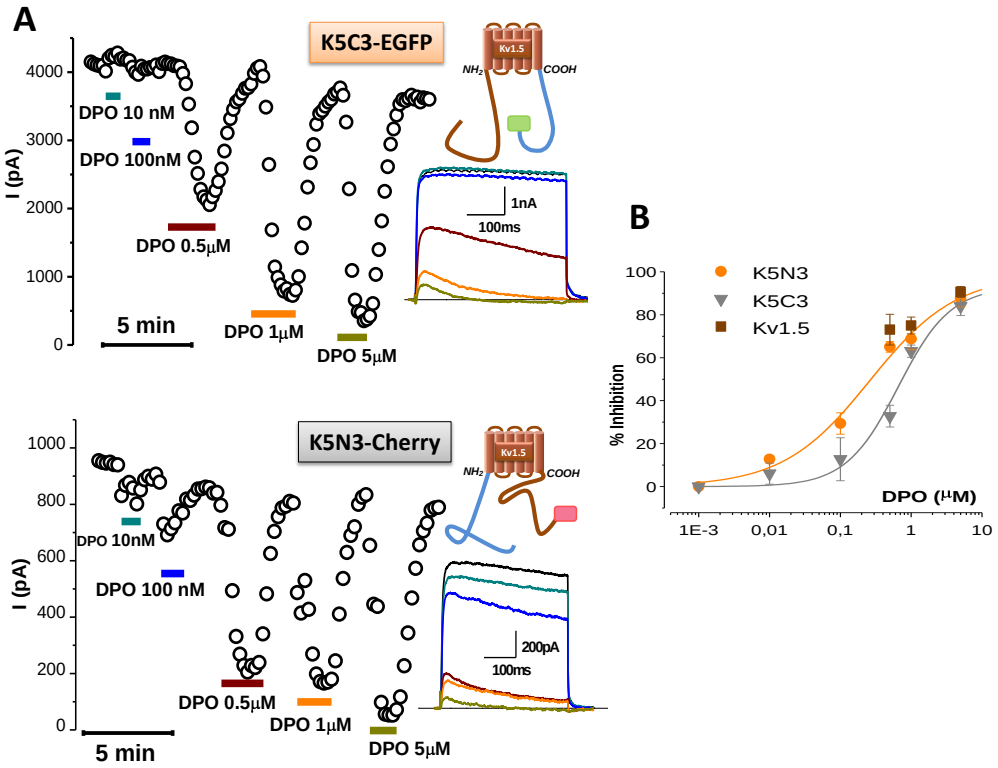


Figure 4.16. A) Representative data showing the effect of DPO (a selective Kv1.5 blocker) on the peak current amplitude elicited by depolarizing pulses to +40 mV in HEK293 cells expressing K5C3EGFP or K5N3Cherry chimeric channels. Current traces at the different DPO concentrations are also shown. B) The plot shows the dose-response curve for the effect of DPO on the current amplitude in both chimeric channels and WT-Kv1.5. Each data point is the mean±SEM of 9-18 cells.

The electrophysiological characterization includes, in addition to the pharmacological profile, an analysis of the kinetic properties of the channels. For this kinetic analysis we used the cell attached configuration, which allows a better space-clamp and a better voltage control. The most conspicuous differences between WT-Kv1.3 and WT-Kv1.5 currents, according to previous data in the literature, refer to the current amplitude (as single channel conductance is larger for Kv1.3 channels), the extent of time-dependent inactivation, and the voltage dependence of activation and

inactivation, in particular the values of the $V_{1/2}$. We first characterized these parameters in our Kv1.3 or Kv1.5 transfected cells.

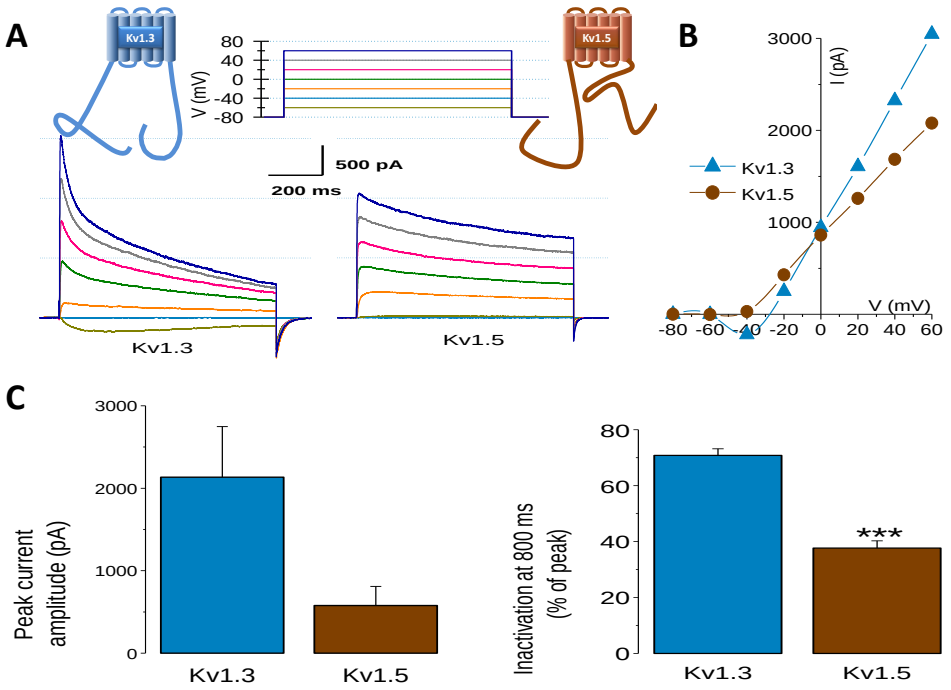


**Figure 4.17. A) Representative traces of HEK293 cells transfected with WT-Kv1.3 and WT-Kv1.5. Currents were elicited by 20 mV steps from -80 to +100 mV (pulse protocol, inset). B) I-V curve of Kv1.3 (blue triangles) and Kv1.5 transfected cells (brown circles). C) Bar plots show the average peak current amplitude and the percentage of peak inactivation at 800 ms of Kv1.3 and Kv1.5 transfected cells. Data are presented as mean±SEM; n=7-11.**

As shown in figure 4.17., Kv1.3 transfected cells expressed larger currents that inactivate faster along the duration of the pulse. To determine half maximal activation and inactivation potentials ($V_{1/2}$) (data shown in table 4.2.), voltage dependence of activation and steady state inactivation curves were normalized and fitted to Boltzmann equations. The analysis of the voltage-dependence of activation and inactivation indicated a clear

hyperpolarizing shift of around 20 mV for Kv1.3 channels (figure 4.18.). Also, the steady-state inactivation curve shows that while the fraction of inactivated current for Kv1.3 is around 90%, it is only half of the current in the case of Kv1.5 (see the differences of the curves at positive values).

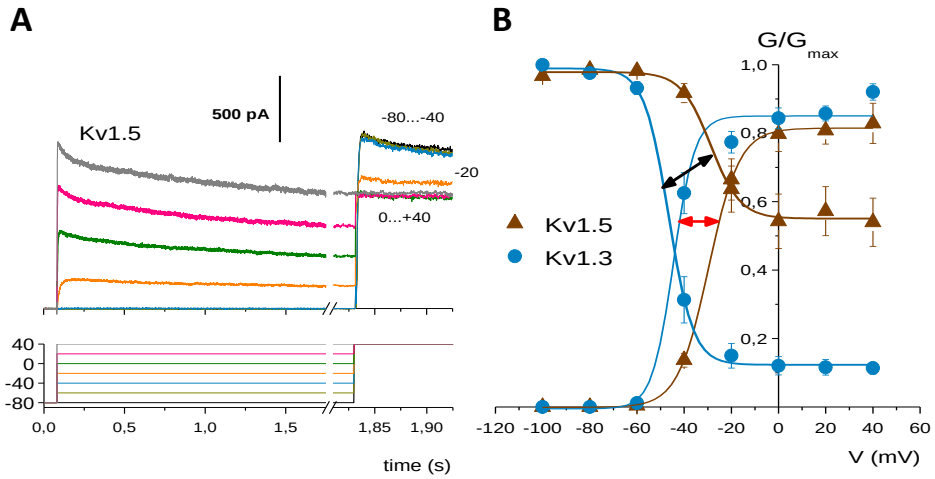


**Figure 4.18. A) Representative traces of Kv1.5 currents evoked by steady-state inactivation protocol (inset) in transfected HEK293 cells. B) Average conductance-voltage relations and Boltzmann fits for activation and inactivation of Kv1.3 or Kv1.5 transfected HEK293 cells. Both voltage dependence of activation and the steady-state inactivation of Kv1.3 shift by 20 mV to more negative potentials. Data are represented as mean±SEM (n=6).**

Voltage dependence of activation and inactivation for the chimeric channels was also studied in cell-attached experiments and the data obtained are shown in table 4.2. K5C3 and K5N3 parameters showed similar activation $V_{1/2}$ values as Kv1.5. However, with regards to inactivation K5N3 transfected HEK293 cells were found to be half inactivated at a similar voltage as Kv1.3, reflecting a Kv1.3 N-type inactivation.

| | Peak current (pA) +40mV | Inactivation at 800ms (%) | Activation | | Inactivation | |
|---|---|---|---|---|---|---|
| | | | $V_{1/2}$ (mV) | slope | $V_{1/2}$ (mV) | slope |
| **Kv1.3** | 2134.3 ± 631.1 (11) | 70.8 ± 2.3 (10) | -46.9 ± 2.8 (8) | 6.2 ± 1 (8) | -46.6 ± 1.7 (6) | 5 ± 0.5 (6) |
| **Kv1.3-Y447A** | 1618.6 ± 283.4 (5) | 62.1 ± 2.8 (5) | -50.2 ± 2.3 (5) | 7 ± 2.7 (5) | -48.7 ± 1.8 (5) | 3.6 ± 0.9 (5) |
| **Kv1.3-S459A** | 2325.2 ± 7094 (5) | 79.3 ± 3.4 (5) | -41.3 ± 4.2 (5) | 4.7 ± 1 (5) | -48.9 ± 7.8 (5) | 3.3 ± 0.5 (5) |
| **K3YS** | ***508.5 ± 139.2* (9)*** | 75.8 ± 4.1 (9) | ***-55.3 ± 2.8* (8)*** | ***3.3 ± 0.6* (8)*** | -44.2 ± 2.6 (6) | 3.9 ± 0.7 (6) |
| **K5C3** | 1077.1 ± 288.2 (13) | 38.9 ± 4.3 (13) | -20.4 ± 1.9 (11) | 10.6 ± 1 (11) | -31 ± 2.2 (6) | 5.3 ± 0.9 (6) |
| **K5N3** | ***41.3 ± 6.1* (7)*** | 35 ± 3 (7) | -25.9 ± 1.5 (7) | 5.3 ± 1 (7) | ***-41.7 ± 1.4** (6)*** | 4.3 ± 0.8 (6) |
| **K5N3+Kvβ2** | 170.7 ± 37.6 (8) | 40.7 ± 4.2 (8) | ***-39.6 ± 1.2** (6)*** | 6.6 ± 1.3 (6) | ***-45.5 ± 1.2*** (7)*** | 6.2 ± 1.3 (7) |
| **K5-532YS** | 241.6 ± 61.4 (8) | 30.9 ± 3.7 (8) | ***-14.8 ± 3.7** (8)*** | ***13.9 ± 1.5** (8)*** | -25.1 ± 1.9 (5) | 6.2 ± 0.7 (5) |
| **K5-613YS** | 252.6 ± 81.6 (10) | 29.6 ± 5 (9) | -22.2 ± 2.3 (10) | 10.7 ± 1.4 (10) | -30.2 ± 4.8 (7) | 5.9 ± 1.3 (7) |
| **Kv1.5** | 577.3 ± 234 (7) | 37.7 ± 2.6 (6) | -27.7 ± 1.6 (7) | 7.2 ± 0.8 (7) | -26.5 ± 3.1 (6) | 6.8 ± 1.9 (6) |

**Table 4.2. Kinetics of activation and inactivation of WT-Kv1.3 (dark blue grids), Kv1.3 mutant and truncated channels (light blue grids), WT-Kv1.5 (dark brown grids), and chimeric channels comprising Kv1.5 backbone (light brown grids). Voltage dependence of activation and steady-state inactivation curves were fitted to Boltzmann functions to obtain the following parameters: potentials of half maximal activation/inactivation ($V_{1/2}$) and the steepness of the relationship between voltage and current (slope). Data are represented as mean±SEM, the sample size is shown in brackets (n). (*) Values significantly different (P<0.05) from WT-Kv1.3 (light blue grids) or from WT-Kv1.5 (light brown grids).**

### 4.2.2. Effects of K5C3 and K5N3 on cell proliferation

Proliferation rate was studied in HEK293 cells transfected with K5N3 and K5C3 chimeras. In all cases, parallel experiments were carried out in cells transfected with WT-Kv1.3, WT-Kv1.5 and a control vector pEGFP-N1. When EdU incorporation assays were performed, both K5C3 chimeric channel and WT-Kv1.3 showed a significant pro-proliferative effect in

comparison with the control vector. On the other hand, K5N3 chimera showed an anti-proliferative effect similar to Kv1.5 and significantly different from the control vector (figure 4.19.). These data suggest that COOH domains in Kv1.3 and Kv1.5 are enrolled in the effects of both channels on HEK293 proliferation.

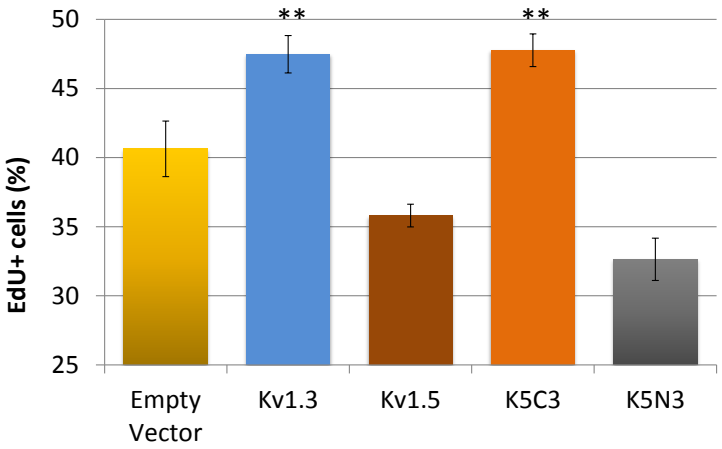


**Figure 4.19. EdU incorporation assay of HEK293 cells transfected with K5C3 and K5N3 chimeric channels in comparison with WT-Kv1.3 and WT-Kv1.5 transfected cells. Cells transfected with an empty vector were used as control. Mean±SEM, n=12-15.**

As for Kv1.5, we explored if the anti-proliferative effect of K5N3 could be due to the induction of apoptotic cell death. HEK293 cells were transfected with a control vector, with pEGFP-N1-hKv1-5 and with pmCherry-N1-K5N3. In addition, a positive and a negative control of the experiment were performed. Figure 4.20. represents average data of TUNEL assays. No differences in the percentage of apoptosis was seen when transfecting cells with K5N3 in comparison to the control vector or to pEGFP-N1-hKv1.5, suggesting that this chimera inhibits proliferation without inducing cell death.

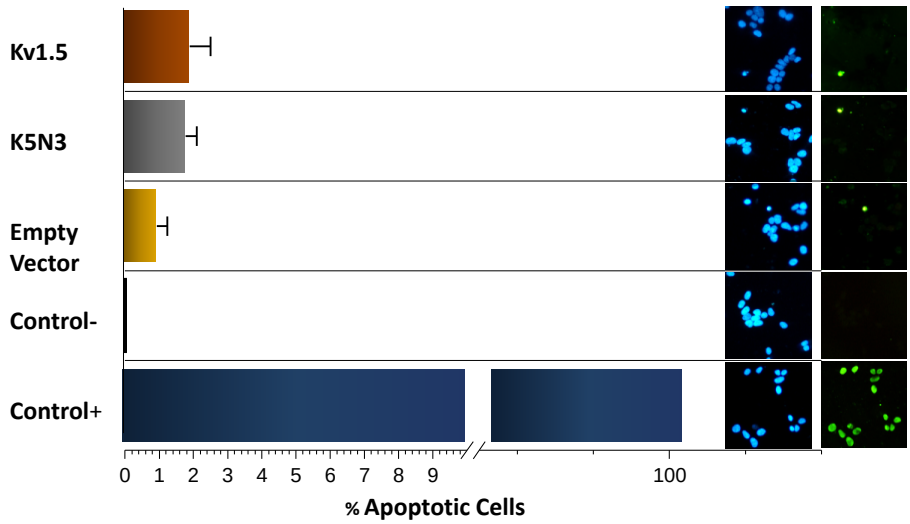


**Figure 4.20. TUNEL assay to determine apoptotic rate of HEK293 cells transfected with K5N3, Kv1.5 and an empty vector. Negative and positive controls of the experiment were carried out. Data are represented as mean±SEM (n=4). Pictures represent a random field of each condition, showing the total number of cells in that field (Hoechst; blue) versus apoptotic cells (green). Each point is mean±SEM of 4 determinations.**

K5N3 immunocytochemical assays revealed cell surface staining, indicating this chimeric channel is trafficking to the membrane. However, images also showed a big fraction of perinuclear staining, which correspond to channel retained in the ER (immature form). Moreover, K5N3 current density was smaller than WT-Kv1.5 or K5C3 chimeric channel currents. Either the reduced protein surface trafficking or the reduced functional expression of K5N3 could be thought to be related to decreased proliferation. To prove this point, we cotransfected K5N3 with the chaperon subunit Kvβ2.1. The chaperon effect of Kvβ2.1 with K5N3 was demonstrated by a significant increased of current density (figure 4.21A) and improved cell surface expression (figure 4.21B) (table 4.1.). By contrast, no significant changes in proliferation rate were observed when comparing HEK293 cells expressing

K5N3 chimera alone or together with Kvβ2.1 (figure 4.21C), so we conclude that the effect of K5N3 on proliferation is solely due to its molecular structure.

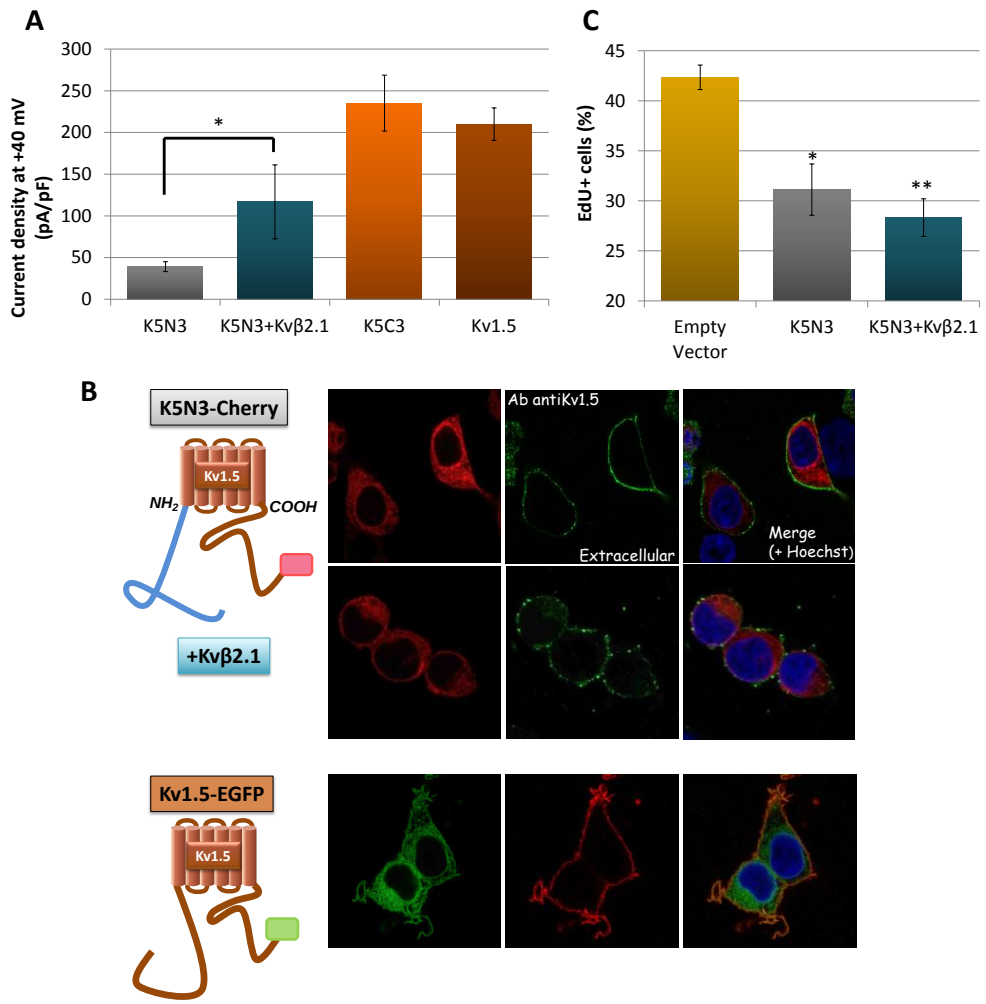


**Figure 4.21. A) Current density at +40 mV of HEK293 cells transfected with WT-Kv1.5, K5C3 chimeric channel and K5N3 alone or in combination with the chaperone subunit Kvβ2.1. Data are represented as mean±SEM (n= 6-17). B) Upper confocal images are nonpermeabilized HEK293 cells transfected with K5N3-Cherry chimeric channel alone or in combination with Kvβ2.1; and labeled with an extracellular anti-Kv1.5 antibody (green). Lower confocal images show nonpermeabilized cells transfected with Kv1.5-EGFP and also labeled with an extracellular anti-Kv1.5 antibody (red). C) EdU incorporation assay of cells transfected with an empty vector as control and K5N3 chimeric channel with or without Kvβ2.1. Mean±SEM (n=4).**

### 4.2.3. Characterization of Kv1.3 C-terminal point mutants

The data presented in the previous section indicate Kv1.3 COOH-terminal domain is involved in Kv1.3 pro-proliferative effect. With this initial result, we sought to investigate in more detail what regions, domains or residues could be responsible for this effect.

The activity of membrane proteins such as ion channels can be modulated by many potential molecular mechanisms. Among all of these mechanisms, protein phosphorylation constitutes one of the major molecular mechanisms influencing properties of voltage-gated channels.

Protein phosphorylation by protein kinases can take place at serine, threonine and tyrosine residues. In this way, protein kinase signaling pathways can participate in the regulation of ion channel properties, altering their metabolic and signaling processes. Thus, several protein kinases can modulate a particular ion channel, each influencing channel activity in a unique way (Levitan, 1994b).

Candidate-site approaches have been used to identify COOH residues critical to phosphorylation-dependent regulation of Kv1.3 function. The contribution of all the predicted phosphorylatable residues within the C-terminus of Kv1.3 has been explored by generating different mutant constructs. Independent point mutations to alanine of 8 residues: T439, Y447, S459, S470, S473, S457, Y477 and T493 have been generated. Some of these residues are part of the protein sequence domains that are recognized by AMP kinase and the insulin receptor motif (see figure 5.2.).

### *Protein expression characterization*

After creating the point mutations to alanine of the selected residues we study whether any of the point mutations was affecting Kv1.3 trafficking by means of immunocytochemistry assays and confocal microscopy analysis.

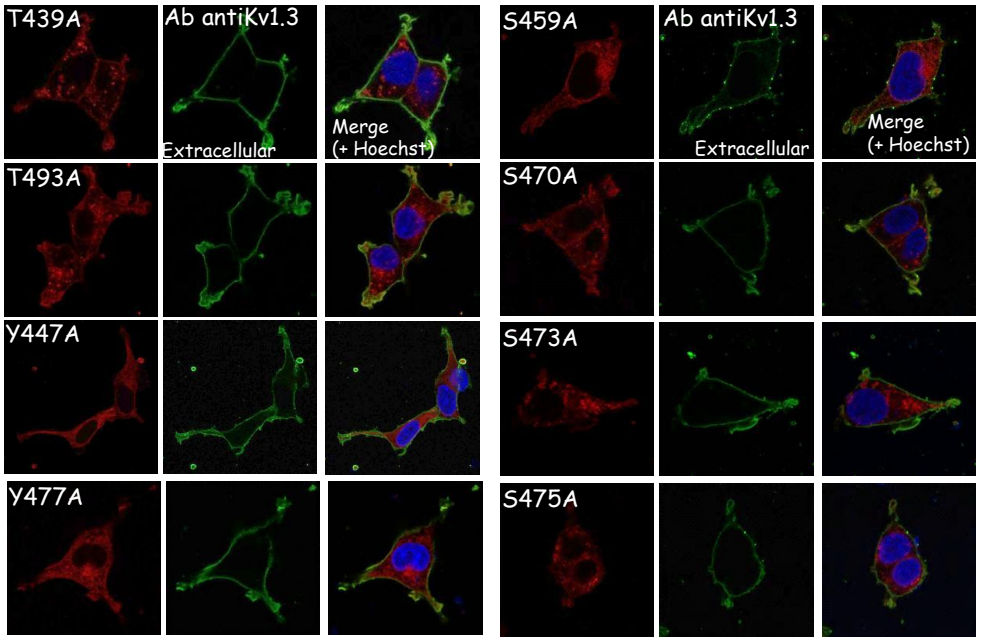


**Figure 4.22. Confocal images from HEK293 cells transfected with the point mutant Kv1.3 channels indicated in the image panels. All mutant channels are expressed as Chery-fusion proteins. Nonpermeabilized cells were labeled with an extracellular anti-Kv1.3 antibody (green). Nuclei were stained with Hoechst (shown in blue). Each point mutation is indicated in the schematic picture.**

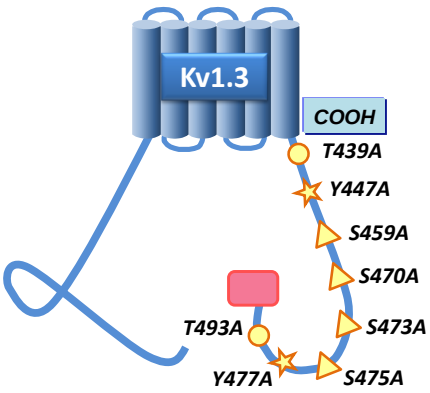

HEK293 cells transfected with Kv1.3 mutant constructs pmCherry-N1-hKv1.3-(T439A, Y447A, S459A, S470A, S473A, S457A, Y477A and T493A) were incubated with rabbit extracellular Kv1.3 primary antibody. Goat anti-Rabbit 488 secondary antibody labeled Kv1.3 green and Nuclei were stained by Hoechst (figure 4.22.). All mutant constructs displayed similar proportions of ER and cell-surface staining pools when comparing them to WT-Kv1.3, suggesting all these mutants formed mature Kv1.3 channels, trafficking properly to the membrane (table 4.3.).

| | Kv1.3 | S475A | S473A | S470A | S459A | T493A | T439A | Y477A | Y447A | K3YS |
|---|---|---|---|---|---|---|---|---|---|---|
| Mean % Cell surface expression | 41,14 | 42,95 | 46,51 | 47,39 | 42,11 | 39,97 | 43,31 | 34,14 | 36,80 | 35,18 |
| SEM | 1,96 | 4,31 | 3,25 | 3,25 | 4,81 | 1,76 | 2,37 | 2,55 | 4,78 | 4,60 |

Table 4.3. Percentage of membrane expression of mutant channels containing Kv1.3 backbone versus wild-type Kv1.3. Average data and SEM are represented (n=10-22).

### *Functional characterization*

In most of the cases, the density of surface expression was also tested with functional studies, determining whole-cell currents (figure 4.23B). As observed in the immunocytochemical analysis, no significant changes in current density were shown in any of the mutants studied in comparison with the WT-Kv1.3. Additionally, we explore in more detail the kinetic properties of Y447A and S459A point mutations. Cell-attached experiments performed in these two mutants provide kinetic parameters indistinguishable from WT Kv1.3 channel (table 4.2.).

### 4.2.4. Effects of single mutations Kv1.3 C-terminal residues on cell proliferation

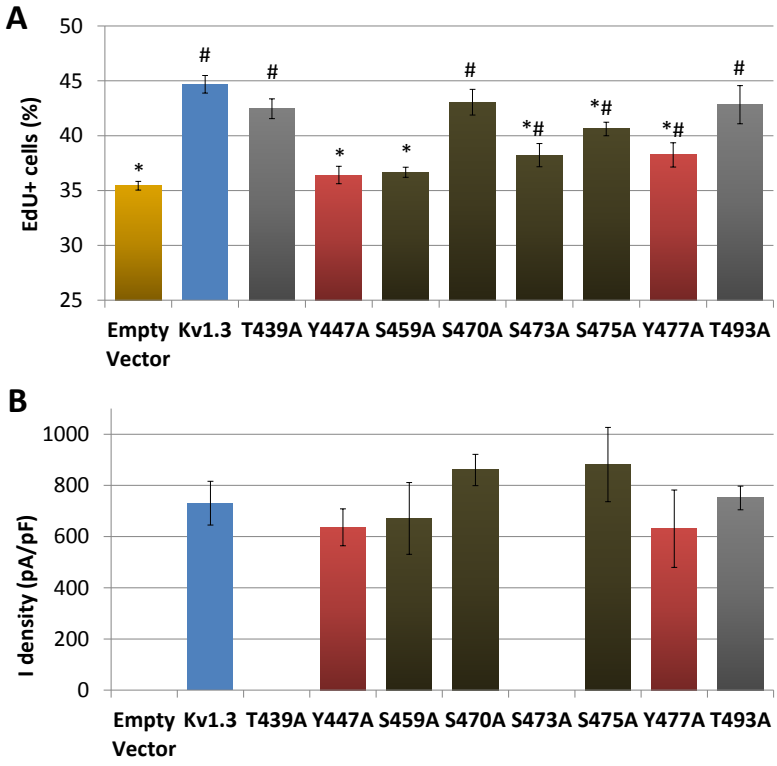


Figure 4.23. A) EdU incorporation assay of HEK293 cells transfected with the point mutant Kv1.3 channels indicated in the plot, WT-Kv1.3 and an empty vector as controls. Data are represented as mean±SEM. Sample size is 6-20 determinations from 7 different experiments. Values significantly different (P<0.05) from WT-Kv1.3 (*) and/or from the empty vector (#) are shown. B) Whole-cell measurements from some of the point mutants and the WT-Kv1.3 channel. N=5-8.

To explore if any of the COOH-terminal mutated residues was involved in the proliferative effect of Kv1.3 channels, EdU incorporation was measured in HEK293 cells transfected with each mutant, pmCherry-N1-hKv1.3 and a control vector. Figure 4.23A plots proliferation rate of all of these constructs. One-way Anova was performed to explore significance among COOH mutants and pmCherry-N1-hKv1.3 (*) and among COOH mutants and the control vector, pmCherry-N1 (#). T439A, S470A and T493A were not

different from WT hKv1.3 channels while S473A, S475A and Y477A were significantly different from both the control vector and hKv1.3. Finally, Y447A and S459A were significantly different from hKv1.3, fully abolishing its pro-proliferative effect, as they were the only two constructs that were not different from control, cherry-transfected cells vector. The latest data suggest these two residues in the COOH-terminal domain of Kv1.3 might play an important role in proliferation. We speculate that one of both these two residues, Y447 and S459 could be the sites of interaction of Kv1.3 with other proteins involved in the signaling cascades leading to cell proliferation.

### 4.2.5. Characterization of K3YS, K5-532YS and K5-613YS chimeric channels

Residues Y447 and S459 seem to determine in an important way the pro-proliferative effect of Kv1.3 channels. Of interest, while phosphorylation of these residues (in particular Y447) has been previously described (Holmes *et al.*, 1996), when searching for consensus phosphorylation sequences, these two residues do not seem to have clearly identified associated kinases. In order to validate their participation in Kv1.3 induced proliferation, we explore if a 16-amino-acid-residue fragment containing Y447 and S459 will suffice to sustain increased proliferation of Kv1.3 and to induce proliferation when present in Kv1.5 channels.

A truncated Kv1.3 channel was created (K3YS) where amino acids 461-523 had been deleted so that only the YS fragment was left. In addition, this fragment was subcloned into two different positions of Kv1.5 COOH-terminus (K5-532YS and K5-613YS). K5-532YS has YS fragment in the

analog Kv1.3 position of the COOH-terminal domain, while in K5-613YS the YS fragment was cloned at the end of the COOH-terminus.

### *Protein expression characterization*

To study subcellular localization trafficking and expression of these chimeras, HEK293 cells were transfected with pmCherry-N1-K3YS, pEGFP-N1-K5-532YS and pEGFP-N1-K5-613YS to be characterized by immunocytochemistry (figure 4.24.). When studying cell surface and ER staining ratio, no significant differences were seen versus their respective WT-channel backbones (table 4.1 and table 4.3.).

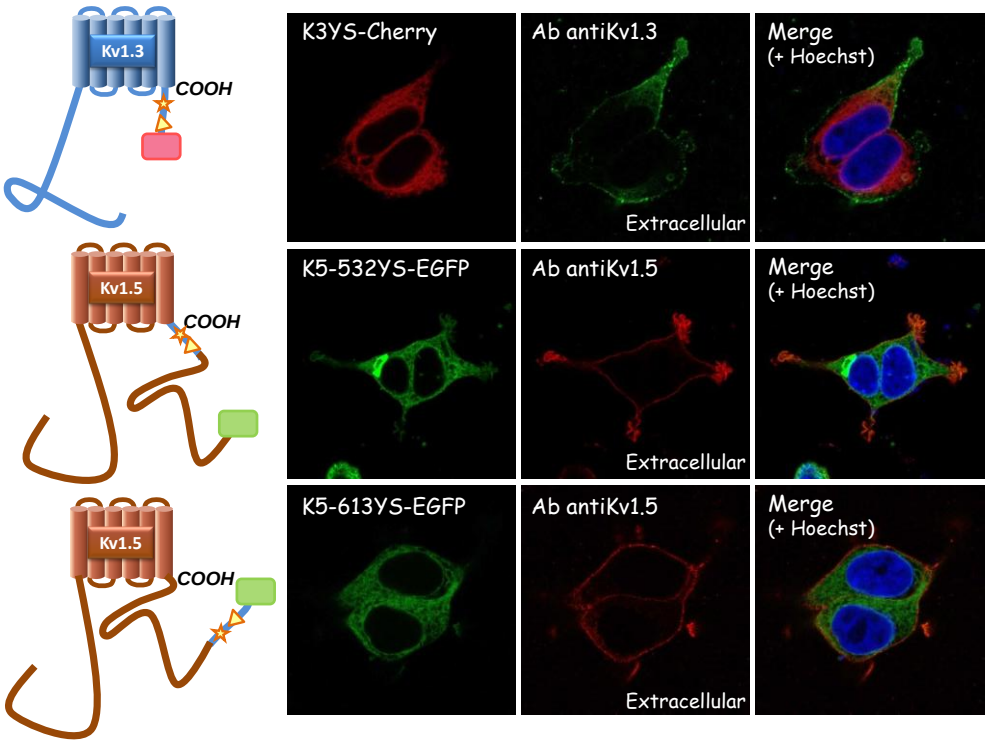


**Figure 4.24. Confocal images of nonpermeabilized HEK293 cells transfected with the truncated channel K3YS-Cherry, and the chimeric channels K5-532YS-EGFP and K5-613YS-EGFP. An extracellular anti-Kv1.3 antibody (green) labelled K3YS, while an extracellular anti-Kv1.5 antibody (red) was used for K5-532YS and K5-613YS chimeras. Nuclei were stained by hoechts (blue). Pictures on the left represent the truncated and chimeric constructs.**

### *Functional characterization*

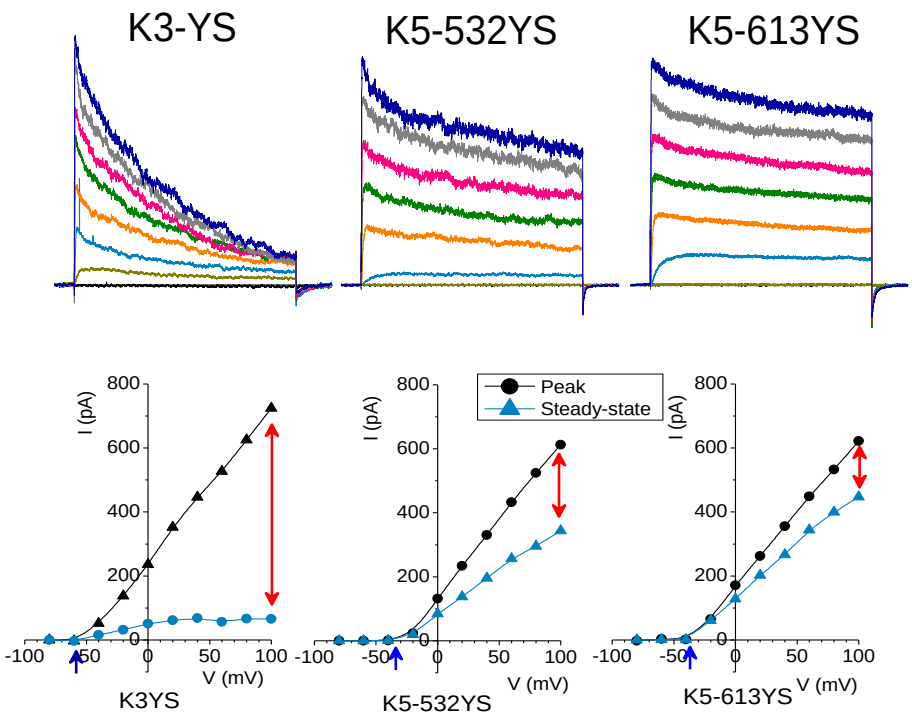


**Figure 4.25. Representative family of traces from transfected HEK293 cells (K3YS, K5-532YS and K5-613YS). Currents were elicited by 20 mV steps from -80 mV to +100 mV. I-V curves were constructed with the values of the peak current amplitude (black curve) and the amplitude at the end of the 800 ms pulse (blue curve) for each voltage, showing the fraction of inactivated channels for each condition (red arrow).**

Cell-attached experiments were performed to determine functional expression and kinetics of the channels. No significant changes in current amplitude were observed among the three mutants (Figure 4.25 and table 4.2). Both voltage dependence of activation and time-dependent inactivation of the K5-532YS and K5-613YS chimeric channel were similar to those in WT-Kv1.5 channel, while in the case of K3YS these parameters were closed

to Kv1.3 ones. Figure 4.25. shows these differences in the activation threshold (blue arrow) and the fraction of inactivated current at the end of the 800 ms pulse (red arrows) between the truncated channel K3YS and the chimeric channels K5-532YS and K5-613YS,. In addition the detailed kinetic analysis showed that K3YS activated at even more hyperpolarized potentials than Kv1.3 and with a steeper voltage-dependency (table 4.2). When compared with Kv1.5 parameters, no differences with K5-613YS were observed, while K5-532YS showed a significant depolarizing shift of the $V_{1/2}$ of activation and a decreased in the voltage-dependency, indicated by a significant increase of the activation slope (table 4.2).

### 4.2.6. Role of YS fragment on cell proliferation

The role in proliferation of the YS fragment from the COOH terminus of Kv1.3 channels, which comprises Y447 and S459 residues, was studied by measuring EdU incorporation of transfected K3YS, K5-532YS and K5-613YS HEK293 cells (figure 4.26.). As controls, we used HEK293 cells transfected with WT-Kv1.3, WT-Kv1.5 and Cherry. As we have seen in previous studies, Kv1.3 was able to significantly increase HEK293 proliferation while Kv1.5 had an opposite effect. When exploring K5-532YS and K5-613YS effects, K5-613YS and WT-Kv1-5 showed similar proliferation rates while K5-532YS showed a significant increased cell proliferation in that was not different from WT-Kv1.3. On the other hand, K3YS was able to increase proliferation over the control but did not reach WT-Kv1.3 proliferative rate. These results suggest that 1) YS fragment is able to induce proliferation but not sufficient to reach WT-Kv1.3 proliferation rate, 2) this

fragment is not able to increase proliferation when subcloned at a random position into Kv1.5, 3) YS fragment is, however, a critical region to increase proliferation when subcloned into Kv1.5 at the Kv1.3 analog position.

Therefore, YS fragment plays a prominent but not exclusive role in Kv1.3 pro-proliferative effect that could be mediated by the interaction of this region with signaling proteins.

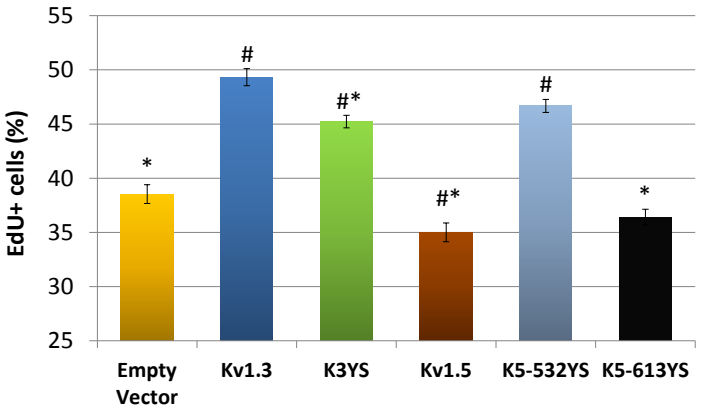


**Figure 4.26. EdU incorporation assay of HEK293 cells transfected with the truncated channel K3YS and the two chimeric channels K5-532YS and K5-613YS. HEK293 cells transfected with an empty vector, WT-Kv1.3 and WT-Kv1.5 are used as controls. Values significantly different (P<0.05) from WT-Kv1.3 (*) and/or from the empty vector (#) are shown.**

### 4.2.7. Study of the involvement of Kv1.3 Y447 and S459 residues in the pro-proliferative signaling pathway

Preliminary work from our group explored the effects of different MAPK blockers on human VSMC proliferation. The results showed that blockers of the MEK1/2-ERK1/2 signaling pathway reduced proliferation significantly, being PD98059 able to significantly reduce, by more than 70%, PDGF-induced proliferation. Moreover, in the presence of PD98059, the

application of PAP-1 (100 nM) or MgTx (10 nM) did not reduce proliferation any further, suggesting Kv1.3 could modulate proliferation through ERK1/2 signaling pathway (Cidad *et al.*, 2014).

Bearing this in mind, we decided to test whether PD98059 could also blocked Kv1.3-induced proliferation in a heterologous system. Additionally, we explored the effects of this blocker in the two Kv1.3 point mutants Y447A and S459A and HEK293 transfected with an empty vector as control. Average data from Click-iT assays is shown in figure 4.27. PD98059 was able to significantly reduce Kv1.3-induced proliferation, while it had no effect on either the control vector or the Kv1.3 point mutants.

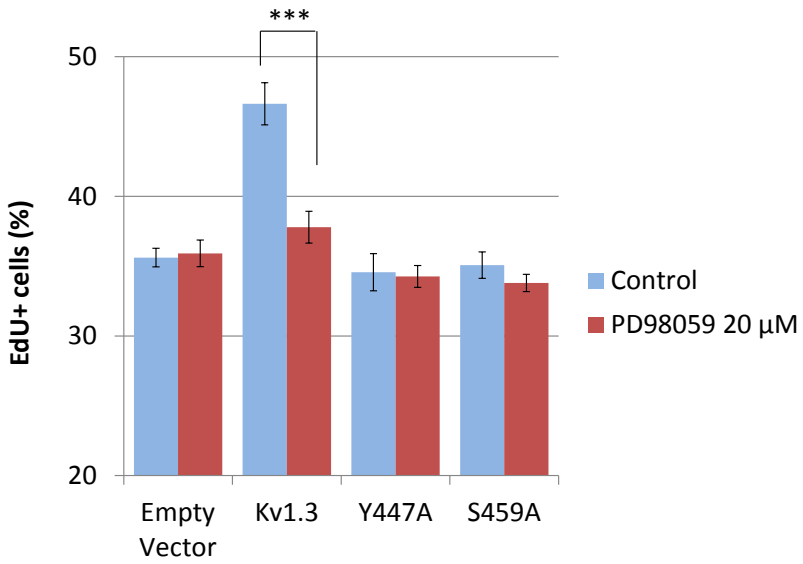


**Figure 4.27. EdU incorporation assay of HEK293 cells transfected with an empty vector, WT-Kv1.3 channel, Kv1.3-Y447A and Kv1.3-S459A mutant channels with (red bars) or without (blue bars) PD98059 (20 µM) treatment.**

These results were confirmed by immunoprecipitation followed by western blot analysis. RFP-TRAP® coupled to agarose beads bound Cherry fusion

proteins and, therefore, its interacting partners. Thus, we were able to pull down WT-Kv1.3 and Kv1.3-Y447A transfected cells that had been pretreated with pervanadate, a protein-tyrosine phosphatase inhibitor, and with or without PD98059. Once the targeted proteins had been immunoprecipitated, immunoblot was performed to measure the tyrosine phosphorylation of the proteins. Mouse Anti-Phosphotyrosine antibody revealed a greater tyrosine phosphorylation level in WT-Kv1.3 transfected cells that was reduced when pretreating cells with PD98059 (figure 4.28.).

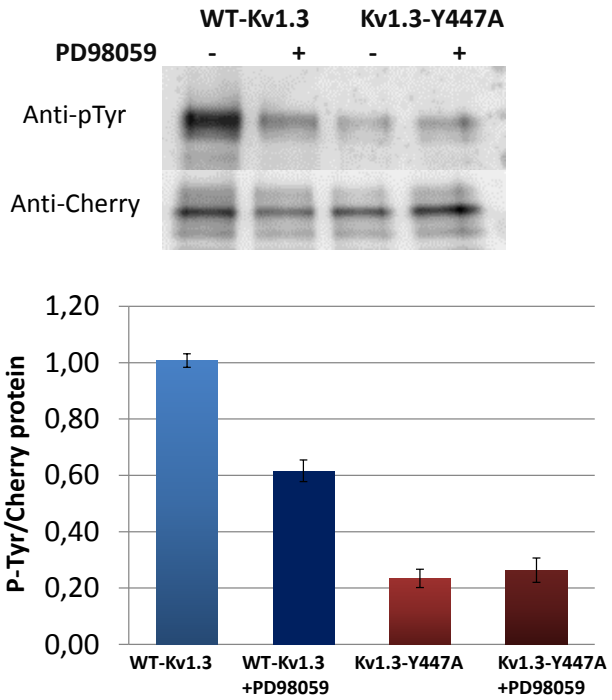


**Figure 4.28. Representative immunoblot and densitiometric (mean±SEM) values of 4-6 different experiments for WT-Kv1.3 and Kv1.3-Y447A transfected HEK293 cells. These cells were immunoprecipitated after incubation with (+) or without (-) PD98059 20 µM, and pervanadate (added to all conditions). The target protein bands were at the expected molecular weight (~84 KDa).**

These data obtained in HEK293 cells supports our results in human VSMC, suggesting that Kv1.3 could be inducing proliferation through ERK1/2 pathway and that both Y447 and S459 residues could play an important role in this pro-proliferative mechanism.

The location of this tyrosine within the channel protein seems to be also relevant for the effect on proliferation (as illustrated with the differences between Kv1.5-532YS and Kv1.5-613YS). This could be attributed to conformational changes of the channel that expose this residue. In Kv channels, these changes occur physiologically upon membrane-potential variations. In support of this observation, we found an increased P-tyr labelling of Kv1.3 channels when the cells are incubated in high extracellular $K^+$ solutions (5.4, 10, 20 and 60 mM $K^+_e$) during 20 minutes, a manoeuvre that promotes depolarization (figure 4.29A). Tyr-phosphorylation of Kv1.3 channels was increased with short (5 min) incubations in media with 60 mM $K^+_e$ (figure 4.29B). The resting $E_M$ value obtained in Kv1.3 transfected cells averaged -43 mV (Cidad *et al.*, 2012), so that we estimate that increasing $K^+_e$ from 5.4 mM to 60 mM will depolarize the cells to -14 mV. This value of $E_M$ is above the $V_{1/2}$ of activation of the channel (table 4.2.). The p-Tyr labelling of Kv1.3 channels decreased to control values when the high $K^+_e$ incubation was maintained for longer times (2 hours), suggesting that this response is determined by the acute conformation change. Also in support of these observations, the degree of Tyr phosphorylarion of Kv1.3 channel mutants is increased in a poreless channel mutant (Kv1.3-W389F), as the channel does not hyperpolarize the cells and resting $V_M$ is around -15 mV. However, in the pore and gating mutant Kv1.3-WF3x, which does not have

voltage gating transitions and, at the resting $V_M$ is in the inactivated stated, the degree of Tyr phosphorylation is decreased (figure 4.29C).

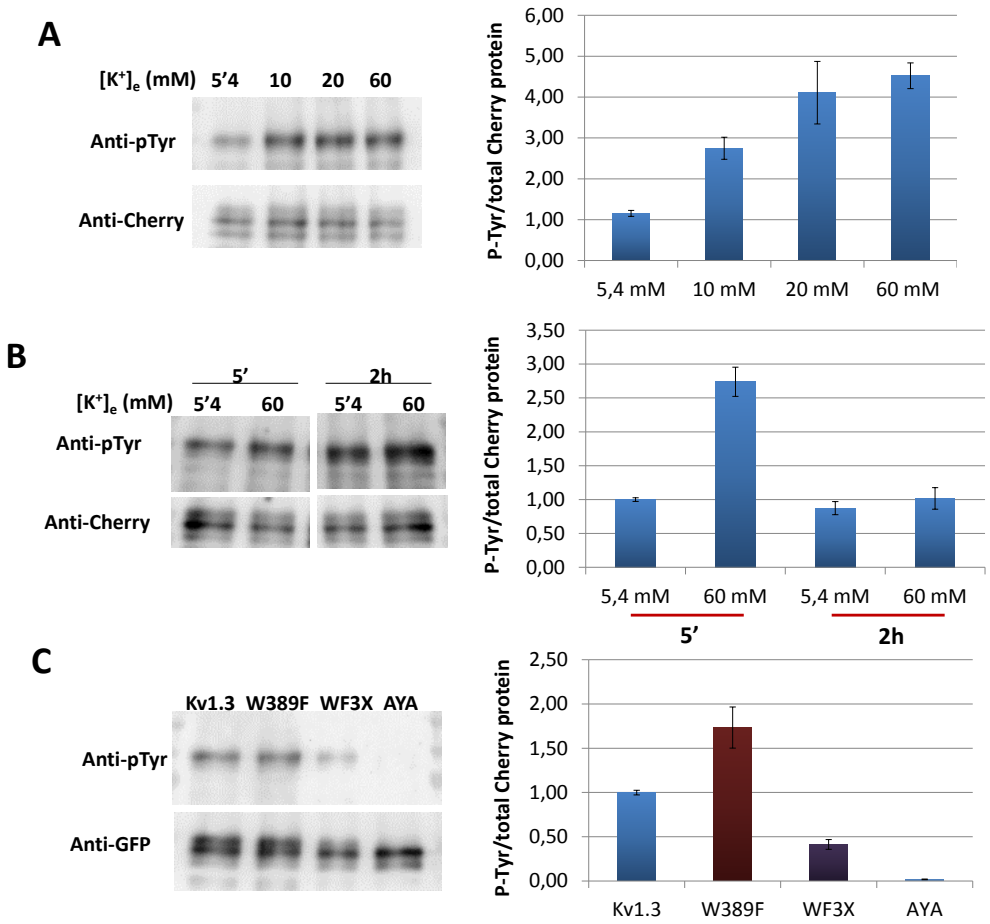


**Figure 4.29. A) Representative immunoblots and summary data from immunoprecipitated HEK293 cells transfected with WT-Kv1.3. Cells were incubated with the indicated $[K^+]_e$ solutions during 20 minutes or B) during 5 minutes or 2 hours. C) Immunoblot and denstiometric values of immunoprecipitated HEK293 cells transfected with WT-Kv1.3 and Kv1.3-W389F, Kv1.3-WF3x and Kv1.3-AYA mutant channels. In all cases, pervanadate incubation was carried out during the last 5 min before collecting the cells. Data are represented as mean±SEM of 3-5 different experiments. The target protein bands were at the expected molecular weight (~84 KDa).**

## Chapter 4.3. Lentiviral vector transduction as a tool to manipulate Kv1.3 and Kv1.5 expression levels in proliferating VSMCs

We have found a good correlation of a low Kv1.5/Kv1.3 ratio and the proliferative phenotype of murine and human VSMCs, mostly due to a complete loss of Kv1.5 channel expression in proliferating cells. As heterologously expressed Kv1.5 channels decreased HEK293 cells proliferation, we first proposed to transduce this channel in proliferating VSMCs (obtained from mice or from human samples from the COLMAH collection).

Since VSMCs are notoriously difficult to transfect with conventional techniques, we decided to use lentiviral vectors. We generated lentivirus carrying Kv1.5-EGFP and Kv1.3-Cherry fusion proteins to be able to check the effects on PDGF induced proliferation. As control we used cells transduced with lentivirus carrying EGFP protein alone. Thus, Kv1.5 and Kv1.3 levels of expression in native tissues could be manipulated.

Successful transduction of primary culture cells requires preparation of highly concentrated viral stocks, which permit a high virus concentration and multiplicity of infection during transduction.

Having optimized lentivirus production and concentration, we next determined optimum culture conditions for transducing primary VSMC. For this optimization we used lentivirus that had been produced using the standard lentivirus production/concentration protocols listed in the material and methods.

To determine the optimal lentiviral transduction efficiency, a range of MOI for each cell type was tested, from 30 to 3000. Multiplicity of Infection (MOI) is the number of transducing lentiviral particles per cell and it was calculated as follows:

(Total number of cells per well) x (desired MOI) = total transducing units needed (TU)

(Total TU needed) / (TU/µl reported on lentivirus tittering protocol) = total µl of lentiviral particles to add to each well.

HEK293 cells and VSMC from coronary, renal or uterine human arteries were transduced with EGFP, Kv1.5-EGFP and Kv1.3-Cherry lentiviral vectors. A high infectivity, greater than 90%, was achieved for all the lentivirus constructs and cell types studied (figure 4.30.). The highest efficiency was displayed even at the lowest MOI tested (30).

Lentivirus transduction offers a promising alternative in VSMC gene transfer, which could be highly advantageous to use in further experiments.

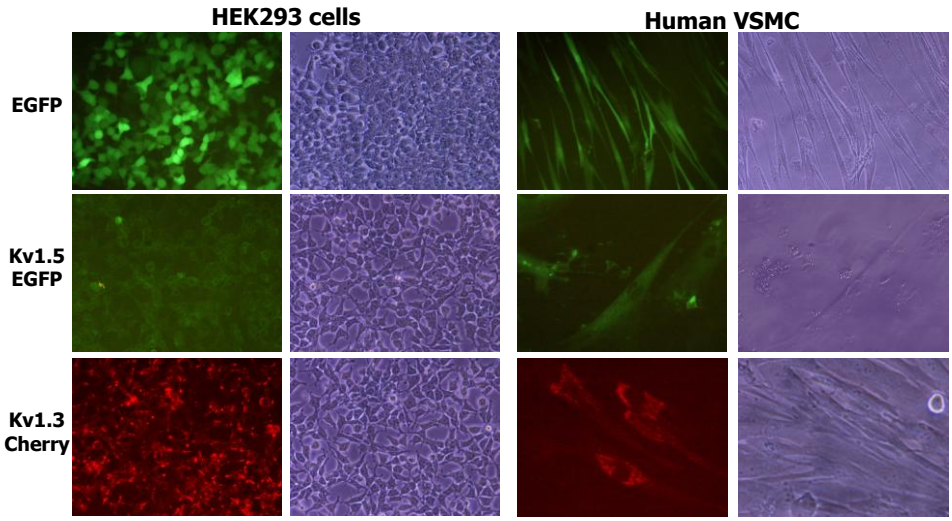


**Figure 4.30. Fluorescence and bright field images from HEK293 cells (left panel) and human VSMC (right panel). Cells were infected with EGFP, Kv1.5-EGFP and Kv1.3-Cherry lentiviral vectors.**

# 5

# Discussion

## Chapter 5.1. Kv1.3 channels can modulate proliferation by an ion-flux independent mechanism

Phenotypic modulation of VSMCs is a relevant issue with important clinical implications, as the cellular responses to vascular injury are important events in the formation of neointima in pathological states such as hypertension and atherosclerosis. The knowledge of the molecular mechanisms controlling VSMC activation and phenotypic modulation may provide points of control that can represent novel therapeuthical opportunities. As previously mentioned, the change in the expression ratio of Kv1.3 and Kv1.5 channels could be a general requirement to facilitate VSMC phenotype modulation, due to differential effects of both channels on the proliferative response. Our group showed evidence indicating that the pro-proliferative role of Kv1.3, previously described in murine VSMCs, can also be observed in human VSMCs obtained from different vascular beds (Cidad *et al.*, 2012;Cidad *et al.*, 2014), suggesting that Kv1.3 channels could constitute a new therapeutical target.

Although the contribution of Kv1.3 to VSMC proliferation seems to be a conserved, vascular bed independent mechanism, the molecular mechanisms through which Kv1.3 induce proliferation have yet to be clarified. Thus, the search for some mechanistic insights into the role of Kv1.3 in proliferation has prompted us to add another preparation to our study, the heterologous system HEK293 cells.

### 5.1.1. Kv1.3 overexpression increases proliferation in HEK293 cells, whereas Kv1.5 has an opposite effect

VSMCs are difficult to obtain in large amounts and hard to transfect efficiently by conventional methods. For these reasons, and with the aim to study the molecular mechanisms through which Kv1.3 was involved in proliferation, we explored if our findings held true in a heterologous system (HEK293 cells) that allowed us to modify Kv channel expression. HEK293 cells are an ideal system to study the effects of Kv1.3 and Kv1.5 channels on proliferation as they express little endogenous Kv protein.

The overexpression of Kv1.3 in HEK293 cells reproduced the effects seen in VSMCs, increasing cell proliferation and thus decreasing cell doubling time significantly. Proliferation assays were carried out both by cell counting and by studying EdU incorporation (Click-iT assay). In order to establish an incubation time in which we could have a reasonable fraction of cells entering the S-phase and a clear effect of the overexpression of the channels and their blockade by specific drugs, we fixed an EdU incubation period of 45 minutes.

The effect of Kv1.3 specific blockers was also confirmed in HEK293 cells, as MgTx and PAP-1 were able to inhibit Kv1.3 pro-proliferative effect. By contrast, Kv1.5 overexpression showed an antagonistic effect, inhibiting cell proliferation, and despite previous reports suggesting a pro-apoptotic role of Kv1.5 (Remillard & Yuan, 2004;Moudgil *et al.*, 2006), no evidence of increased apoptosis was observed in TUNEL assays.

Both Kv1.3 and Kv1.5 effects were significant up to 60 hours after transfection, decreasing at longer times probably due to a loss of the

transient transfection. The opposite effects of Kv1.3 and Kv1.5 channels in HEK293 cells points to concurrent changes in Kv1.3 and Kv1.5 channel expression in native systems as a requirement for the functional changes associated with phenotypic switch. The effects on HEK293 cells were not very large but very consistent. In fact, considering our transfection efficiencies (42.58±1.75%, mean±SEM), and the fast growth rate of HEK293 cells, they were probably underestimated.

Kv1.3 effect over proliferation was appreciated even at concentrations as low as 5 ng, reaching a saturated functional expression and saturated effect at 250 ng. Cotransfection of Kv1.3+Kvβ2.1 led to an increased HEK293 cell proliferation that could be simply explained by its chaperone role, increasing functional expression of Kv1.3 channels. Thus, once Kv1.3 expression had saturated, no additional effects were seen when cotransfecting Kvβ2.1. Interestingly, these saturating concentrations were relatively low, which is consistent with the effects of Kv1.3 channels on the proliferation of native VSMCs, as Kv1.3 current density remains low in cultured VSMCs (Cidad et al., 2012)

Kv1.3 pro-proliferative effects have been described in tumoral cells and VMSCs from several vascular beds, as we have previously mentioned (Pardo, 2004;Cidad *et al.*, 2010;Wonderlin & Strobl, 1996). However, this effect has never been described in a heterologous system. The fact that Kv1.3 effects can be reproduced in HEK293 cells suggests that the molecular mechanisms involved in the pro-proliferative role may be conserved, widening the possibilities for exploring the mechanisms through which Kv1.3 increases proliferation.

### 5.1.2. Kv1.3 pore and gating mutants as tools to explore the pro-proliferative mechanisms

Several findings have shown that many ion channels demonstrate biological activity that is unrelated to ion conduction (Kaczmarek, 2006). Moreover, our previous results indicated that depolarization, induced by channel blockers that were different from Kv1.3 specific blockers, or induced by high $[K^+]_e$, did not affect cell proliferation in femoral VSMCs (Cidad *et al.*, 2010). Bearing the latter in mind, and the finding that Kv1.3 and Kv1.5 channels promoted the opposite processes of proliferation, we speculated that Kv1.3 action was unlikely to be mediated solely through $K^+$ flux.

To study our hypothesis we first generated Kv1.3 fusion proteins. Fusion of fluorescent proteins is a useful tool to obtain information of the distribution of the protein of interest. In order to discard that our fusion tagging could produce substantial changes in the properties of the channel, Kv1.3 pro-proliferative effects were validated both in a bicistronic vector and as a fusion protein, obtaining comparable results.

Voltage-dependent ion channels have two functional domains, the ion pore itself and the voltage sensor that regulates ion flux. The two pore mutant constructs (pEGFP-N3-Kv1.3AYA and pEGFP-N3-Kv1.3W389F) and the pore and voltage sensor mutant (pEGFP-N3-Kv1.3WF3x) were generated with the purpose of getting evidence of the possible mechanisms by which Kv1.3 induced proliferation.

### 5.1.3. Kv1.3-mediated proliferation requires gating movement but not $K^+$ permeation

Kv channels can modulate proliferation by functioning either as $V_M$ modulators, so that proliferation is affected by the change in $V_M$ induced by ion fluxes through the channels; or as $V_M$ sensors, so that $V_M$ induced conformational changes could affect associated proteins that participate in proliferation pathways. The first possibility underlies the current hypothesis for $K^+$ channels-mediated proliferation, stating that cell hyperpolarization by $K^+$ channels activation will increase the driving force for $Ca^{2+}$ entry. However, our work suggests that membrane Kv1.3 channels only need their voltage-sensing capability to impact proliferation, being their effect on $V_M$ irrelevant, since Kv1.3-W389F, but not Kv1.3-WF3x, was able to increase proliferation with a time course and magnitude similar as WT-Kv1.3. This finding could accommodate the data obtained in native tissue, where we observed that although several Kv channel blockers depolarized VSMCs, only Kv1.3 channels blockade affected proliferation (Cidad *et al.*, 2010). Moreover, in femoral arteries, the phenotypic switch associates with a shift toward a more depolarized resting membrane potential (from –50.33±2.85 in freshly dissociated to –40.34±1.66 mV in cultured VSMCs; mean±SEM of 12–20 cells), stressing the fact that the physiological relevance of the change in the Kv1.3:Kv1.5 ratio is not related to the hyperpolarizing role of $K^+$ channels. Furthermore, the absolute value of $V_M$ seems to be irrelevant for HEK293 cells, because Kv1.3 and Kv1.3W389F have similar effects on proliferation with a very different effect on $V_M$, whereas Kv1.3 and Kv1.5 have similar effects on $V_M$ and opposite effects on proliferation. Therefore, we propose that Kv1.3 behaves as a sensor of $V_M$ changes occurring during the cell

cycle, which translate into a proliferative signal through coupling to some yet unknown pro-proliferative pathway (figure 5.1.).

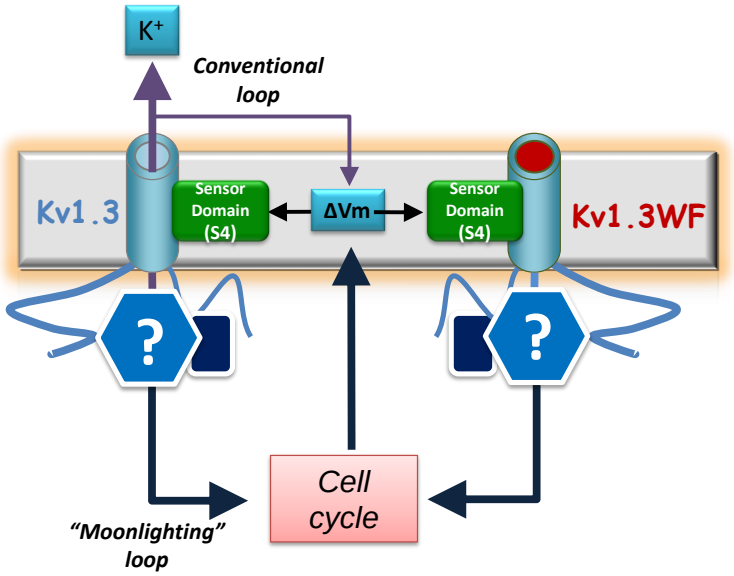


**Figure 5.1. Proposed model to frame the results obtained in this work. Kv1.3 channels are voltage sensors which respond to changes in membrane potential ($V_M$) with a conformational change. This conformational change translates into a change in the potassium flux through the channel that aims to recover the original potential (Conventional loop). We propose that in addition to determine ion flux, this conformational change could promote the association and/or the activation of intracellular proteins that modulate cell progression through the cell-cycle (Moonlighting loop). Since the conventional loop does not seem to be required to modulate proliferation, we propose that Kv1.3 channels behave as sensors of changes in the VM that occur during the cell cycle, and interact with the appropriate set of intracellular effectors to facilitate cell cycle progression.**

Some *in vivo* studies have also suggested that the effects of Kv1.3 are unlikely to result purely from changes in membrane potential or $K^+$ flux. For instance, in olfactory bulb, where Kv1.3 is highly expressed, $Kv1.3^{-/-}$ mice presented elevated levels of various signaling molecules, in comparison with WT-mice (Fadool *et al.*, 2004). These effects have not been reported for animals in which other $K^+$ genes have been eliminated, suggesting that

these actions of Kv1.3 are unlikely to be attributed simply to changes in membrane excitability.

The role of voltage-dependent ion channels as voltage sensors is reminiscent of other well characterized physiological processes such as the conformational coupling between the L-type calcium channel and the ryanodine receptor in the skeletal muscle (Catterall, 1991). In a more related scenario, similar mechanisms have been described for EAG-induced proliferation of fibroblasts and myoblasts, where the voltage-dependent conformational change of the channel seems to be the signaling switch that modulates cell proliferation (Hegle *et al.*, 2006). Similarly, $K^+$ efflux with the consequent hyperpolarization and enhanced $Ca^{2+}$ entry are not necessary for IK1-induced HEK293 cell proliferation (Millership *et al.*, 2011). In this case IK1 does not even seem to behave as a voltage sensor because expression at the cell membrane is not required to potentiate proliferation. This fact is contrary to our studies where Kv1.3-AYA, which was unable to traffic to the cell surface, had no effect on proliferation.

### 5.1.4. Kv1.3 pore blockers inhibit the effect of Kv1.3W389F on proliferation by affecting gating movement

The effect on proliferation of Kv1.3 and the nonpermeant Kv1.3W389F is inhibited by selective Kv1.3 blockers (MgTx and PAP-1), that have been previously considered as open channel blockers with no effects on the kinetics of the channel (Wulff *et al.*, 2009;Aiyar *et al.*, 1995;Garcia-Calvo *et al.*, 1993). Their inhibitory effect on proliferation seems to be in open contradiction with the observation that ion flux through the channels is not

required to induce proliferation. Characterization of the gating charge movements in the Kv1.3-W389F mutant showed that PAP-1 and MgTx clearly affected the voltage-sensing mechanism. This effect could explain the inhibition of Kv1.3-induced proliferation by these drugs.

*As a whole, these data suggest that conformational changes of Kv1.3 in response to $V_M$, but not changes in ion fluxes, are the key element in the proliferation signaling pathway.*

## Chapter 5.2. Identificacion of the molecular determinants and signalling pathways involved in the pro-proliferative mechanism induced by Kv1.3

Ion channels that have non-conducting functions can participate in coupled biochemical reactions or communicate directly with cytoplasmic and nuclear signaling pathways. The ability of enzymes and second messenger systems to assemble with a Kv channel opens up the possibility of translating changes in membrane potential into biological signals. Henceforth, we speculate that changes in resting membrane potential that contribute to cell-cycle progression could be sensed and transduced through Kv1.3 channels. However, the requirement of Kv1.3 channels (and not a closely related Kv1 subfamily member such as Kv1.5) for the potentiation of proliferation indicates that either Kv1.3 channel itself or other closely associated molecules must be targets and/or effectors in the proliferation signalling pathway. Thus, we postulated the existence of specific docking sites within the channel molecule whose exposure to proliferative stimulus is regulated

by voltage-dependent conformational changes and that could potentiate cell proliferation.

The cytoplasmic domains of Kv channels have a number of unusual features, playing a key role in cellular signalling pathways. For instance, EAG channels have putative nuclear localization signals in their C-terminus, and an N-terminal PAS domain that has been found to regulate transcription or protein kinase activity (Hegle *et al.*, 2006;Kaczmarek, 2006). In the same way, Kv1.3 is known to participate in cell signaling pathways given a number of molecular motifs that serve as protein-protein interaction domains in its N- and C- terminal domains (Marks & Fadool, 2007). Protein-protein interactions occur between proteins at discreet modules that may or may not require phosphorylation for recognition of the signaling motif (Cook & Fadool, 2002).

### 5.2.1. The effects of Kv1.3 and Kv1.5 on HEK cells proliferation seem to be mediated by their cytoplasmic COOH domains

A high stringency search for predicted motif sites in human Kv1.3 was performed using Scansite (http://scansite3.mit.edu) (figure 5.2.). Kv1.3 intracellular domains can associate with proteins involved in key signaling pathways such as protein kinase A (PKA) or MAPK1. Moreover, Kv1.3 intracellular termini comprises sequences required for association with scaffolding and adapter proteins, including Src-homology 3 (SH3) and Src-homology 2 (SH2) proteins, allowing the channel to assemble large protein complexes at the plasma membrane.

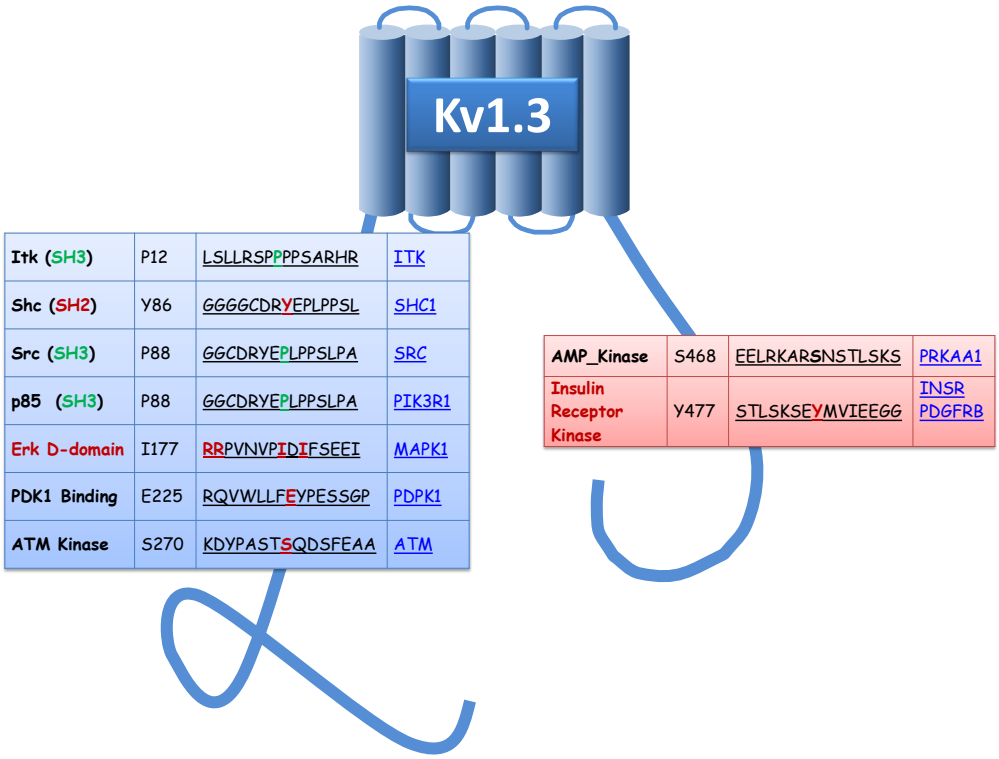


**Figure 5.2. Diagram of a human Kv1.3 α subunit showing speculative motifs in the cytosolic N-terminal domain (blue box) and C-terminal domain (red box).**

In order to identify the specific Kv1.3 domains involved in cell proliferation, we undertook the molecular dissection of the channel and the parallel changes observed in HEK293 cells proliferation. First of all, we generated two Kv1.3/Kv1.5 chimeric channels by switching either N-terminus or C-terminus of Kv1.3 into Kv1.5 channel backbone (K5C3 and K5N3 chimeric channels). Proliferation assays revealed a pro-proliferative role of K5C3 with statistically indistinguishable effects from those of the wild type Kv1.3 channel. This result suggests that a key domain underlying Kv1.3-induced proliferation resides in the cytoplasmic C-terminal tail of Kv1.3.

K5N3 chimeric channel showed an inhibitory effect similar to that seen in Kv1.5 transfected cells, whilst a pro-apoptotic role of this chimeric channel was discarded by TUNEL assays. This fact not only discards Kv1.3 N-terminus as the main responsible of the pro-proliferative effect, but also may imply Kv1.5 C-terminal domain as a key part in Kv1.5 inhibitory effect.

With regard to pharmacological and kinetics profile characterizations, both K5C3 and K5N3 were sensitive to DPO blockade and showed similar activation $V_{1/2}$ values as Kv1.5. However, K5N3 transfected cells were half inactivated at a similar voltage as Kv1.3, displaying a Kv1.3 N-type inactivation. These two features have been previously associated with molecular determinants located in the N-terminal domain (Bielanska *et al.*, 2009). However, we observed differences in the trafficking of these two chimeras. Immunostaining assays showed K5C3 was mainly present in the cell surface, whilst a higher proportion of K5N3 was present inside the cell.

The surface expression is determined by the balance between ERR (Endoplasmic Reticulum Retention) and forward trafficking signals (Misonou & Trimmer, 2004b). There exist several ERR signals within the pore and C- and N-terminal domains of the channels that determine traffic and surface expression (Misonou & Trimmer, 2004a;Manganas *et al.*, 2001). In fact, Kv1.3 has intracellular motifs near the T1 tetramerization domain that serve as ERR signals (Colley *et al.*, 2007;Martinez-Marmol *et al.*, 2013). Nevertheless, it has been reported that Kv1.3 C-terminal domain is necessary for an effective membrane surface targeting of this channel. Indeed, a cluster (YMVIEE) at the C-terminus of the channel was found to be responsible for efficient Kv1.3 forward trafficking. In particular, the two

glutamic acids (E) at positions 483 and 484 were identified as part of the cell membrane sorting sequence and their mutations decreased protein surface expression significantly (Martinez-Marmol *et al.*, 2013). YMVIEE signature is a conserved motif that has been found to be present in Kv1.1, Kv1.2 and Kv1.4 channels, however this forward trafficking sequence is absent in Kv1.5 channels.

By contrast, Kv1.5 has been described to associate with α-actinin-2 through its N-terminal region, thus linking it to the actin cytoskeleton (Maruoka *et al.*, 2000). This interaction may play an important role in clustering Kv1.5 channels to relevant cellular domains. Furthermore, point mutations within the T1 domain of Kv1.5 decrease protein expression, being mutant channels mainly retained in intracellular packets instead of localizing to the plasma membrane (Burg *et al.*, 2010b).

The importance of these domains in Kv1.3 and Kv1.5 trafficking may help to understand differences in trafficking of Kv1.3-Kv1.5 chimeric channels. Some studies reported that a chimeric Kv1.3 channel with the Kv1.5 N-terminus was able to target to the membrane in a similar way to the WT-Kv1.3, but a chimeric Kv1.3 with the Kv1.5 C-terminus displayed greater intracellularly retention, in a pattern similar to the WT-Kv1.5 channel (Martinez-Marmol *et al.*, 2013). Our experiments showed similar results, as virtually all K5C3 channels trafficked to the cell membrane, but K5N3 chimeric channels were retained in the ER to a greater extend than both WT-Kv1.3 and WT-Kv1.5.

These results suggest that Kv1.3 C-terminus could be responsible for targeting K5C3 to the membrane. Moreover, the low cell surface expression

of K5N3 channels could be due to the absence of forward trafficking sequences in Kv1.3 N-terminus or to ERR elements, such as the previously mentioned residues in this domain, acting as dominant signals in the absence of the Kv1.3 C-terminus. Another explanations would be that Kv1.5 N-terminus was exclusively determinant in channel trafficking or that potent ERR signatures were present in Kv1.5 C-terminus (figure 5.3.). Thus, the channel abundance at the cell surface is determined by the balance and strength of forward trafficking and ERR signals present in intracellular domains of the channels (Misonou and Trimmer, 2004).

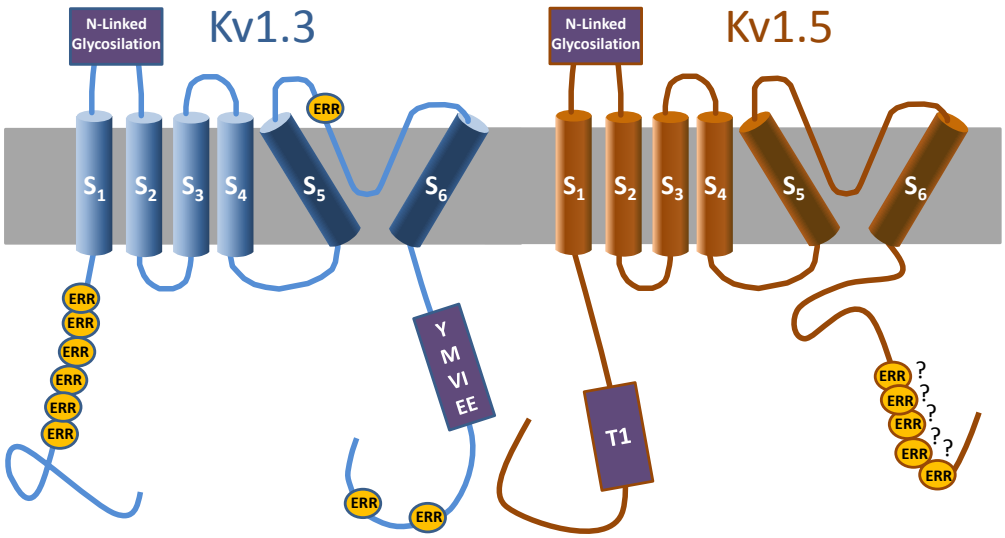


**Figure 5.3. Cartoon summary of predicted determinants of Kv1.3 and Kv1.5 channel expression and location. Sites defined as important determinants of forward trafficking are shown in purple, while described and predicted ER retention motifs (ERR) are shown in yellow. Adapted from (Misonou & Trimmer, 2004b).**

In principle, the differences in channel expression could question our results in proliferation. However, as the channels are overexpressed in HEK293 cells and our results have shown that even small amounts of transfected

Kv1.3 (250 ng) are able to reach a saturated effect, a possible reduction in the mutant channel's targeting to the membrane should have no impact on the measurement of proliferation. In fact, contransfection of Kvβ2.1 subunits was able to partially rescue functional and membrane expression of K5N3. Nevertheless, no increase in cell proliferation was observed despite the chaperone association. Therefore, this excludes reduced membrane expression levels accounting for the inhibitory effect mediated by K5N3.

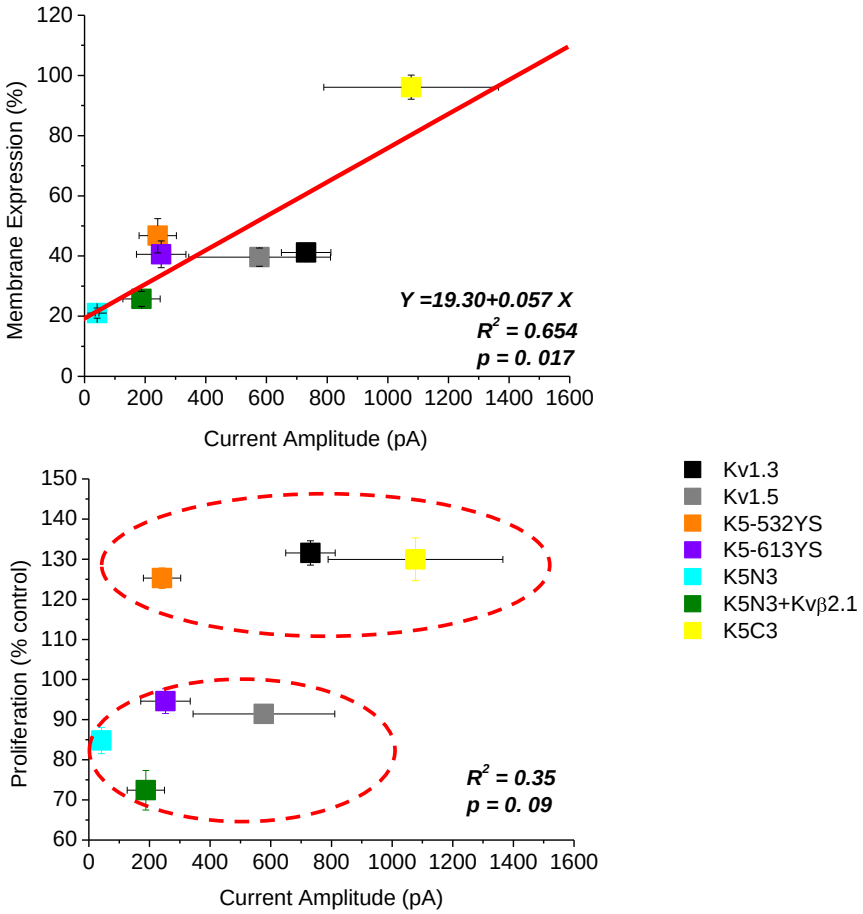


**Figure 5.4. Correlation between current amplitude and the percentage of membrane expression and between current amplitude and the percentage of proliferating HEK293 cells transfected with WT-Kv1.3 (black), WT-Kv1.5 (grey) and the different chimeric constructs containing Kv1.5 backbone.**

Membrane expression quantification was validated though its correlation with functional expression measured by patch-clamp electrophysiology. While we found a good, significant correlation between membrane expression values and current density (figure 5.4, upper graph), there is no relationship between functional expression and proliferation (or membrane expression, data not shown) and proliferation (lower graph, $R^2$=0.35, p=0.1). As shown in the figure, the effects on proliferation discriminate two groups of constructs, which are unrelated to their functional expression, as similar values of current density were found in constructs decreasing proliferation (K5-613YS, Kv1.5) and constructs increasing it (K5-532YS, Kv1.3).

### 5.2.2. Single mutations of the C-terminal tyrosine Y447A or serine S459A abolish the pro-proliferative effect of Kv1.3

The Kv1.3 C-terminus contains several domains that could mediate the signaling activity of Kv1.3. such as the AMP kinase and the insulin receptor kinase motifs (see figure 5.2.). Moreover, eight kinase specific phosphorylation sites within the Kv1.3 C-terminal domain were predicted by NetPhos 2.0 Server. To identify the domain(s) or residue(s) contributing to the signaling activity of Kv1.3, we first examined by EdU incorporation assays, the effects of mutations in every phosphosite from the C-terminal tail. The results showed that only Y447A and S459A mutations decreased proliferation to a level comparable to control vector transfected cells. Our results are of great interest since, although they do not form part of any predicted consensus phosphorylation sequence or have clearly identified kinases, Y447 and S459 were capable of modulating proliferation. Moreover,

the effects of phosphorylation of Y447 have been studied in terms of changes in channel currents (Fadool *et al.*, 2000), but the role of this residue in cell proliferation has not been studied to date.

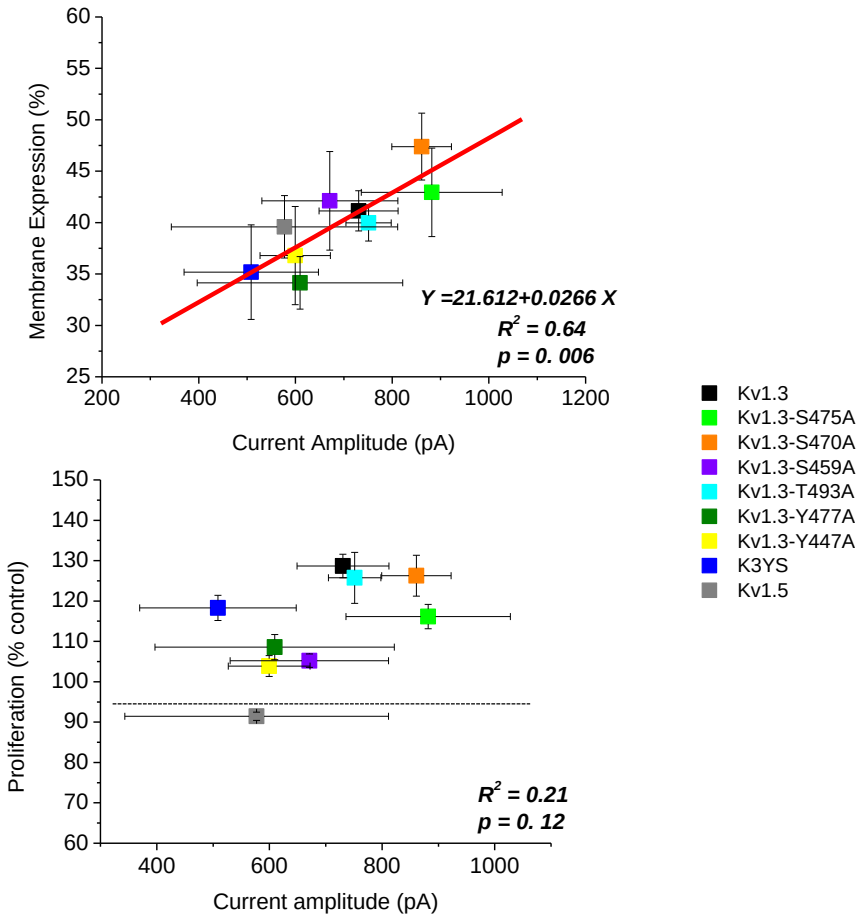


**Figure 5.5. Correlation between current amplitude and the percentage of membrane expression and between current amplitude and the percentage of proliferating HEK293 cells transfected with WT-Kv1.3 (black), WT-Kv1.5 (grey) and the different chimeric and point mutant constructs containing Kv1.3 backbone.**

Again, as in the case of Kv1.5 chimeric channels, the reduced proliferation observed with mutations in the Y447 and S459 residues could not be

explained by changes in surface expression, since immunostaining quantification revealed no significant differences in expression levels between the various C-terminal domain mutations and the wild-type Kv1.3 channel. Furthermore, Y447A and S459A mutants exhibited outward currents comparable to those observed for WT-Kv1.3, and no significant differences were shown in their kinetic profiles in comparison with WT-Kv1.3. Thus, although we found a good correlation between surface and functional expression, there was no correlation between proliferation and functional expression (figure 5.5.).

These data suggest that Y447 and S459 residues are essential for Kv1.3-mediated proliferation. However, they do not rule out possible contributions of other regions or residues of the channel. In fact, there are other point mutations that also show a decrease proliferation ratio, significantly different from Kv1.3, such as Y479A, although the induction of proliferation is not fully abolished.

### 5.2.3. YS fragment plays a prominent but not exclusive role in the pro-proliferative effect by means of the interaction with signaling proteins

In order to validate our previous results and confirm the role of Y447 and S459 residues, we explore the effect of a short fragment that includes these two residues , the YS fragment. The effect of YS fragment was explored through the generation of K3YS, K5-532YS and K5-613YS mutant channels. Despite the clear effect of Y447 and S459 residues on proliferation, we confirm that the potentiation of proliferation was not only due to these two residues, as the truncated K3YS channel was not able to reach the pro-

proliferative levels of the wild-type channel. These data suggest that other residues within the Kv1.3 C-terminal domain participate, in a cooperative way, in the pro-proliferative effect. Nevertheless, the proliferation rate of cells transfected with K3YS was significantly higher than the rate of cells transfected with the control vector, confirming the important role of both residues mediating cell growth. Although K3YS truncated channel lacked the Kv1.3 forward trafficking sequence mentioned above (YMVIEE), its slightly lower membrane expression level was not significantly different from that of WT-Kv1.3 channel. Moreover, as previously shown, no correlation was observed between proliferation and functional expression among Kv1.3 mutant constructs (figure 5.4.).

Our results when overexpressing the chimeric Kv1.5 channels containing the YS fragment suggest that the location of these residues within the channel molecule also determines its contribution to proliferation. Thus, K5-532YS (YS fragment inserted in the equivalent location in Kv1.3 channels) was able to significantly induce proliferation at rates similar to those of WT-Kv1.3, while K5-613YS (YS fragment located at the end of the protein) showed an inhibitory effect indistinguishable from the wild-type Kv1.5 channel.

The effect of these mutant channels cannot be explained by changes in the cell surface/ER ratio as both K5-532YS and K5-613YS showed similar membrane expression rates (figure 5.3.).

### 5.2.4. Y447 phosphorylation is essential for Kv1.3-mediated MAPK signaling pathway

Previous work from our group explored the role of PLCγ, PI3K and the MAPKs JNK, p38 and ERK1/2 in PDGF-induced proliferation of human coronary VSMCs (Cidad *et al.*, 2014). The results indicated that ERK1/2, PI3K and PLCγ signalling contributed to cell proliferation, consistent with many other studies pointing to a relevant contribution of these pathways to the phenotypic switch of VSMCs (Muto *et al.*, 2007;Zhan *et al.*, 2002;Hafizi *et al.*, 2004). Moreover, the search for the mechanisms involved in the pro-proliferative effect of Kv1.3 channels on human VSMCs demonstrated that the activity of these channels modulated proliferation acting on ERK1/2 signalling pathway. In fact, inhibition of proliferation by PAP-1 was occluded in the presence of selective inhibitors (PD98059) of ERK1/2, suggesting competition for the same site of action.

In the present study, we have found that Kv1.3-induced proliferation of HEK293 cells can be fully abolished by two point mutations that eliminate two phosphorylation sites at the C-terminal domain: Y447A and S459A. Interestingly, PD98059 treatment was also able to abolish Kv1.3-induced proliferation in HEK293 cells, not having any effect on the Y447A transfected cells.

With the aim to explore whether Y447 phosphorylation could be a trigger of the ERK1/2 pathway, the effect of PD98059 over pTyr labelling was measured in wild-type Kv1.3 and the mutant channel Y447A. Our results demonstrated that PD98059 reduced pTyr levels in the WT-Kv1.3, and that Y447A mutant channel has a significantly lower basal tyrosine phosphorylation which is not affected by PD98059 treatment. We conclude

that the phosphorylation of Y447 residue mediates proliferation through the activity of MEK/ERK kinases.

This fact is not supported with our high stringency search for predicted motif sites, since the predicted D-domain for ERK1/2 is located in the N-terminus of the protein. However, Kv1.3 N-terminal domain seems to have hardly any influence on Kv1.3-induced proliferation, since K5C3 but not K5N3 chimeric channel was able to induce proliferation, suggesting the existence of a pro-proliferative pathway associated to the C-terminus of the channel. Our data illustrate how , in the absence of experimental studies, the data from in-silico bioinformatics searches should be interpreted with caution, as it is possible that some of the predicted sites might be unavailable or masked by post-translational modifications and/or the presence of other proteins that compete for those sites.

### 5.2.5. Kv1.3-mediated signaling is regulated by channel conformation

We speculate that the exposure of Y447 site for phosphorylation requires a conformational change of the channel. Our results studying pTyr labelling of mutant Kv1.3 channels or wild type channels in the presence of high extracellular [$K^+$] suggest that voltage-dependent transitions from a closed to an open state could represent this conformational change. Moreover, our data suggest that we need one particular channel, and not any voltage-dependent channel, as a voltage sensor to activate the signalling pathway facilitating proliferation. The effect is lost when the channel is not able to sense the voltage, being permanently in the inactivated state (Kv1.3WF3x), and is increased when the voltage-dependent transitions are facilitated

(Kv1.3W389F or WT-Kv1.3). However, the changes in membrane potential are not sufficient to promote proliferation, as illustrated by the overexpression of Kv1.5 channels which promote a similar depolarization but in the absence of the specific domains are not able to induce proliferation (in fact they have the opposite effect). Nevertheless, when some of the molecular determinants identified in Kv1.3 channels are inserted in Kv1.5 channels we could obtain an effect on proliferation similar to that of Kv1.3 channels.

Although many signalling molecules are known to associate with ion channels and modulate their properties (Levitan, 2006), the finding that an integral element of the channel can catalyse an enzymatic reaction or participate in cell-cell interactions suggests that changes in channel activity could influence these processes.

There is evidence of a reciprocal modulatory interaction between Kv channels and protein tyrosine phosphorylation signaling pathways. Protein phosphorylation can be modulated by cell membrane potential (Siciliano *et al.*, 1994;Woodrow *et al.*, 1992) and potassium conductances. Specifically, Kv1.3 heterologous expression has been shown to attenuate v-Src-induced protein tyrosine phosphorylation while a non-conducting mutant Kv1.3 channel did not affect these phosphorylation levels (Holmes *et al.*, 1997). The attenuation of protein phosphotyrosine levels can correlate with the gating properties of Kv channels. In this same study, channels that exhibited different gating properties, such as Kv1.4 (fast inactivation) and Kv1.5 (slow inactivation) were coexpressed with v-Src. Whilst Kv1.4 showed little effect on v-Src induced protein tyrosine phosphorylation, Kv1.5 strongly

suppressed it (Holmes *et al.*, 1997). However, although changes in membrane potential and gating can modulate tyrosine phosphorylation, other mechanisms cannot be excluded.

Our results suggest that Kv1.3 signaling in proliferation depends on voltage-dependent conformations of the channel, linking channel conformational switch to the activity of intracellular messengers or signalling pathways. The Kv1.3 signaling mechanism described here suggests a function for the voltage sensor that is distinct from its role in regulating ion flux. This bifunctional mechanism has also been described to channels that regulate calcium influx and to EAG channels (Hegle *et al.*, 2006). However, contrary to Kv1.3 channels, EAG-induced proliferation was shown to be highest when EAG channels were predominantly in a close conformation.

Altogether, these observations indicate that even though VM could represent a valuable biolectrical signal associated to cell cycle progression and cell proliferation, the specific contribution of ion channels to these two processes is starting to be known. In the case of Kv channels, there are very few studies dissecting the contribution to the cell cycle of both conducting and non-conducting properties of ion channels, as this requires the use of genetic or pharmacological tools to selectively abolish ion permeation. Even more scarce is the information regarding the link(s) between voltage-dependent gating of Kv channels and cell cycle progression, although some clues are provided by the characterization of the proteins associated with Kv channels in the macromolecular complexes. These proteins include growth factor receptors and cytoskeleton associated molecules, such as integrin receptors, that cooperate to transduce extracellular signals into second

messengers cascades. However, the dynamic interactions of these macromolecular complexes, or the relation of ion fluxes through the channels with the signalling cascades leading to proliferation have not been described.

These data open interesting questions to identify the signalling pathways by which Kv1.3 channels (and not Kv1.5 channels) potentiate cell proliferation in several native systems. The contribution of Kv1.3 channels to cell proliferation in these systems can be related to their role as effectors of the cell-cycle machinery, by way of the modulation of their expression and function along the cell cycle. However, they can also participate in the regulation of signalling cascades via protein-protein interactions. The knowledge of which are these signalling cascades and the identification of the proteins and processes involved in the role of Kv channels in cell proliferation will provide a better understanding of these processes, and will pave the way for the development of new, more specific therapies based on ion channels for the treatment of unwanted proliferation.

## Chapter 5.3. Optimized lentiviral vector transduction to manipulate Kv1.3 and Kv1.5 levels of expression in human VSMCs

As previously reported, the functional expression of Kv1.3 in murine and human VSMCs was explored electrophysiologically, and its contribution to proliferation was demonstrated by the anti-proliferative effects of the selective blockers PAP-1 and MgTx. Our data indicated that the upregulated functional expression of Kv1.3 channels contributed to the phenotypic switch

of VSMCs (Cidad *et al.*, 2010;Cidad *et al.*, 2012;Cidad *et al.*, 2014). Nevertheless, an alternative explanation for the phenotypic modulation could be that the relevant change was Kv1.5 downregulation so that VSMC proliferation would not take place if Kv1.5 decrease is prevented. This idea is consistent with the observation that while Kv1.3 overexpression is able to increase HEK293 cell proliferation, Kv1.5 overexpression significantly decreases it. The latter fact has yet to be studied in VSMCs, since transient transfection has certain experimental limitations, showing poor and variable transfection rates in cultured VSMCs.

By contrast, lentiviral transduction has enabled us to overexpress both Kv1.3 and Kv1.5 channels in VSMCs with a high efficiency. There are many advantageous characteristics suggesting that lentiviral vectors are favorable gene delivery vectors for vascular gene transfer. While both plasmid DNA and adenovirus DNA are unstable due to the lack of chromosomal integration, lentiviral vectors integrate into the host cell chromatin, even in nondividing cells, thus providing a permanent genetic modification of the target cells (Cefai *et al.*, 2005;Chick *et al.*, 2012). Lentiviral vectors have been described to be highly efficient at transducing vascular cells (Dishart *et al.*, 2003;Cefai *et al.*, 2005;Qian *et al.*, 2006;Yang *et al.*, 2010). Indeed, our results here indicate that efficient transgene expression (more than 90% infectivity) can be achieved by lentiviral vectors not only in HEK293 cells, but also in human coronary, renal and uterine VSMCs.

Therefore, lentiviral vectors can be a useful tool to determine whether in native proliferating VSMCs the functional expression of Kv1.5 channels is linked to anti-proliferative signaling. This might be achieved by using Kv1.5

lentivirus together with lentiviral vectors carrying siRNA against Kv1.3 channels to abolish its pro-proliferative effect. Another possibility would be to determine if it is the formation of Kv1.3/Kv1.5 heteromultimers what occludes the pro-proliferative signaling pathways mediated by Kv1.3 channels. The latter could be studied by transducing VSMCs with different ratios of Kv1.3/Kv1.5 lentiviral vectors. Moreover, stably transduced VSMCs in which the endogenous KCNA3 had been replaced with the Kv1.3-Y447A version of the gene would provide a better cell culture system in which to study the effects of this mutation.

# 6

# CONCLUSIONS

Kv1.3 overexpression in a heterologous system (HEK293 cells) is able to increase cell proliferation significantly, while Kv1.5 overexpression inhibits proliferation without affecting apoptosis.

The pore mutants (Kv1.3-W389F and Kv1.3-AYA) and the pore and gating mutant (Kv1.3-WF3x) do not contribute to resting membrane potential, so that they can be used to explore the pro-proliferative mechanisms mediated by Kv1.3 channel molecule independently of ion fluxes. All mutants but Kv1.3-AYA traffic properly to the plasma membrane.

Kv1.3 effects on HEK293 cell proliferation requires membrane expression and intact voltage-sensing mechanisms, but is independent of the $K^+$ flux through the channel, thus the effects of Kv1.3 could be reproduced by pore mutants with intact voltage sensing mechanisms (Kv1.3-W389F). In addition, the effects of Kv1.3 pore blockers (MgTx and PAP-1) on Kv1.3-W389F indicate that these drugs also modulate the movement of the voltage sensor. These results suggest that Kv1.3 could be a bifunctional protein that not only regulates $K^+$ flux but also intracellular signalling pathways.

The two chimeric channels, K5C3 and K5N3, form functional channels in the cell membrane (albeit with different efficiency) and have a DPO sensitivity that does not differ from Kv1.5 channels. Both show activation $V_{1/2}$ values indistinguishable from Kv1.5, and K5N3 transfected cells are half inactivated at a similar voltage as Kv1.3, reflecting a Kv1.3 N-type inactivation.

Kv1.3 and K5C3 chimeric channel show similar pro-proliferative rates, while Kv1.5 and K5N3 have similar anti-proliferative effects, suggesting

that the effects of Kv1.3 and Kv1.5 on HEK293 cells proliferation are mediated by their cytoplasmic COOH domains.

The inhibition of proliferation observed with K5N3 is not associated to increased levels of apoptosis. Moreover, the combination of K5N3 with excess of the chaperone subunit Kvβ2.1 increases membrane and functional expression of K5N3 channels without inducing changes in proliferation, excluding a correlation between expression levels and proliferation for this construct.

Among all the phosphorilatable residues in the Kv1.3 C-terminal domain, only Kv1.3-Y447A and Kv1.3-S459A point mutations fully prevent Kv1.3-induced proliferation. Furthermore, a truncated K3YS channel comprising these residues is able to induce proliferation. Therefore, these data confirm an important role of these phosphosites to the pro-proliferative effect mediated by Kv1.3.

A short fragment of the C-terminal domain of Kv1.3 comprising Y447 and S459 residues (YS fragment) is able to recapitulate proliferation when inserted in an analogous position in the Kv1.5 C-terminus (K5-532YS) but not when inserted at the end of the Kv1.5 protein (K5-613YS). We speculate that conformational changes of the channel molecule are important to determine the accessibility of these residues, so that their position is relevant for the pro-proliferative effect.

A blocker of the MEK1/2-ERK1/2 signaling pathway, PD98059, significantly reduces Kv1.3-induced proliferation, not having any effect on Kv1.3-Y447A or Kv1.3-S459A mutant channels. This signaling

pathway has also been implicated on the proliferative effect of native Kv1.3 channels in human VSMCs. In agreement with these data, Tyr-phosphorylation levels are significantly reduced in the Kv1.3-Y447A mutant channel and become insensitive to PD98059 treatment. We conclude that ERK1/2-mediated Tyr-phosphorylation of Kv1.3 at Y447 is an important determinant of the signaling pathway leading to proliferation.

The increase in phospho-Tyr labelling of Kv1.3 shows a clear correlation with the effect of the channel inducing proliferation. We observe transient Tyr- phosphorylation in response to conformational changes of Kv1.3 channel upon depolarization. We postulate that the voltage-induced transition of the channel molecule from close to open conformation is able to trigger Tyr-phosphorylation. In agreement with this hypothesis, increased phospho-Tyr labelling is detected in Kv1.3-W389F mutant channel but not in Kv1.3-WF3x, which remains in the inactivated state. We conclude that Kv1.3-induced proliferation is dependent on conformational changes of the channel that expose these residues.

Lentiviral vectors expressing EGFP, Kv1.5-EGFP or Kv1.3-Cherry show high transduction efficiencies (>90%) not only in HEK293 cells, but also in human VSMCs, representing a valuable tool for genetic manipulation of VSMCs in primary culture.

# 7

# REFERENCES

1. Accili, E. A., Kiehn, J., Yang, Q., Wang, Z., Brown, A. M., & Wible, B. A. (1997). Separable Kvbeta subunit domains alter expression and gating of potassium channels. *J Biol Chem* **272**, 25824-25831.

2. Accili, E. A., Kuryshev, Y. A., Wible, B. A., & Brown, A. M. (1998). Separable effects of human Kvbeta1.2 N- and C-termini on inactivation and expression of human Kv1.4. *J.Physiol* **512 ( Pt 2)**, 325-336.

3. Aggarwal, S. K. & MacKinnon, R. (1996). Contribution of the S4 segment to gating charge in the Shaker K+ channel. *Neuron* **16**, 1169-1177.

4. Aiyar, J., Withka, J. M., Rizzi, J. P., Singleton, D. H., Andrews, G. C., Lin, W., Boyd, J., Hanson, D. C., Simon, M., Dethlefs, B., Lee, C. l., Hall, J. E., Gutman, G. A., & George Chandy, K. (1995). Topology of the pore-region of a K+ channel revealed by the NMR-derived structures of scorpion toxins. *Neuron* **15**, 1169-1181.

5. Artym, V. V. & Petty, H. R. (2002). Molecular proximity of Kv1.3 voltage-gated potassium channels and beta(1)-integrins on the plasma membrane of melanoma cells: Effects of cell adherence and channel blockers. *Journal of General Physiology* **120**, 29-37.

6. Bahring, R., Milligan, C. J., Vardanyan, V., Engeland, B., Young, B. A., Dannenberg, J., Waldschutz, R., Edwards, J. P., Wray, D., & Pongs, O. (2001). Coupling of voltage-dependent potassium channel inactivation and oxidoreductase active site of Kvbeta subunits. *J Biol Chem* **276**, 22923-22929.

7. Baukrowitz, T. & Yellen, G. (1995). Modulation of K+ current by frequency and external [K+]: a tale of two inactivation mechanisms. *Neuron* **15**, 951-960.

8. Beck, E. J. & Covarrubias, M. (2001). Kv4 channels exhibit modulation of closed-state inactivation in inside-out patches. *Biophys.J* **81**, 867-883.

9. Beech, D. J. (2007). Ion channel switching and activation in smooth-muscle cells of occlusive vascular diseases. *Biochemical Society Transactions* **035**, 890-894.

10. Bekele-Arcuri, Z., Matos, M. F., Manganas, L., Strassle, B. W., Monaghan, M. M., Rhodes, K. J., & Trimmer, J. S. (1996). Generation and characterization of subtype-specific monoclonal antibodies to K+ channel alpha- and beta-subunit polypeptides. *Neuropharmacology* **35**, 851-865.

11. Bezanilla, F. (2008). How membrane proteins sense voltage. *Nat Rev Mol Cell Biol* **9**, 323-332.

12. Bezanilla, F., Perozo, E., Papazian, D. M., & Stefani, E. (1991). Molecular basis of gating charge immobilization in Shaker potassium channels. *Science* **254**, 679-683.

13. Bezanilla, F., White, M. M., & Taylor, R. E. (1982). Gating currents associated with potassium channel activation. *Nature* **296**, 657-659.

14. Bielanska, J., Hernandez-Losa, J., Moline, T., Somoza, R., Cajal, S., Condom, E., Ferreres, J. C., & Felipe, A. (2012a). Differential expression of Kv1.3 and Kv1.5 voltage-dependent K+ channels in human skeletal muscle sarcomas. *Cancer Invest* **30**, 203-208.

15. Bielanska, J., Hernandez-Losa, J., Moline, T., Somoza, R., Cajal, S. R., Condom, E., Ferreres, J. C., & Felipe, A. (2012b). Increased voltage-dependent K(+) channel Kv1.3 and Kv1.5 expression correlates with leiomyosarcoma aggressiveness. *Oncol.Lett.* **4**, 227-230.

16. Bielanska, J., Hernandez-Losa, J., Moline, T., Somoza, R., Ramon, Y. C., Condom, E., Ferreres, J. C., & Felipe, A. (2010). Voltage-dependent potassium channels Kv1.3 and Kv1.5 in human fetus. *Cell Physiol Biochem* **26**, 219-226.

17. Bielanska, J., Hernandez-Losa, J., Perez-Verdaguer, M., Moline, T., Somoza, R., Ramon, Y. C., Condom, E., Ferreres, J. C., & Felipe, A. (2009). Voltage-dependent potassium channels Kv1.3 and Kv1.5 in human cancer. *Curr.Cancer Drug Targets.* **9**, 904-914.

18. Bixby, K. A., Nanao, M. H., Shen, N. V., Kreusch, A., Bellamy, H., Pfaffinger, P. J., & Choe, S. (1999). Zn2+-binding and molecular determinants of tetramerization in voltage-gated K+ channels. *Nat Struct.Biol* **6**, 38-43.

19. Blank, R. S. & Owens, G. K. (1990). Platelet-derived growth factor regulates actin isoform expression and growth factor regulates actin isoform expression and growth state in cultured rat aortic smooth muscle cells. *Journal of Cellular Physiology* **142**, 635-642.

20. Bowlby, M. R., Fadool, D. A., Holmes, T. C., & Levitan, I. B. (1997). Modulation of the Kv1.3 potassium channel by receptor tyrosine kinases. *J Gen.Physiol* **110**, 601-610.

21. Bryksin, A. V. & Matsumura, I. (2010). Overlap extension PCR cloning: a simple and reliable way to create recombinant plasmids. *BioTechniques* **48**, 463-465.

22. Burg, E. D., Platoshyn, O., Tsigelny, I. F., Lozano-Ruiz, B., Rana, B. K., & Yuan, J. X. (2010a). Tetramerization domain

mutations in KCNA5 affect channel kinetics and cause abnormal trafficking patterns. *AJP - Cell Physiology* **298**, C496-C509.

23. Burg, E. D., Platoshyn, O., Tsigelny, I. F., Lozano-Ruiz, B., Rana, B. K., & Yuan, J. X. J. (2010b). Tetramerization domain mutations in KCNA5 affect channel kinetics and cause abnormal trafficking patterns. *American Journal of Physiology - Cell Physiology* **298**, C496-C509.

24. Cachero, T. G., Morielli, A. D., & Peralta, E. G. (1998). The small GTP-binding protein RhoA regulates a delayed rectifier potassium channel. *Cell* **93**, 1077-1085.

25. Cahalan, M. D. & Chandy, K. G. (1997). Ion channels in the immune system as targets for immunosuppression. *Curr.Opin.Biotechnol.* **8**, 749-756.

26. Cahalan, M. D. & Chandy, K. G. (2009). The functional network of ion channels in T lymphocytes. *Immunological Reviews* **231**, 59-87.

27. Cai, Y. C. & Douglass, J. (1993). In vivo and in vitro phosphorylation of the T lymphocyte type n (Kv1.3) potassium channel. *J Biol Chem* **268**, 23720-23727.

28. Campomanes, C. R., Carroll, K. I., Manganas, L. N., Hershberger, M. E., Gong, B., Antonucci, D. E., Rhodes, K. J., & Trimmer, J. S. (2002). Kvbeta Subunit Oxidoreductase Activity and Kv1 Potassium Channel Trafficking. *Journal of Biological Chemistry* **277**, 8298.

29. Catterall, W. A. (1991). Excitation-contraction coupling in vertebrate skeletal muscle: a tale of two calcium channels. *Cell* **64**, 871-874.

30. Cefai, D., Simeoni, E., Ludunge, K. M., Driscoll, R., von Segesser, L. K., Kappenberger, L., & Vassalli, G. (2005). Multiply attenuated, self-inactivating lentiviral vectors efficiently transduce human coronary artery cells in vitro and rat arteries in vivo. *J Mol Cell Cardiol.* **38**, 333-344.

31. Cerda, O. & Trimmer, J. S. (2010). Analysis and functional implications of phosphorylation of neuronal voltage-gated potassium channels. *Neurosci Lett.* **486**, 60-67.

32. Cheong, A., Bingham, A. J., Li, J., Kumar, B., Sukumar, P., Munsch, C., Buckley, N. J., Neylon, C. B., Porter, K. E., Beech, D. J., & Wood, I. C. (2005). Downregulated REST transcription factor is a switch enabling critical potassium channel expression and cell proliferation. *Mol Cell* **20**, 45-52.

33. Chick, H. E., Nowrouzi, A., Fronza, R., McDonald, R. A., Kane, N. M., Alba, R., Delles, C., Sessa, W. C., Schmidt, M., Thrasher, A. J., & Baker, A. H. (2012). Integrase-deficient lentiviral vectors mediate efficient gene transfer to human vascular smooth muscle cells with minimal genotoxic risk. *Hum.Gene Ther* **23**, 1247-1257.

34. Chittajallu, R., Chen, Y., Wang, H., Yuan, X., Ghiani, C. A., Heckman, T., McBain, C. J., & Gallo, V. (2002). Regulation of Kv1 subunit expression in oligodendrocyte progenitor cells and their role in G(1)/S phase progression of the cell cycle. *Proceedings of the National Academy of Sciences of the United States of America* **99**, 2350-2355.

35. Choi, K. L., Aldrich, R. W., & Yellen, G. (1991). Tetraethylammonium blockade distinguishes two inactivation mechanisms in voltage-activated K+ channels. *Proc.Natl.Acad.Sci.U.S.A* **88**, 5092-5095.

36. Choi, K. L., Mossman, C., Aube, J., & Yellen, G. (1993). The internal quaternary ammonium receptor site of Shaker potassium channels. *Neuron* **10**, 533-541.

37. Cidad, P., Jimenez-Perez, L., Garcia-Arribas, D., Miguel-Velado, E., Tajada, S., Ruiz-McDavitt, C., Lopez-Lopez, J. R., & Perez-Garcia, M. T. (2012). Kv1.3 channels can modulate cell proliferation during phenotypic switch by an ion-flux independent mechanism. *Arteriosclerosis, Thrombosis, and Vascular Biology* **32**, 1299-1307.

38. Cidad, P., Miguel-Velado, E., Ruiz-McDavitt, C., Alonso, E., Jimenez-Perez, L., Asuaje, A., Carmona, Y., Garcia-Arribas, D., Lopez, J., Marroquin, Y., Fernandez, M., Roque, M., Perez-Garcia, M. T., & Lopez-Lopez, J. R. (2014). Kv1.3 channels modulate human vascular smooth muscle cells proliferation independently of mTOR signaling pathway. *Pflugers Arch*.

39. Cidad, P., Moreno-Dominguez, A., Novensa, L., Roque, M., Barquin, L., Heras, M., Perez-Garcia, M. T., & Lopez-Lopez, J. R. (2010). Characterization of ion channels involved in the proliferative response of femoral artery smooth muscle cells. *Arteriosclerosis, Thrombosis, and Vascular Biology* **30**, 1203-1211.

40. Coetzee, W. A., Amarillo, Y., Chiu, J., Chow, A., Lau, D., McCormack, T., Moreno, H., Nadal, M. S., Ozaita, A., Pountney, D., Saganich, M., Vega-Saenz, d. M., & Rudy, B. (1999). Molecular diversity of K+ channels. *Ann.N.Y.Acad.Sci.* **868:233-85.**, 233-285.

41. Colley, B. S., Biju, K. C., Visegrady, A., Campbell, S., & Fadool, D. A. (2007). Neurotrophin B receptor kinase increases Kv subfamily member 1.3 (Kv1.3) ion channel

half-life and surface expression. *Neuroscience* **144**, 531-546.

42. Coma, M., Vicente, R., Busquets, S., Carbo, N., Tamkun, M. M., Lopez-Soriano, F. J., Argiles, J. M., & Felipe, A. (2003). Impaired voltage-gated K+ channel expression in brain during experimental cancer cachexia. *FEBS Lett.* **536**, 45-50.

43. Comes, N., Bielanska, J., Vallejo-Gracia, A., Serrano-Albarras, A., Marruecos, L., Gomez, D., Soler, C., Condom, E., Ramon, Y. C., Hernandez-Losa, J., Ferreres, J. C., & Felipe, A. (2013). The voltage-dependent K(+) channels Kv1.3 and Kv1.5 in human cancer. *Front Physiol* **4**, 283.

44. Cook, K. K. & Fadool, D. A. (2002). Two adaptor proteins differentially modulate the phosphorylation and biophysics of Kv1.3 ion channel by SRC kinase. *J Biol Chem* **277**, 13268-13280.

45. Cornetta, K. & Anderson, W. F. (1989). Protamine sulfate as an effective alternative to polybrene in retroviral-mediated gene-transfer: implications for human gene therapy. *J Virol.Methods* **23**, 187-194.

46. Cox, R. H. (2005). Molecular Determinants of Voltage-Gated Potassium Currents in Vascular Smooth Muscle. *Cell Biochem.Biophys.* **42**, 167-196.

47. Decher, N., Pirard, B., Bundis, F., Peukert, S., Baringhaus, K. H., Busch, A. E., Steinmeyer, K., & Sanguinetti, M. C. (2004). Molecular basis for Kv1.5 channel block: conservation of drug binding sites among voltage-gated K+ channels. *J Biol Chem* **279**, 394-400.

48. Dishart, K. L., Denby, L., George, S. J., Nicklin, S. A., Yendluri, S., Tuerk, M. J., Kelley, M. P., Donahue, B. A., Newby, A. C., Harding, T., & Baker, A. H. (2003). Third-generation lentivirus vectors efficiently transduce and phenotypically modify vascular cells: implications for gene therapy. *J Mol Cell Cardiol.* **35**, 739-748.

49. Doyle, D. A., Morais, C. J., Pfuetzner, R. A., Kuo, A., Gulbis, J. M., Cohen, S. L., Chait, B. T., & MacKinnon, R. (1998). The structure of the potassium channel: molecular basis of K+ conduction and selectivity. *Science* **280**, 69-77.

50. Drain, P., Dubin, A. E., & Aldrich, R. W. (1994). Regulation of Shaker K+ channel inactivation gating by the cAMP- dependent protein kinase. *Neuron* **12**, 1097-1109.

51. Du, Y. m., Zhang, X. x., Tu, D. n., Zhao, N., Liu, Y. j., Xiao, H., Sanguinetti, M. C., Zou, A., & Liao, Y. h. (2010). Molecular determinants of Kv1.5 channel block by diphenyl phosphine

oxide-1. *Journal of Molecular and Cellular Cardiology* **48**, 1111-1120.

52. Eldstrom, J., Doerksen, K. W., Steele, D. F., & Fedida, D. (2002). N-terminal PDZ-binding domain in Kv1 potassium channels. *FEBS Lett.* **531**, 529-537.

53. Erdogan, A., Schaefer, C. A., Schaefer, M., Luedders, D. W., Stockhausen, F., Abdallah, Y., Schaefer, C., Most, A. K., Tillmanns, H., Piper, H. M., & Kuhlmann, C. R. (2005). Margatoxin inhibits VEGF-induced hyperpolarization, proliferation and nitric oxide production of human endothelial cells. *J Vasc Res* **42**, 368-376.

54. Fadool, D. A., Tucker, K., Perkins, R., Fasciani, G., Thompson, R. N., Parsons, A. D., Overton, J. M., Koni, P. A., Flavell, R. A., & Kaczmarek, L. K. (2004). Kv1.3 channel gene-targeted deletion produces "Super-Smeller Mice" with altered glomeruli, interacting scaffolding proteins, and biophysics. *Neuron* **41**, 389-404.

55. Fadool, D. A., Tucker, K., Phillips, J. J., & Simmen, J. A. (2000). Brain insulin receptor causes activity-dependent current suppression in the olfactory bulb through multiple phosphorylation of Kv1.3. *Journal of Neurophysiology* **83**, 2332-2348.

56. Fan, Z., Ji, X., Fu, M., Zhang, W., Zhang, D., & Xiao, Z. (2012). Electrostatic interaction between inactivation ball and T1-S1 linker region of Kv1.4 channel. *Biochim.Biophys.Acta* **1818**, 55-63.

57. Felipe, A., Vicente, R., Villalonga, N., Roura-Ferrer, M., Martinez-Marmol, R., Sole, L., Ferreres, J. C., & Condom, E. (2006). Potassium channels: new targets in cancer therapy. *Cancer Detect.Prev.* **30**, 375-385.

58. Fink, M., Duprat, F., Lesage, F., Heurteaux, C., Romey, G., Barhanin, J., & Lazdunski, M. (1996). A new K+ channel beta subunit to specifically enhance Kv2.2 (CDRK) expression. *J Biol Chem* **271**, 26341-26348.

59. Frid, M. G., Shekhonin, B. V., Koteliansky, V. E., & Glukhova, M. A. (1992). Phenotypic changes of human smooth muscle cells during development: late expression of heavy caldesmon and calponin. *Dev.Biol* **153**, 185-193.

60. Gabbiani, G., Schmid, E., Winter, S., Chaponnier, C., de Ckhastonay, C., Vandekerckhove, J., Weber, K., & Franke, W. W. (1981). Vascular smooth muscle cells differ from other smooth muscle cells: predominance of vimentin filaments and a specific alpha-type actin. *Proc Natl.Acad.Sci U S.A* **78**, 298-302.

61. Gandhi, C. S., Loots, E., & Isacoff, E. Y. (2000). Reconstructing voltage sensor-pore interaction from a fluorescence scan of a voltage-gated K+ channel. *Neuron* **27**, 585-595.

62. Garcia Calvo, M., Leonard, R. J., Novick, J., Stevens, S. P., Schmalhofer, W., Kaczorowski, G. J., & Garcia, M. L. (1993). Purification, characterization, and biosynthesis of margatoxin, a component of Centruroides margaritatus venom that selectively inhibits voltage-dependent potassium channels. *J.Biol.Chem.* **268**, 18866-18874.

63. Garcia-Calvo, M., Leonard, R. J., Novick, J., Stevens, S. P., Schmalhofer, W., Kaczorowski, G. J., & Garcia, M. L. (1993). Purification, characterization, and biosynthesis of margatoxin, a component of Centruroides margaritatus venom that selectively inhibits voltage-dependent potassium channels. *Journal of Biological Chemistry* **268**, 18866-18874.

64. Gimona, M., Sparrow, M. P., Strasser, P., Herzog, M., & Small, J. V. (1992). Calponin and SM 22 isoforms in avian and mammalian smooth muscle. Absence of phosphorylation in vivo. *Eur J Biochem* **205**, 1067-1075.

65. Gollasch, M., Haase, H., Ried, C., Lindschau, C., Morano, I., Luft, F. C., & Haller, H. (1998). L-type calcium channel expression depends on the differentiated state of vascular smooth muscle cells. *The FASEB Journal* **12**, 593-601.

66. Grissmer, S., Nguyen, A. N., Aiyar, J., Hanson, D. C., Mather, R. J., Gutman, G. A., Karmilowicz, M. J., Auperin, D. D., & Chandy, K. G. (1994). Pharmacological characterization of five cloned voltage-gated K+ channels, types Kv1.1, 1.2, 1.3, 1.5, and 3.1, stably expressed in mammalian cell lines. *Molecular Pharmacology* **45**, 1227-1234.

67. Gubitosi-Klug, R. A., Mancuso, D. J., & Gross, R. W. (2005). The human Kv1.1 channel is palmitoylated, modulating voltage sensing: Identification of a palmitoylation consensus sequence. *Proc Natl.Acad.Sci U S.A* **102**, 5964-5968.

68. Hafizi, S., Wang, X., Chester, A. H., Yacoub, M. H., & Proud, C. G. (2004). ANG II activates effectors of mTOR via PI3-K signaling in human coronary smooth muscle cells. *American Journal of Physiology - Heart and Circulatory Physiology* **287**, H1232-H1238.

69. Hartmann, H. A., Kirsch, G. E., Drewe, J. A., Taglialatela, M., Joho, R. H., & Brown, A. M. (1991). Exchange of conduction pathways between two related K+ channels. *Science* **251**, 942-944.

70. Heginbotham, L. (1999). Growing momentum in the molecular study of ion channels. *Nat Struct.Biol* **6**, 811-814.

71. Heginbotham, L., Lu, Z., Abramson, T., & MacKinnon, R. (1994). Mutations in the K+ channel signature sequence. *Biophys.J* **66**, 1061-1067.

72. Hegle, A. P., Marble, D. D., & Wilson, G. F. (2006). A voltage-driven switch for ion-independent signaling by ether-a-go-go K+ channels. *Proc Natl.Acad.Sci U S.A* **103**, 2886-2891.

73. Heinemann, S. H., Rettig, J., Wunder, F., & Pongs, O. (1995). Molecular and functional characterization of a rat brain Kv beta 3 potassium channel subunit. *FEBS Lett.* **377**, 383-389.

74. Higashita, R., Li, L., Van, P., V, Yamamura, Y., Zarinetchi, F., Heasley, L., & Nemenoff, R. A. (1997). Galpha16 mimics vasoconstrictor action to induce smooth muscle alpha-actin in vascular smooth muscle cells through a Jun-NH2-terminal kinase-dependent pathway. *J Biol Chem* **272**, 25845-25850.

75. Holmes, T. C., Fadool, D. A., & Levitan, I. B. (1996). Tyrosine phosphorylation of the Kv1.3 potassium channel. *J Neurosci* **16**, 1581-1590.

76. Holmes, T. C., Berman, K., Swartz, J. E., Dagan, D., & Levitan, I. B. (1997). Expression of Voltage-Gated Potassium Channels Decreases Cellular Protein Tyrosine Phosphorylation. *The Journal of Neuroscience* **17**, 8964-8974.

77. Hoshi, T., Zagotta, W. N., & Aldrich, R. W. (1990). Biophysical and molecular mechanisms of Shaker potassium channel inactivation. *Science* **250**, 533-538.

78. Hoshi, T., Zagotta, W. N., & Aldrich, R. W. (1991). Two types of inactivation in *Shaker* $K^+$ channels: effects of alterations in the carboxy-terminal region. *Neuron* **7**, 547-556.

79. Hu, L., Gocke, A. R., Knapp, E., Rosenzweig, J. M., Grishkan, I. V., Baxi, E. G., Zhang, H., Margolick, J. B., Whartenby, K. A., & Calabresi, P. A. (2012). Functional Blockade of the Voltage-gated Potassium Channel Kv1.3 Mediates Reversion of T Effector to Central Memory Lymphocytes through SMAD3/p21cip1 Signaling. *Journal of Biological Chemistry* **287**, 1261-1268.

80. Hunter, T. (1998). The Croonian Lecture 1997. The phosphorylation of proteins on tyrosine: its role in cell growth and disease. *Philos.Trans.R.Soc Lond B Biol Sci* **353**, 583-605.

81. Jackson, W. F. (2000). Ion Channels and Vascular Tone. *Hypertension* **35**, 173.

82. Jindal, H. K., Folco, E. J., Liu, G. X., & Koren, G. (2008). Posttranslational modification of voltage-dependent potassium channel Kv1.5: COOH-terminal palmitoylation modulates its biological properties. *AJP - Heart and Circulatory Physiology* **294**, H2012-H2021.

83. Jonas, E. A. & Kaczmarek, L. K. (1996). Regulation of potassium channels by protein kinases. *Curr.Opin.Neurobiol.* **6**, 318-323.

84. Kaczmarek, L. K. (2006). Non-conducting functions of voltage-gated ion channels. *Nat Rev Neurosci* **7**, 761-771.

85. Klemic, K. G., Shieh, C. C., Kirsch, G. E., & Jones, S. W. (1998). Inactivation of Kv2.1 Potassium Channels. *Biophysical Journal* **74**, 1779-1789.

86. Kohler, R., Wulff, H., Eichler, I., Kneifel, M., Neumann, D., Knorr, A., Grgic, I., Kampfe, D., Si, H., Wibawa, J., Real, R., Borner, K., Brakemeier, S., Orzechowski, H. D., Reusch, H. P., Paul, M., Chandy, K. G., & Hoyer, J. (2003). Blockade of the Intermediate-Conductance Calcium-Activated Potassium Channel as a New Therapeutic Strategy for Restenosis. *Circulation* **108**, 1119-1125.

87. Komuro, I., Kurihara, H., Sugiyama, T., Yoshizumi, M., Takaku, F., & Yazaki, Y. (1988). Endothelin stimulates c-fos and c-myc expression and proliferation of vascular smooth muscle cells. *FEBS Lett.* **238**, 249-252.

88. Kosolapov, A., Tu, L., Wang, J., & Deutsch, C. (2004). Structure acquisition of the T1 domain of Kv1.3 during biogenesis. *Neuron* **44**, 295-307.

89. Kotecha, S. A. & Schlichter, L. C. (1999). A Kv1.5 to Kv1.3 Switch in Endogenous Hippocampal Microglia and a Role in Proliferation. *Journal of Neuroscience* **19**, 10680-10693.

90. Kumar, B., Dreja, K., Shah, S. S., Cheong, A., Xu, S. Z., Sukumar, P., Naylor, J., Forte, A., Cipollaro, M., McHugh, D., Kingston, P. A., Heagerty, A. M., Munsch, C. M., Bergdahl, A., Hultgardh-Nilsson, A., Gomez, M. F., Porter, K. E., Hellstrand, P., & Beech, D. J. (2006). Upregulated TRPC1 channel in vascular injury in vivo and its role in human neointimal hyperplasia. *Circulation Research* **98**, 557-563.

91. Kupper, J. (1998). Functional expression of GFP-tagged Kv1.3 and Kv1.4 channels in HEK 293 cells. *Eur J Neurosci* **10**, 3908-3912.

92. Kurata, H. T., Doerksen, K. W., Eldstrom, J. R., Rezazadeh, S., &

Fedida, D. (2005). Separation of P/C- and U-type inactivation pathways in Kv1.5 potassium channels. *Journal of Physiology* **568**, 31-46.

93. Lagrutta, A., Wang, J., Fermini, B., & Salata, J. J. (2006). Novel, Potent Inhibitors of Human Kv1.5 K+ Channels and Ultrarapidly Activating Delayed Rectifier Potassium Current. *Journal of Pharmacology and Experimental Therapeutics* **317**, 1054-1063.

94. Larsson, H. P. & Elinder, F. (2000). A conserved glutamate is important for slow inactivation in K+ channels. *Neuron* **27**, 573-583.

95. Lecar, H., Larsson, H. P., & Grabe, M. (2003). Electrostatic model of S4 motion in voltage-gated ion channels. *Biophys.J* **85**, 2854-2864.

96. Ledoux, J., Werner, M. E., Brayden, J. E., & Nelson, M. T. (2006). Calcium-Activated Potassium Channels and the Regulation of Vascular Tone. *Physiology* **21**, 69-78.

97. Leonard, R. J., Garcia, M. L., Slaughter, R. S., & Reuben, J. P. (1992). Selective blockers of voltage-gated K+ channels depolarize human T lymphocytes: mechanism of the antiproliferative effect of charybdotoxin. *Proc Natl.Acad.Sci U S.A* **89**, 10094-10098.

98. Lev, S., Moreno, H., Martinez, R., Canoll, P., Peles, E., Musacchio, J. M., Plowman, G. D., Rudy, B., & Schlessinger, J. (1995). Protein tyrosine kinase PYK2 involved in Ca(2+)-induced regulation of ion channel and MAP kinase functions. *Nature* **376**, 737-745.

99. Levick J.R. (2010). *An Introduction to Cardiovascular Physiology.*, Fifth ed. Hodder Arnold, London.

100. Levin, G., Keren, T., Peretz, T., Chikvashvili, D., Thornhill, W. B., & Lotan, I. (1995). Regulation of RCK1 currents with a cAMP analog via enhanced protein synthesis and direct channel phosphorylation. *J Biol Chem* **270**, 14611-14618.

101. Levitan, I. B. (1994b). Modulation of ion channels by protein phosphorylation and dephosphorylation. *Annu.Rev Physiol* **56**, 193-212.

102. Levitan, I. B. (1994a). Modulation of ion channels by protein phosphorylation and dephosphorylation. *Annu.Rev Physiol* **56**, 193-212.

103. Levitan, I. B. (2006). Signaling protein complexes associated with neuronal ion channels. *Nat Neurosci* **9**, 305-310.

104. Levite, M., Cahalon, L., Peretz, A., Hershkoviz, R., Sobko, A., Ariel, A., Desai, R., Attali, B., & Lider, O.

(2000). Extracellular K+ and Opening of Voltage-Gated Potassium Channels Activate T Cell Integrin Function: Physical and Functional Association between Kv1.3 Channels and {beta}1 Integrins. *The Journal of Experimental Medicine* **191**, 1167-1176.

105. Levy, M. N. & Pappano, A. J. (2007). *Cardiovascular Physiology*, 9th ed. Philadelphia.

106. Li, M., Jan, Y. N., & Jan, L. Y. (1992). Specification of subunit assembly by the hydrophilic amino-terminal domain of the Shaker potassium channel. *Science* **257**, 1225-1230.

107. Long, S. B., Campbell, E. B., & MacKinnon, R. (2005a). Crystal structure of a mammalian voltage-dependent Shaker family K+ channel. *Science* **309**, 897-903.

108. Long, S. B., Campbell, E. B., & Mackinnon, R. (2005b). Crystal structure of a mammalian voltage-dependent Shaker family K+ channel. *Science* **309**, 897-903.

109. Lu, J., Robinson, J. M., Edwards, D., & Deutsch, C. (2001). T1-T1 interactions occur in ER membranes while nascent Kv peptides are still attached to ribosomes. *Biochemistry* **40**, 10934-10946.

110. Ludin, B. & Matus, A. (1998). GFP illuminates the cytoskeleton. *Trends Cell Biol* **8**, 72-77.

111. Mack, C. P. (2011). Signaling Mechanisms That Regulate Smooth Muscle Cell Differentiation. *Arteriosclerosis, Thrombosis, and Vascular Biology* **31**, 1495-1505.

112. MacKinnon, R. (1995). Pore loops: an emerging theme in ion channel structure. *Neuron* **14**, 889-892.

113. Manganas, L. N. & Trimmer, J. S. (2000). Subunit composition determines Kv1 potassium channel surface expression. *J.Biol.Chem.* **275**, 29685-29693.

114. Manganas, L. N., Wang, Q., Scannevin, R. H., Antonucci, D. E., Rhodes, K. J., & Trimmer, J. S. (2001). Identification of a trafficking determinant localized to the Kv1 potassium channel pore. *Proceedings of the National Academy of Sciences* **98**, 14055-14059.

115. Marks, D. R. & Fadool, D. A. (2007). Post-synaptic density perturbs insulin-induced Kv1.3 channel modulation via a clustering mechanism involving the SH3 domain. *J Neurochem.* **103**, 1608-1627.

116. Martinez-Marmol, R., Perez-Verdaguer, M., Roig, S. R., Vallejo-Gracia, A., Gotsi, P., Serrano-

Albarras, A., Bahamonde, M. I., Ferrer-Montiel, A., Fernandez-Ballester, G., Comes, N., & Felipe, A. (2013). A non-canonical di-acidic signal at the C-terminus of Kv1.3 determines anterograde trafficking and surface expression. *J Cell Sci* **126**, 5681-5691.

117. Maruoka, N. D., Steele, D. F., Au, B. P., Dan, P., Zhang, X., Moore, E. D., & Fedida, D. (2000). alpha-actinin-2 couples to cardiac Kv1.5 channels, regulating current density and channel localization in HEK cells. *FEBS Lett.* **473**, 188-194.

118. Matz, M. V., Fradkov, A. F., Labas, Y. A., Savitsky, A. P., Zaraisky, A. G., Markelov, M. L., & Lukyanov, S. A. (1999). Fluorescent proteins from nonbioluminescent Anthozoa species. *Nat Biotechnol.* **17**, 969-973.

119. McCormack, K., McCormack, T., Tanouye, M., Rudy, B., & Stuhmer, W. (1995). Alternative splicing of the human Shaker K+ channel beta 1 gene and functional expression of the beta 2 gene product. *FEBS Lett.* **370**, 32-36.

120. McCormack, T., McCormack, K., Nadal, M. S., Vieira, E., Ozaita, A., & Rudy, B. (1999). The effects of Shaker beta-subunits on the human lymphocyte K+ channel Kv1.3. *J Biol Chem.* **274**, 20123-20126.

121. Miguel-Velado, E., Moreno-Dominguez, A., Colinas, O., Cidad, P., Heras, M., Perez-Garcia, M. T., & López-López, J. R. (2005). Contribution of Kv Channels to Phenotypic Remodeling of Human Uterine Artery Smooth Muscle Cells. *Circulation Research* **97**, 1280-1287.

122. Miguel-Velado, E., Perez-Carretero, F. D., Colinas, O., Cidad, P., Heras, M., Lopez-Lopez, J. R., & Perez-Garcia, M. T. (2010). Cell-cycle dependent expression of Kv3.4 channels modulates proliferation of human uterine artery smooth muscle cells. *Cardiovascular Research* **86**, 383-391.

123. Miller, A. G. & Aldrich, R. W. (1996). Conversion of a delayed rectifier K+ channel to a voltage-gated inward rectifier K+ channel by three amino acid substitutions. *Neuron* **16**, 853-858.

124. Millership, J. E., Devor, D. C., Hamilton, K. L., Balut, C. M., Bruce, J. I. E., & Fearon, I. M. (2011). Calcium-activated K+ channels increase cell proliferation independent of K+ conductance. *American Journal of Physiology - Cell Physiology* **300**, C792-C802.

125. Misonou, H. & Trimmer, J. S. (2004a). Determinants of voltage-gated potassium channel surface expression and localization in

Mammalian neurons. *Crit Rev Biochem Mol Biol* **39**, 125-145.

126. Misonou, H. & Trimmer, J. S. (2004b). Determinants of voltage-gated potassium channel surface expression and localization in Mammalian neurons. *Crit Rev Biochem Mol Biol* **39**, 125-145.

127. Mitchell, D. A., Vasudevan, A., Linder, M. E., & Deschenes, R. J. (2006). Protein palmitoylation by a family of DHHC protein S-acyltransferases. *J Lipid Res* **47**, 1118-1127.

128. Morales, M. J., Castellino, R. C., Crews, A. L., Rasmusson, R. L., & Strauss, H. C. (1995). A novel beta subunit increases rate of inactivation of specific voltage-gated potassium channel alpha subunits. *J Biol Chem* **270**, 6272-6277.

129. Moudgil, R., Michelakis, E. D., & Archer, S. L. (2006). The role of k+ channels in determining pulmonary vascular tone, oxygen sensing, cell proliferation, and apoptosis: implications in hypoxic pulmonary vasoconstriction and pulmonary arterial hypertension. *Microcirculation* **13**, 615-632.

130. Muto, A., Fitzgerald, T. N., Pimiento, J. M., Maloney, S. P., Teso, D., Paszkowiak, J. J., Westvik, T. S., Kudo, F. A., Nishibe, T., & Dardik, A. (2007). Smooth muscle cell signal transduction: Implications of vascular biology for vascular surgeons. *Journal of Vascular Surgery* **45**, A15-A24.

131. Nagai, R., Kuro-o M, Babij, P., & Periasamy, M. (1989). Identification of two types of smooth muscle myosin heavy chain isoforms by cDNA cloning and immunoblot analysis. *J Biol Chem* **264**, 9734-9737.

132. Nagaya, N. & Papazian, D. M. (1997). Potassium channel alpha and beta subunits assemble in the endoplasmic reticulum. *J Biol Chem.* **272**, 3022-3027.

133. Nakahira, K., Shi, G., Rhodes, K. J., & Trimmer, J. S. (1996). Selective interaction of voltage-gated K+ channel beta-subunits with alpha-subunits. *J.Biol.Chem.* **271**, 7084-7089.

134. Nelson, M. T., Cheng, H., Rubart, M., Santana, L. F., Bonev, A. D., Knot, H. J., & Lederer, W. J. (1995). Relaxation of arterial smooth muscle by calcium sparks. *Science* **270**, 633-637.

135. Nelson, M. T. & Quayle, J. M. (1995). Physiological roles and properties of potassium channels in arterial smooth muscle. *AJP - Cell Physiology* **268**, C799-C822.

136. Neylon, C. B., Lang, R. J., Fu, Y., Bobik, A., & Reinhart, P. H. (1999). Molecular cloning and characterization of the

intermediate-conductance Ca(2+)-activated K(+) channel in vascular smooth muscle: relationship between K(Ca) channel diversity and smooth muscle cell function. *Circ.Res.* **85**, e33-e43.

137. Neylon, C. B. (2002). Potassium channels and vascular proliferation. *Vascular Pharmacology* **38**, 35-41.

138. Obenauer, J. C., Cantley, L. C., & Yaffe, M. B. (2003). Scansite 2.0: Proteome-wide prediction of cell signaling interactions using short sequence motifs. *Nucleic Acids Res* **31**, 3635-3641.

139. Ogielska, E. M., Zagotta, W. N., Hoshi, T., Heinemann, S. H., Haab, J., & Aldrich, R. W. (1995). Cooperative subunit interactions in C-type inactivation of K channels. *Biophys.J.* **69**, 2449-2457.

140. Owens, G. K. (1995). Regulation of differentiation of vascular smooth muscle cells. *Physiological Reviews* **75**, 487-517.

141. Owens, G. K. (1998). Molecular control of vascular smooth muscle cell differentiation. *Acta Physiol Scand.* **164**, 623-635.

142. Owens, G. K., Kumar, M. S., & Wamhoff, B. R. (2004). Molecular regulation of vascular smooth muscle cell differentiation in development and disease. *Physiol Rev.* **84**, 767-801.

143. Papazian, D. M., Timpe, L. C., Jan, Y. N., & Jan, L. Y. (1991). Alteration of voltage-dependence of Shaker potassium channel by mutations in the S4 sequence. *Nature* **349**, 305-310.

144. Parcej, D. N. & Dolly, J. O. (1989). Dendrotoxin acceptor from bovine synaptic plasma membranes. Binding properties, purification and subunit composition of a putative constituent of certain voltage-activated K+ channels. *Biochem J* **257**, 899-903.

145. Parcej, D. N., Scott, V. E., & Dolly, J. O. (1992). Oligomeric properties of alpha-dendrotoxin-sensitive potassium ion channels purified from bovine brain. *Biochemistry* **31**, 11084-11088.

146. Pardo, L. A. & Stuhmer, W. (2014). The roles of K(+) channels in cancer. *Nat Rev Cancer* **14**, 39-48.

147. Pardo, L. A. (2004). Voltage-Gated Potassium Channels in Cell Proliferation. *Physiology* **19**, 285-292.

148. Park, K. S., Yang, J. W., Seikel, E., & Trimmer, J. S. (2008). Potassium channel phosphorylation in excitable cells: providing dynamic functional variability to a diverse family of ion channels. *Physiology (Bethesda.)* **23**, 49-57.

149. Pérez-García, M. T., López-López, J. R., & Gonzalez, C. (1999). Kvβ1.2 subunit coexpression in HEK293 cells confers $O_2$ sensitivity to kv4.2 but not to Shaker channels. *J.Gen.Physiol* **113**, 897-907.

150. Pérez-García, M. T., López-López, J. R., Riesco, A. M., Hoppe, U. C., Marban, E., Gonzalez, C., & Johns, D. C. (2000). Viral gene transfer of dominant-negative Kv4 construct suppresses an O2- sensitive K+ current in chemoreceptor cells. *J.Neurosci.* **20**, 5689-5695.

151. Perozo, E., MacKinnon, R., Bezanilla, F., & Stefani, E. (1993). Gating currents from a nonconducting mutant reveal open-closed conformations in Shaker K+ channels. *Neuron* **11**, 353-358.

152. Pongs, O. (1995). Regulation of the activity of voltage-gated potassium channels by ß subunits. *Seminars in the Neurosciences* **7**, 137-146.

153. Qian, Z., Haessler, M., Lemos, J. A., Arsenault, J. R., Aguirre, J. E., Gilbert, J. R., Bowler, R. P., & Park, F. (2006). Targeting vascular injury using Hantavirus-pseudotyped lentiviral vectors. *Mol Ther* **13**, 694-704.

154. Rasmusson, R. L., Morales, M. J., Wang, S., Liu, S., Campbell, D. L., Brahmajothi, M. V., & Strauss, H. C. (1998). Inactivation of voltage-gated cardiac K+ channels. *Circulation Research* **82**, 739-750.

155. Remillard, C. V. & Yuan, J. X. (2004). Activation of K+ channels: an essential pathway in programmed cell death. *Am J Physiol Lung Cell Mol Physiol* **286**, L49-L67.

156. Rettig, J., Heinemann, S. H., Wunder, F., Lorra, C., Parcej, D. N., Dolly, J. O., & Pongs, O. (1994). Inactivation properties of voltage-gated K+ channels altered by presence of beta-subunit. *Nature* **369**, 289-294.

157. Rhodes, K. J., Keilbaugh, S. A., Barrezueta, N. X., Lopez, K. L., & Trimmer, J. S. (1995). Association and colocalization of K+ channel alpha- and beta-subunit polypeptides in rat brain. *J.Neurosci.* **15**, 5360-5371.

158. Rhodes, K. J., Monaghan, M. M., Barrezueta, N. X., Nawoschik, S., Bekele-Arcuri, Z., Matos, M. F., Nakahira, K., Schechter, L. E., & Trimmer, J. S. (1996). Voltage-gated K+ channel beta subunits: expression and distribution of Kv beta 1 and Kv beta 2 in adult rat brain. *J.Neurosci.* **16**, 4846-4860.

159. Rhodes, K. J., Strassle, B. W., Monaghan, M. M., Bekele-Arcuri, Z., Matos, M. F., & Trimmer, J. S. (1997). Association and colocalization of the Kvbeta1 and Kvbeta2 beta-subunits with Kv1

alpha-subunits in mammalian brain K+ channel complexes. *J.Neurosci.* **17**, 8246-8258.

160. Robbins, J. R., Lee, S. M., Filipovich, A. H., Szigligeti, P., Neumeier, L., Petrovic, M., & Conforti, L. (2005). Hypoxia modulates early events in T cell receptor-mediated activation in human T lymphocytes via Kv1.3 channels. *Journal of Physiology* **564**, 131-143.

161. Rodman, D. M., Reese, K., Harral, J., Fouty, B., Wu, S., West, J., Hoedt-Miller, M., Tada, Y., Li, K. X., Cool, C., Fagan, K., & Cribbs, L. (2005). Low-Voltage-Activated (T-Type) Calcium Channels Control Proliferation of Human Pulmonary Artery Myocytes. *Circulation Research* **96**, 864-872.

162. Schmitz, A., Sankaranarayanan, A., Azam, P., Schmidt-Lassen, K., Homerick, D., Hansel, W., & Wulff, H. (2005). Design of PAP-1, a selective small molecule Kv1.3 blocker, for the suppression of effector memory T cells in autoimmune diseases. *Molecular Pharmacology* **68**, 1254-1270.

163. Schwetz, T. A., Norring, S. A., & Bennett, E. S. (2010). N-glycans modulate K(v)1.5 gating but have no effect on K(v)1.4 gating. *Biochim.Biophys.Acta* **1798**, 367-375.

164. Scott, V. E., Rettig, J., Parcej, D. N., Keen, J. N., Findlay, J. B., Pongs, O., & Dolly, J. O. (1994). Primary structure of a beta subunit of alpha-dendrotoxin-sensitive K+ channels from bovine brain. *Proc.Natl.Acad.Sci U S.A* **91**, 1637-1641.

165. Seoh, S. A., Sigg, D., Papazian, D. M., & Bezanilla, F. (1996). Voltage-sensing residues in the S2 and S4 segments of the Shaker K+ channel. *Neuron* **16**, 1159-1167.

166. Sewing, S., Roeper, J., & Pongs, O. (1996). Kv$\beta$1 subunit binding specific for *shaker*-related potassium channel $\alpha$ subunits. *Neuron* **16**, 455-463.

167. Shanahan, C. M. & Weissberg, P. L. (1998). Smooth muscle cell heterogeneity: patterns of gene expression in vascular smooth muscle cells in vitro and in vivo. *Arteriosclerosis, Thrombosis, and Vascular Biology* **18**, 333-338.

168. Shen, N. V., Chen, X., Boyer, M. M., & Pfaffinger, P. J. (1993). Deletion analysis of K+ channel assembly. *Neuron* **11**, 67-76.

169. Shen, N. V. & Pfaffinger, P. J. (1995). Molecular recognition and assembly sequences involved in the subfamily-specific assembly of voltage-gated K+ channel subunit proteins. *Neuron* **14**, 625-633.

170. Shi, G., Nakahira, K., Hammond, S., Rhodes, K. J., Schechter, L. E., & Trimmer, J. S. (1996). Beta subunits promote K+ channel surface expression through effects early in biosynthesis. *Neuron* **16**, 843-852.

171. Siciliano, J. C., Gelman, M., & Girault, J. A. (1994). Depolarization and neurotransmitters increase neuronal protein tyrosine phosphorylation. *J Neurochem.* **62**, 950-959.

172. Snyders, D. J. (1999b). Structure and function of cardiac potassium channels. *Cardiovasc Res* **42**, 377-390.

173. Snyders, D. J. (1999c). Structure and function of cardiac potassium channels. *Cardiovasc Res* **42**, 377-390.

174. Snyders, D. J. (1999a). Structure and function of cardiac potassium channels. *Cardiovasc Res* **42**, 377-390.

175. Solway, J., Seltzer, J., Samaha, F. F., Kim, S., Alger, L. E., Niu, Q., Morrisey, E. E., Ip, H. S., & Parmacek, M. S. (1995). Structure and expression of a smooth muscle cell-specific gene, SM22 alpha. *J Biol Chem* **270**, 13460-13469.

176. Somlyo, A. P. & Somlyo, A. V. (1994). Signal transduction and regulation in smooth muscle. *Nature* **372**, 231-236.

177. Stauber, R. H., Horie, K., Carney, P., Hudson, E. A., Tarasova, N. I., Gaitanaris, G. A., & Pavlakis, G. N. (1998). Development and applications of enhanced green fluorescent protein mutants. *BioTechniques* **24**, 462-471.

178. Stuhmer, W., Ruppersberg, J. P., Schroter, K. H., Sakmann, B., Stocker, M., Giese, K. P., Perschke, A., Baumann, A., & Pongs, O. (1989). Molecular basis of functional diversity of voltage-gated potassium channels in mammalian brain. *EMBO J* **8**, 3235-3244.

179. Sun, X. X., Hodge, J. J., Zhou, Y., Nguyen, M., & Griffith, L. C. (2004). The eag potassium channel binds and locally activates calcium/calmodulin-dependent protein kinase II. *J.Biol.Chem.* **279**, 10206-10214.

180. Swanson, R., Marshall, J., Smith, J. S., Williams, J. B., Boyle, M. B., Folander, K., Luneau, C. J., Antanavage, J., Oliva, C., Buhrow, S. A., & . (1990). Cloning and expression of cDNA and genomic clones encoding three delayed rectifier potassium channels in rat brain. *Neuron* **4**, 929-939.

181. Tamkun, M. M., Knoth, K. M., Walbridge, J. A., Kroemer, H., Roden, D. M., & Glover, D. M.

(1991). Molecular cloning and characterization of two voltage-gated K+ channel cDNAs from human ventricle. *FASEB J* **5**, 331-337.

182. ten Dijke, P. & Arthur, H. M. (2007). Extracellular control of TGFbeta signalling in vascular development and disease. *Nat Rev Mol Cell Biol* **8**, 857-869.

183. Thyberg, J. (1996). Differentiated properties and proliferation of arterial smooth muscle cells in culture. *Int.Rev.Cytol.* **169**, 183-265.

184. Timpe, L. C. & Fantl, W. J. (1994). Modulation of a voltage-activated potassium channel by peptide growth factor receptors. *J Neurosci* **14**, 1195-1201.

185. Tsai, W., Morielli, A. D., Cachero, T. G., & Peralta, E. G. (1999). Receptor protein tyrosine phosphatase alpha participates in the m1 muscarinic acetylcholine receptor-dependent regulation of Kv1.2 channel activity. *EMBO J* **18**, 109-118.

186. Tu, L., Santarelli, V., Sheng, Z., Skach, W., Pain, D., & Deutsch, C. (1996). Voltage-gated K+ channels contain multiple intersubunit association sites. *J Biol Chem* **271**, 18904-18911.

187. Valiyaveetil, F. I., Leonetti, M., Muir, T. W., & MacKinnon, R. (2006). Ion selectivity in a semisynthetic K+ channel locked in the conductive conformation. *Science* **314**, 1004-1007.

188. Vennekamp, J., Wulff, H., Beeton, C., Calabresi, P. A., Grissmer, S., Hansel, W., & Chandy, K. G. (2004). Kv1.3-blocking 5-phenylalkoxypsoralens: a new class of immunomodulators. *Molecular Pharmacology* **65**, 1364-1374.

189. Vicente, R., Escalada, A., Coma, M., Fuster, G., Sanchez-Tillo, E., Lopez-Iglesias, C., Soler, C., Solsona, C., Celada, A., & Felipe, A. (2003a). Differential voltage-dependent K+ channel responses during proliferation and activation in macrophages. *J Biol Chem* **278**, 46307-46320.

190. Vicente, R., Escalada, A., Villalonga, N., Texido, L., Roura-Ferrer, M., Martin-Satue, M., Lopez-Iglesias, C., Soler, C., Solsona, C., Tamkun, M. M., & Felipe, A. (2006). Association of Kv1.5 and Kv1.3 contributes to the major voltage-dependent K+ channel in macrophages. *J Biol Chem* **281**, 37675-37685.

191. Vicente, R. n., Villalonga, N. +., Calvo, M., Escalada, A., Solsona, C., Soler, C., Tamkun, M. M., & Felipe, A. (2008). Kv1.5 Association Modifies Kv1.3 Traffic and Membrane Localization. *Journal of Biological Chemistry* **283**, 8756-8764.

192. Vicente, R., Escalada, A., Coma, M., Fuster, G., Sanchez-Tillo, E., Lopez-Iglesias, C., Soler, C., Solsona, C., Celada, A., & Felipe, A. (2003b). Differential Voltage-dependent K+ Channel Responses during Proliferation and Activation in Macrophages. *Journal of Biological Chemistry* **278**, 46307-46320.

193. Villalonga, N., Escalada, A., Vicente, R., Sanchez-Tillo, E., Celada, A., Solsona, C., & Felipe, A. (2007a). Kv1.3/Kv1.5 heteromeric channels compromise pharmacological responses in macrophages. *Biochem Biophys.Res Commun.* **352**, 913-918.

194. Villalonga, N., Ferreres, J. C., Argiles, J. M., Condom, E., & Felipe, A. (2007b). Potassium channels are a new target field in anticancer drug design. *Recent Pat Anticancer Drug Discov.* **2**, 212-223.

195. Villalonga, N., David, M., Bielanska, J., Vicente, R., Comes, N., Valenzuela, C., & Felipe, A. (2010). Immunomodulation of voltage-dependent K+ channels in macrophages: molecular and biophysical consequences. *The Journal of General Physiology* **135**, 135-147.

196. Villalonga, N., Martínez-Marmol, R., Roura-Ferrer, M., David, M., Valenzuela, C., Soler, C., & Felipe, A. (2008). Cell cycle-dependent expression of Kv1.5 is involved in myoblast proliferation. *Biochimica et Biophysica Acta (BBA) - Molecular Cell Research* **1783**, 728-736.

197. Wallner, M., Meera, P., & Toro, L. (1996). Determinant for beta-subunit regulation in high-conductance voltage-activated and Ca(2+)-sensitive K+ channels: an additional transmembrane region at the N terminus. *Proc Natl.Acad.Sci U S.A* **93**, 14922-14927.

198. Wamhoff, B. R., Bowles, D. K., & Owens, G. K. (2006). Excitation-transcription coupling in arterial smooth muscle. *Circulation Research* **98**, 868-878.

199. Wang, Z., Robertson, B., & Fedida, D. (2007). Gating currents from a Kv3 subfamily potassium channel: charge movement and modification by BDS-II toxin. *Journal of Physiology* **584**, 755-767.

200. Watanabe, I., Zhu, J., Recio-Pinto, E., & Thornhill, W. B. (2004). Glycosylation affects the protein stability and cell surface expression of Kv1.4 but Not Kv1.1 potassium channels. A pore region determinant dictates the effect of glycosylation on trafficking. *J Biol Chem* **279**, 8879-8885.

201. Watanabe, I., Zhu, J., Sutachan, J. J., Gottschalk, A., Recio-Pinto, E.,

& Thornhill, W. B. (2007). The glycosylation state of Kv1.2 potassium channels affects trafficking, gating, and simulated action potentials. *Brain Res* **1144**, 1-18.

202. Welschoff, J., Matthey, M., & Wenzel, D. (2014). RGD peptides induce relaxation of pulmonary arteries and airways via beta3-integrins. *FASEB J* **28**, 2281-2292.

203. Wonderlin, W. F. & Strobl, J. S. (1996). Potassium channels, proliferation and G1 progression. *J Membr.Biol.* **154**, 91-107.

204. Woodrow, S., Bissoon, N., & Gurd, J. W. (1992). Depolarization-dependent tyrosine phosphorylation in rat brain synaptosomes. *J Neurochem.* **59**, 857-862.

205. Wulff, H., Castle, N. A., & Pardo, L. A. (2009). Voltage-gated potassium channels as therapeutic targets. *Nat Rev Drug Discov.* **8**, 982-1001.

206. Xu, J., Yu, W., Jan, Y. N., Jan, L. Y., & Li, M. (1995). Assembly of voltage-gated potassium channels. Conserved hydrophilic motifs determine subfamily-specific interactions between the alpha-subunits. *J.Biol.Chem.* **270**, 24761-24768.

207. Yang, J., Jiang, H., Chen, S. S., Chen, J., Li, W. Q., Xu, S. K., & Wang, J. C. (2010). Lentivirus-mediated RNAi targeting CREB binding protein attenuates neointimal formation and promotes re-endothelialization in balloon injured rat carotid artery. *Cell Physiol Biochem* **26**, 441-448.

208. Yang, J. W., Vacher, H., Park, K. S., Clark, E., & Trimmer, J. S. (2007). Trafficking-dependent phosphorylation of Kv1.2 regulates voltage-gated potassium channel cell surface expression. *Proc Natl.Acad.Sci U S.A* **104**, 20055-20060.

209. Yifrach, O. & MacKinnon, R. (2002). Energetics of pore opening in a voltage-gated K(+) channel. *Cell* **111**, 231-239.

210. Yu, W., Xu, J., & Li, M. (1996). NAB domain is essential for the subunit assembly of both $\alpha$-$\alpha$ and $\alpha$-$\beta$ complexes of shaker-like potassium channels. *Neuron* **16**, 441-453.

211. Yuan, J. X., Aldinger, A. M., Juhaszova, M., Wang, J., Conte, J. V., Jr., Gaine, S. P., Orens, J. B., & Rubin, L. J. (1998a). Dysfunctional voltage-gated K+ channels in pulmonary artery smooth muscle cells of patients with primary pulmonary hypertension. *Circulation* **98**, 1400-1406.

212. Yuan, X. J., Wang, J., Juhaszova, M., Gaine, S. P., & Rubin, L. J. (1998b). Attenuated K+ channel

gene transcription in primary pulmonary hypertension. *Lancet* **351**, 726-727.

213. Zagotta, W. N., Hoshi, T., & Aldrich, R. W. (1990). Restoration of inactivation in mutants of Shaker potassium channels by a peptide derived from ShB. *Science* **250**, 568-571.

214. Zhan, Y., Kim, S., Yasumoto, H., Namba, M., Miyazaki, H., & Iwao, H. (2002). Effects of dominant-negative c-Jun on platelet-derived growth factor-induced vascular smooth muscle cell proliferation. *Arteriosclerosis, Thrombosis, and Vascular Biology* **22**, 82-88.

215. Zhou, Y., Morais-Cabral, J. H., Kaufman, A., & MacKinnon, R. (2001). Chemistry of ion coordination and hydration revealed by a K+ channel-Fab complex at 2.0 A resolution. *Nature* **414**, 43-48.

216. Zhu, J., Watanabe, I., Gomez, B., & Thornhill, W. B. (2001b). Determinants involved in Kv1 potassium channel folding in the endoplasmic reticulum, glycosylation in the Golgi, and cell surface expression. *J Biol Chem* **276**, 39419-39427.

217. Zhu, J., Watanabe, I., Gomez, B., & Thornhill, W. B. (2001a). Determinants involved in Kv1 potassium channel folding in the endoplasmic reticulum, glycosylation in the Golgi, and cell surface expression. *J Biol Chem* **276**, 39419-39427.

218. Zhu, J., Watanabe, I., Gomez, B., & Thornhill, W. B. (2003a). Heteromeric Kv1 potassium channel expression: amino acid determinants involved in processing and trafficking to the cell surface. *J Biol Chem* **278**, 25558-25567.

219. Zhu, J., Watanabe, I., Poholek, A., Koss, M., Gomez, B., Yan, C., Recio-Pinto, E., & Thornhill, W. B. (2003b). Allowed N-glycosylation sites on the Kv1.2 potassium channel S1-S2 linker: implications for linker secondary structure and the glycosylation effect on channel function. *Biochemical Journal* **375**, 769-775.

220. Zhu, J., Yan, J., & Thornhill, W. B. (2012). N-glycosylation promotes the cell surface expression of Kv1.3 potassium channels. *FEBS Journal* **279**, 2632-2644.

# 8

# RESUMEN

## 8.1. Introducción

Las células de músculo liso vascular (CMLV) son capaces de pasar de un fenotipo contráctil a un fenotipo proliferativo en respuesta a diversos factores o estímulos que actúan sobre el vaso. La proliferación de estas células es importante en todos los estados del desarrollo y es crítica en la reparación tisular frente a diversas lesiones (Owens, 1995). Sin embargo, además de este papel fisiológico, la plasticidad de las CMLV contribuye de forma importante a numerosas patologías cardiovasculares, como la hipertensión, la ateroesclerosis o la restenosis tras angioplastia. En todas estas situaciones existen factores fisiológicos o patológicos que desencadenan la modulación fenotípica de las CMLV, induciendo su desdiferenciación con la expresión de genes que codifican para proteínas reguladoras del crecimiento, la migración y la proliferación celular.

Los cambios coordinados en la expresión de canales iónicos son también un componente integral de esta plasticidad. De hecho, los cambios en la expresión de los canales de $K^+$ se asocian con alteraciones en las propiedades funcionales de las CMLV (Neylon, 2002). En trabajos previos de nuestro grupo se generó un perfil de expresión de 87 genes de canales iónicos de CMLV de arteria femoral de ratón, en fenotipo contráctil y en dos modelos diferentes de proliferación: un modelo in vitro (CMLV en cultivo) y un modelo in vivo (CMLV desdiferenciadas procedentes de lesiones endoluminales). Este abordaje permitió identificar cambios en la expresión de los canales iónicos asociados al fenotipo proliferativo en las dos condiciones experimentales estudiadas. Así, se observó una sobreexpresión de dos genes, el canal Kv1.3 y la subunidad accesoria de este canal, Kvβ2.1. Por otra parte, la expresión funcional del Kv1.5, el canal más

abundante en el fenotipo contráctil, desapareció tras el cambio fenotípico (Cidad et al., 2010). Estos cambios en la expresión de los canales Kv1.3 y Kv1.5 tras el cambio fenotípico se vieron conservados en otros lechos vasculares de ratón (CMLV de arteria aorta y mesentérica), determinando que el cociente entre la expresión de los canales Kv1.3 y Kv1.5 podría constituir un indicador de la modulación fenotípica.

El bloqueo del Kv1.3 con agentes selectivos redujo significativamente la proliferación y la capacidad de migración de las CMLV en cultivo, demostrando que existe una asociación entre el aumento de la expresión funcional de los canales Kv1.3 y la capacidad de proliferación de estas células (Cidad et al., 2010). Estos datos se han descrito también en otros lechos vasculares de ratón (arterias mesentéricas) (Cidad et al., 2012) y en diversos lechos vasculares humanos (Cidad et al., 2014).

A pesar de que existen otros canales cuya expresión y/o función también se han relacionado con un aumento en la proliferación de las CMLV (Miguel-Velado et al., 2010;Kohler et al., 2003), la asociación de estos canales y la proliferación no se ha visto conservada en otros lechos vasculares.

Por tanto, el hecho de que el efecto pro-proliferativo de los canales Kv1.3 se haya descrito en CMLV de diferentes lechos vasculares y especies podría reflejar una asociación de estos canales con el remodelamiento vascular, pudiendo representar una diana terapeútica.

## 8.2. Objetivos

El principal objetivo de este trabajo es la caracterización del papel de los canales Kv1.3 en la proliferación celular. Para ello, estudiaremos los determinantes moleculares del Kv1.3 relacionados con la proliferación, así como los mecanismos y las vías de señalización involucradas.

## 8.3. Materiales y Métodos

Para la realización de los principales experimentos de esta tesis se ha usado la línea celular HEK293. En estas células se han transfectado distintos vectores de expresión mediante Lipofectamina 2000. Los vectores usados son plásmidos bicistrónicos que codifican para Kv1.3 o Kv1.5, proteínas de fusión de ambos canales generadas por PCR, mutantes puntuales del Kv1.3 y canales quiméricos Kv1.3-Kv1.5. Las mutaciones puntuales se han generado usando el kit de mutagénesis dirigida QuikChange (mutantes del poro: Kv1.3-AYA y Kv1.3-W389F, mutante del poro y del sensor de voltaje: Kv1.3-WF3x y mutantes de todos los residuos fosforilables del extremo carboxilo del Kv1.3-(T439A, Y447A, S459A, S470A, S473A, S475A, Y477A, T493A). Las quimeras usadas se han generado bien por PCR convencional (K5N3 y K5C3), mediante alineamiento de oligos (K5-613YS) o por PCR de extensión por solapamiento (K5-532YS). Por último, se ha generado también un vector truncado del Kv1.3 (K3YS) mediante alineamiento de oligos.

La caracterización de la expresión en membrana de estos mutantes se ha llevado a cabo mediante inmunocitoquímica, mientras que la caracterización funcional y el estudio de la cinética de estos canales se ha realizado con

estudios de patch-clamp, usando las conformaciones de whole-cell, parche perforado y cell-attached. La expresión proteica y los cambios en la fosforilación del Kv1.3 se han estudiado por immunoblot. Finalmente, los ensayos de proliferación se realizaron mediante contaje celular y estudiando la incorporación de EdU, un análogo de la timidina que se incorpora durante la fase S del ciclo celular.

Con el objetivo de realizar transferencias génicas en CMLV (uterinas, coronarias y renales) se han usado lentivirus.

## 8.4. Resultados

Los resultados obtenidos en CMLV han sido validados en un sistema heterólogo como son las células HEK293. La sobreexpresión de Kv1.3 condujo a un aumento significativo de la proliferación celular, mientras que la sobreexpresión de Kv1.5 inhibió la proliferación. El efecto pro-proliferativo del Kv1.3 fue inhibido por bloqueantes selectivos de este canal, como el PAP-1 y la Margatoxina. Además, el estudio de los efectos sobre la proliferación de los mutantes del poro y/o del sensor de voltaje indicó que el efecto pro-proliferativo del Kv1.3 puede ser reproducido por mutantes del poro pero no por un mutante del sensor de voltaje.

Mediante la sobreexpresión de las quimeras K5N3 y K5C3, se determinó que los determinantes moleculares responsables de la proliferación inducida por Kv1.3 residen en el dominio carboxilo. En particular, identificamos dos residuos cercanos (Y447 y S459) cuyas mutaciones inhibieron el efecto del Kv1.3 sobre la proliferación. De hecho, en quimeras del Kv1.5 que

contenían el fragmento YS se observó un aumento significativo de la proliferación únicamente cuando este segmento había sido clonado en el sitio análogo del Kv1.3.

El uso del bloqueante PD98059, inhibidor de la vía de señalización de MEK/ERK, redujo la proliferación de manera significativa en células transfectadas con Kv1.3 pero no en células transfectadas con los mutantes Kv1.3-Y447 o Kv1.3-S459. Cuando estudiamos los efectos sobre la fosforilación de la proteína, PD98059 fue capaz de inhibir la fosforilación en tirosinas (p-Tyr) de Kv1.3, no observándose ningún efecto en el mutante Y447A. Al estudiar los niveles de p-Tyr asociados al cambio conformacional del canal, observamos que esta fosforilación aumentaba en aquellas células que habíamos incubado con una alta concentración de potasio extracelular. Sin embargo, al incubar las células con esta solución durante periodos más largos no observamos un aumento en la proliferación. Estos datos, apoyan nuestros resultados en células transfectadas con los mutantes del poro y/o del sensor de voltaje, en los que vemos un aumento en p-Tyr sólo en el mutante Kv1.3-W389F (capaz de sentir el voltaje), pero no en Kv1.3-WF3x, el cual permanece en el estado inactivado.

Por último, y con el objetivo de extrapolar los resultados obtenidos en células HEK293 a un sistema nativo, optimizamos un método de transferencia génica en CMLV mediante el uso de lentivirus. Este vehículo de transferencia nos permitió obtener eficiencias de transducción de más del 90 % no sólo en células HEK293 sino en también en CMLV de arteria uterina, renal y coronaria.

## 8.5. Discusión y Conclusiones

La sobreexpresión de Kv1.3 en un sistema heterólogo (células HEK293) aumenta significativamente la proliferación celular, mientras que la sobreexpresión de Kv1.5 inhibe la proliferación sin inducir apoptosis.

El uso de los mutantes del poro y/o del sensor de voltaje indica que el efecto del Kv1.3 sobre la proliferación de las células HEK293 requiere la expresión en membrana del canal y que éste sea capaz de sentir el voltaje, induciendo cambios conformacionales. Estos resultados sugieren que el Kv1.3 podría ser una proteína bifuncional que no sólo regula el flujo de $K^+$ sino también vías de señalización intracelulares.

La quimera K5C3 presenta efectos pro-proliferativos similares a los del Kv1.3, mientras que la quimera K5N3 inhibe la proliferación al igual que el Kv1.5, demostrando que los efectos de los canales Kv1.3 y Kv1.5 están mediados por sus dominios carboxilo.

Entre todos los residuos fosforilables del dominio carboxilo del Kv1.3, sólo las mutaciones en Y447 y S459 abolen completamente el efecto pro-proliferativo del Kv1.3, por tanto estos residuos podrían jugar un papel importante en los mecanismos a través de los cuales el Kv1.3 induce proliferación. De hecho, la quimera K5-532YS, la cual contiene el fragmento YS clonado en el sitio análogo del Kv1.3, es capaz de inducir proliferación. Esto demuestra que la posición de estos residuos es relevante.

Los resultados con el bloqueante de la vía de MEK/ERK (PD98059) y los estudios de los niveles de fosforilación en tirosina demuestran que ERK1/2 modula la fosforilación del residuo Y447, el cual es un determinante

importante de la vía de señalización a través de la cual el Kv1.3 induce proliferación. Además, la fosforilación de Y447 se observa en el Kv1.3 y en el mutante del poro Kv1.3-W389F, pero no en el mutante del poro y el sensor del voltaje: Kv1.3-WF3x, el cual permanece en un estado inactivado. Estos resultados indican que los cambios conformacionales del canal son los responsables de determinar la accesibilidad de estos residuos, desencadenando así la vía de señalización mediante la cual el Kv1.3 induce proliferación.

Por último, el uso de vectores lentivirales como herramienta de transferencia génica en CMLV representa una buena técnica para manipular los niveles de expresión de los canales Kv1.3 y Kv1.5 en cultivos primarios y estudiar los efectos de estos mutantes.